UNIVERSITA' DEGLI STUDI DI PARMA

Dottorato di Ricerca

Biologia e Patologia Molecolare

Ciclo XXVI

In vivo molecular imaging: a useful tool in respiratory drug discovery to visualize key components of lung inflammation

Coordinatore

Chiar.mo Prof.ssa Valeria Dall'Asta

Tutor

Chiar.mo Prof. Gaetano Donofrio

Dottorando Franco Fabio Stellari

BACKGROUND

Chronic respiratory diseases are major causes of morbidity and mortality, comprising 7% of deaths and 4% of disability adjusted life years (DALYs) worldwide (1-2). Asthma and chronic obstructive pulmonary disease (COPD) affect approximately 300 and 210 million people, respectively, with most of the deaths associated with both disorders occurring in low- and middle-income countries. In 2005 asthma was responsible for 255,000 deaths, whereas COPD was the cause of approximately 3 million deaths worldwide. The majority of asthma deaths occur in individuals with a severe form of the disease (5–10% of asthmatics), which is not effectively managed with the standard asthma therapy (i.e., glucocorticoid and β2-adrenoceptor agonist combination therapy). Similarly in COPD, there are no treatments that can halt the progression of the disease. Additionally, acute exacerbations of both asthma and COPD (where disease symptoms become acutely more severe) are major causes of hospitalizations and death in patients. Again, there is little that can be done to effectively limit the severity or reduce the frequency of these events. With asthma being the most common chronic disease amongst children and COPD predicted to become the 3rd leading cause of death by 2030, clearly these two conditions represent very large unmet medical needs that require urgent attention. In recent years, drug discovery efforts have largely centered around two different approaches – the improvements on existing therapies like bronchodilators and glucocorticoids, and novel therapeutic approaches aimed at specific molecular targets. Where, the latter approaches are becoming particularly important. For such approach, biological models of disease are vital for the development of all therapies, for instance, it has become commonplace to validate the “central role” of a particular molecular target in the pathogenesis of either asthma or COPD by characterizing the responses of particular target gene, either

knocked-out or overexpressed, in the most relevant system before in vitro and after in vivo models. Therefore, the development of a new drug is the direct consequence of the model system quality employed.

Clearly, data from clinical specimens demonstrating the target has an association with the disease or correlation with disease progression is as, if not more, important for validating a particular target for drug discovery purposes; however, data from biological models provide the cause–effect relationship between target and disease-like phenotype that is a very powerful form of evidence that cannot be easily obtained in the clinic.

ASTHMA and COPD is a prime example of a “complex disease,” a term that has become popular for characterizing those pathologies that appear to have multifaceted etiologist and an entanglement of underlying mechanisms. The moniker of complex disease, however, often tends to belie a general lack of understanding about what is going on, and this pathologists are no exception. Indeed, asthma and COPD is more properly regarded as a syndrome than a disease because it is defined on the basis of clinical characteristics rather than underlying mechanisms, and there remains a great deal of controversy about which of the possible mechanisms are the most important (3). The principal characteristics of asthma are reversible airflow obstruction, hyperresponsiveness of the lungs to challenge with smooth muscle agonists, and airway inflammation. Not surprisingly, allergy heads the list of causative suspects, but it is by no means alone. Exercise, cold air, and emotional stress are also known triggers of asthma (4), leading to the notion that asthma itself represents merely the common clinical endpoint of a number of distinct disease processes (5-6).

As with most human diseases, studies in laboratory animals have produced much of what we currently think we know about the mechanisms responsible

for asthma. Obviously, the relevance and validity of these studies are tied to how well we can produce accurate animal equivalents of human asthma. The development of such “animal models” is still very much a work in progress; although many of the various features of asthma have been convincingly recapitulated in animals, invariably every animal model misses some important aspect of the human syndrome (7). Also, very few animals spontaneously develop a condition with any similarity to asthma, the most reminiscent being an allergic syndrome in cats (8) and the condition known as heaves in horses (9).

If asthma is a condition peculiar to humans for some reason, then having it manifest in its entirety in a laboratory animal may simply be impossible. On the other hand, given that we still do not fully understand what asthma in humans actually is, it remains difficult to know whether an animal really has it or not. Accordingly, much of the challenge in studying animal models of asthma lies in phenotyping them properly, particularly as asthma is defined in humans in terms of phenotype rather than underlying pathology**.**

In this thesis, we therefore focus on the issue of how to assess the relevant function, structure molecular events in the mice lungs, fusing together: histological, FACS analysis and non-invasive *in vivo* molecular imaging technologies.

ASTHMA and COPD

Along with chronic obstructive pulmonary disease (COPD), bronchitis and emphysema, asthma is a disease of the airways: in the past it had been very difficult to define asthma, since, as we now know, the basic characteristics (airway inflammation, airway hyper responsiveness, airway obstruction and airway remodeling) of all the chronic lung diseases partially overlap.

A recent definition given by Global Initiative for Astma (GINA) states that "*asthma is a chronic inflammatory disorder of the airways in which many cells and cellular elements play a role. The chronic inflammation is associated with airway hyper responsiveness that leads to recurrent episodic of wheezing, breathlessness, chest tightness, and coughing, particularly at night or in the early morning. These episodes are usually associated with widespread, but variable, airflow obstruction within the lung that is often reversible either spontaneously or with treatment"* (10).

Asthma treatment either with β_2-adrenoceptor agonists or glucocorticoids is nowadays more likely to control and decrease the frequency of clinical symptoms as well as its eventual exacerbations, rather than to cure the cause of asthma disease.

Asthma pathogenesis is complex and heterogeneous as it is driven by different risk factors including environmental and genetic factors which are not to be considered independent but interactive in asthma inception (11). The identification of the risk factors underlying the onset, expression and morbidity of asthma has been very important and helpful to better understand some features of its pathogenesis.

Although the cause of asthma is unknown, there are several risk factors that influence the development of asthma. These can be divided into host factors and environmental risk factors (12).

The allelic distribution of genes pre-disposing to atopy or airway hyper responsiveness is a typical host factor which determines asthma development and phenotype. Typical environmental factors are allergens (indoor or outdoor allergens, such as these originating from domestic mites, furred animals, cockroach, fungi, molds, yeasts and pollen), infections (mainly viruses), occupational sensitizers, tobacco smoke (both active and passive smoking) and indoor or outdoor pollution by gasses and particulate matter (PM).

Allergens such as dust mite, ragweed and aspergillus are among the potential inducers of asthma. (13).

Dust mite is a very small creature invisible to unaided eye that lives indoors in warm, moist places like the insides of pillows and mattresses. The digestive proteins in its feces are one of the major inducers of allergic reactions like asthma by inhalation. Pollens grains released into the air by ragweed, a weed that grows in rural, warm and humid areas, are determinant in hay fever an asthma-triggering condition. *Aspergillus fumigatus* is a fungal which airborne spores can aggravate asthmatic conditions promoting pulmonary airway hyperreactivity (AHR) and remodeling after repeated contact. Allergen-driven asthma is known as allergic or atopic asthma and it’s often defined as the estrinsic form of this disease while the intrinsic form intended as non-atopic asthma is triggered by other stimuli (viral respiratory infections, air pollution, smoke exposure, sensitizing agents in work environment, exercise and cold) (14-15); it usually develops in childhood persisting also in adulthood.

In their efforts to unravel the pathogenesis of asthma, researchers have mainly focussed on the basic immunologic mechanisms resulting in unwanted or exaggerated inflammation. Many uncertainties remain concerning why and how asthma develops during lifetime. The emerging hypothesis is that a failure of endogenous immune regulated tolerance mechanisms might be

Involved. Alternatively, exposure to a more or less specific cocktail of allergens or pollutants might also lead to the development of an asthmatic phenotype. Regardless of the mechanism, exposure of the airways to foreign agents (allergens or chemical agents) often represents the very first cause for an immune derailment.

In later stages, sensitized individuals will be more susceptible to develop airway inflammation and symptoms. These processes can be present for a limited time or become chronic. In that view, the pathogenesis of allergic asthma comprises 3 phases: sensitization, acute inflammation and chronic disease.

The association between exposure to inhalable pollutants such as cigarette smoke and particularly matter (e.g. diesel exhaust) and respiratory morbidity has been recognized for a long time. The epidemiological association of increased exposure to air pollutants and the rise in frequency of wheezing illnesses led to the assumption that these pollutants are actively involved in the pathogenesis of asthma. While there is no doubt that inhaled pollutants can exacerbate the symptoms of asthma, it is also considerable (though less well established) that they play a role in inducing asthma or at least in driving incipient asthma into clinically obvious manifestations of the disease.

Asthma has a significant genetic component, in fact, thanks to the genome-wide screening approach, it is now known that there are different genes predisposing to airway hyper responsiveness and to atopy (allergic reactions) associated with the developing of the asthmatic phenotype (16-17).

The definition of asthma derives from analysis of bronchoalveolar lavage (BAL) fluids and induced sputum of asthmatics as well as from bronchoscopy analysis, lung specimen biopsies and autopsy in patients with fatal asthma. These were the primary methods used to study asthma and they have been very successful in evidencing the role of inflammation in asthma disorder.

Nonetheless, the advancement of asthma knowledge and the underlying pathophysiological mechanisms have been achieved through studies in animal models which have shed light on the cellular and molecular events that occur in asthma pathology (18.)

Allergic asthma has been the asthmatic phenotype mostly used to outline the disease pathogenesis because it is very easy to replicate in laboratory under controlled conditions. In fact, upon inhalation of allergens which have the capacity to penetrate mucus and epithelial barriers, a cascade of immune-mediated reactions that leads to chronic airway inflammation occurs in sensitized subjects. Th2 cytokines are the major actors triggering the activation and the infiltration of inflammatory cells (eosinophils, lymphocytes T CD4+ and mast cells) in the airways, as well as inducing the airway obstruction. There are two major mechanisms underlying airway obstruction in asthma: the type I hypersensitivity and the type IV hypersensitivity. The former mechanism is based on immune-mediated reactions that can be divided in two phases: the early phase and the late phase responses. During the early phase response which usually resolves within an hour, Th2-cytokines IL-4 and IL-9 activate either lymphocytes B for the synthesis of immunoglobulin E (IgE) and the airway mast cells which release pro-inflammatory mediators such as histamine, prostaglandins, cysteinyl leukotrienes and reactive oxygen species that induce contraction of airway smooth muscle, mucus secretion and edema (figure 1). These reactions are the bases of the acute airway inflammation characterized by bronchospasm and mucus hyper-secretion which are also controlled by the stimulation of the parasympathetic nervous system. Figure 2 better show the complexity of the disease. In the late-phase response which occurs 6-9 hours after antigen challenge, other Th2-cytokines like IL-5 and IL-13 induce the recruitment and activation of inflammatory cells (eosinophils, lymphocytes, basophils and

macrophages) in the bronchial airways which release further inflammatory mediators promoting airway obstruction. The type IV hypersensitivity characterizing the non-atopic asthma inception also involves Th2 cytokines (19-20). The activation of inflammatory and immune cells is crucial in the perpetuation of airway inflammation: the resulting chronic inflammation, deriving from repeated exposure to allergen, seems to be responsible for epithelial cell shedding due to tight junction and extracellular matrix destruction caused by mast cell and eosinophil proteolytic enzymes.

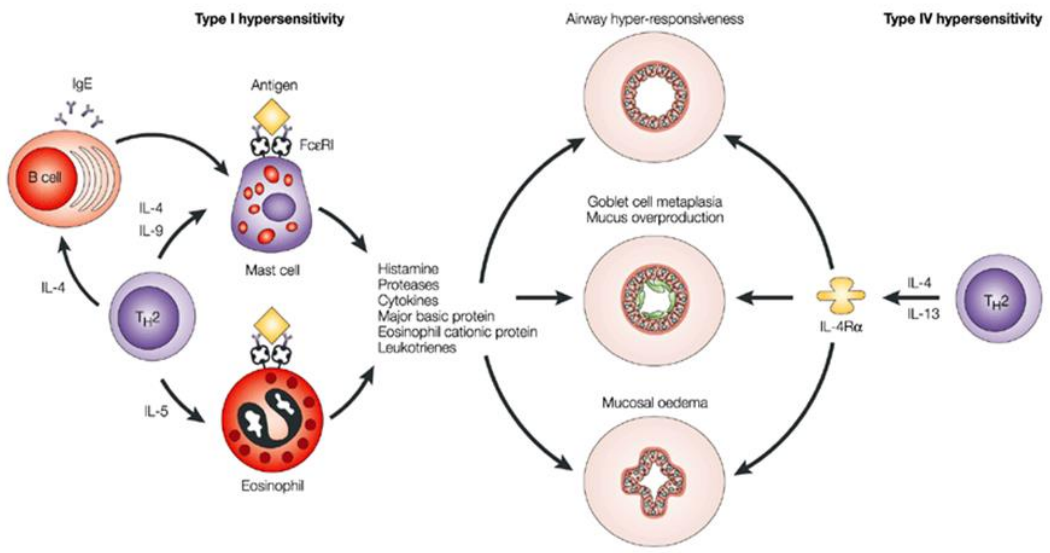

Figure 1. There are two mechanisms underlying airway obstruction in asthma: the type I hypersensitivity and the type IV hypersensitivity.

These latter have been shown to alter the epithelia cells attachment to the basement membrane and the bronchial smooth muscle function. When injured, the epithelium has an intrinsic capacity to reconstitute and it has been observed in asthmatic patients that once epithelium is reformed, the goblet-cells and submucosal glands undergo hyperplastic, hypertrophic and metaplastic alterations while the lamina reticularis of the basement membrane looks thicker because of deposition of collagen resulting in the so called “subephithelial fibrosis” (21-22-23) All these events, together with

smooth muscles hyperplasia and hypertrophy lead to a thickened, engorged and edematous airway wall as well as a narrowing of the airway lumen which in addition to plasma exudation reduces airway calibre and mucociliary clearance (24-25) (figure 2). These structural changes are known as airway remodeling and contribute to the decrease of the elastic recoil of the lung parenchyma leading to airflow obstruction and to an increased bronchial hyperreactivity to a variety of stimuli (26). Considering airflow limitation, lung function heterogeneity and variability, symptom frequencies and levels as well as responsesiveness to treatments, asthma can be subdivided in four forms: intermittent, mild persistent, moderate persistent and severe persistent. Asthma is sustained by the activity of T lymphocytes bearing CD4+ receptors. T lymphocytes CD4+ releases Th2-cyotkines and enhance the perpetuation of airway inflammation because of their long-lived nature and their “immune memory” (27).

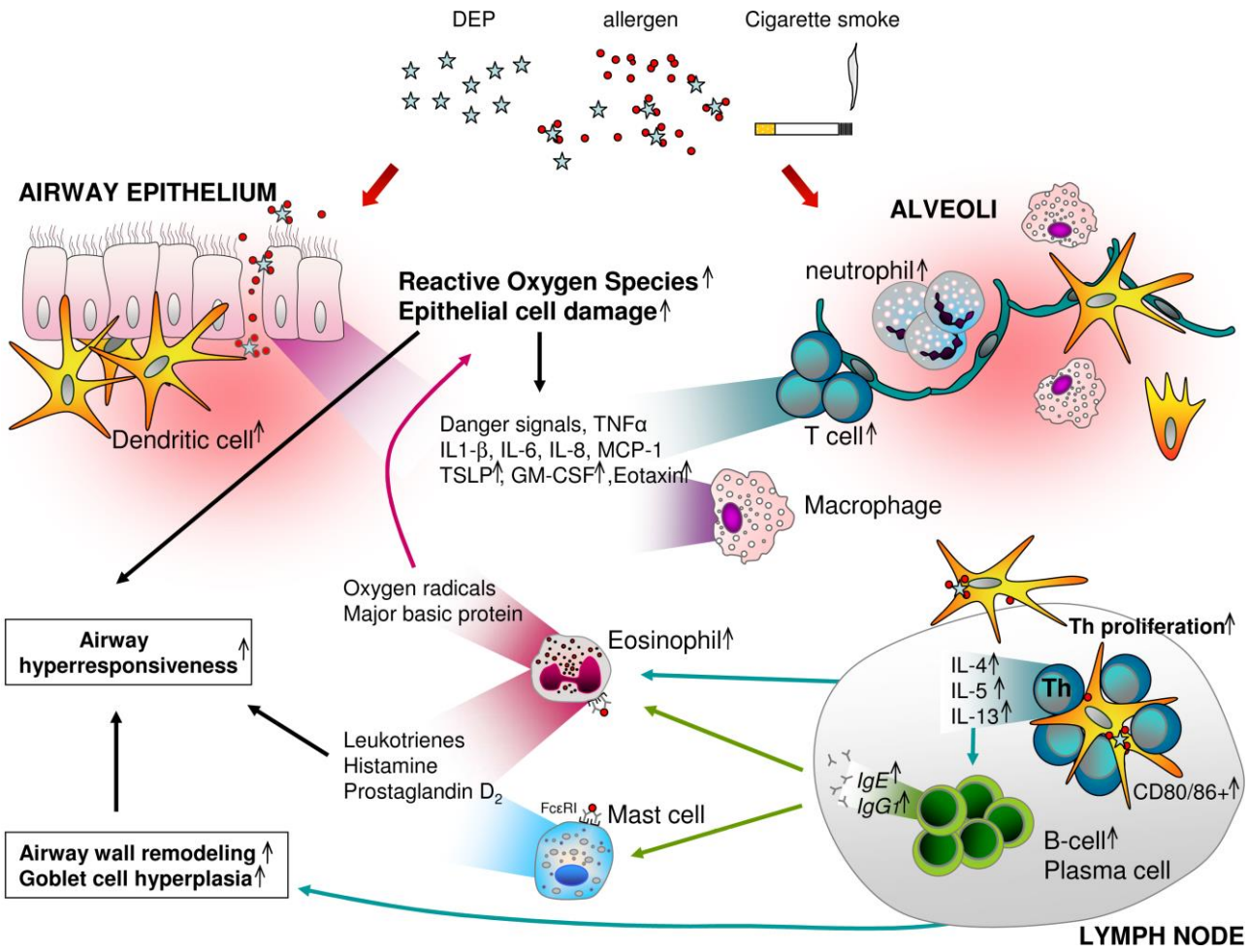

Figure 2. Diesel exhaust particles (DEP) and cigarette smoke affect allergic sensitization and the development or exacerbation of asthma. Similar proposed mechanisms for both inhalable pollutants, obtained from human, mouse and in vitro data are shown. Both DEP and cigarette smoke induce tissue damage and oxidative stress, resulting in a pulmonary inflammation with increased neutrophils and T-cells, and increased pro-inflammatory cytokines. This creates an environment which facilitates allergic sensitization. Cell types and mediators that are increased upon the combination of allergen and inhalable pollutant exposure (both DEP and cigarette smoke) and which are specifically associated with allergic asthma are indicated with a small black arrow. ***(Maes et al. Respiratory Research 2010, 11:7)***

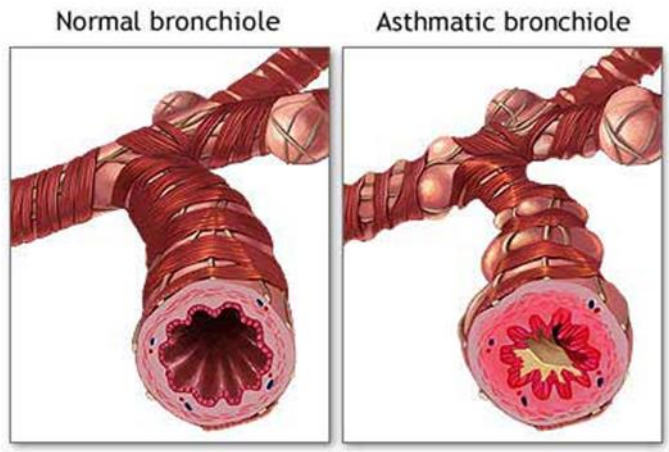

Figure 3. Asthma histopathology. Differences between a bronchial with a normal airflow and a bronchial with an obstructed airflow consisting in a contracted smooth muscle, decreased lumen diameter, mucous hypersecretion, inflammation and swelling.

Eosinophils are thought to be the key effectors in asthma pathogenesis and airway inflammation since they have been found to be present in an increased number in sputum and BAL fluid of asthmatics. In addition it has been proved that there is a significant association between asthma severity and eosinophil activation in the airways (28-29).

Eosinophils maturation is driven by IL-5 and, once matured, they are very rich in crystalloid granules that are source of inflammatory proteins including major basic protein (MBP), eosinophil cationic proteins (ECP), eosinophil-derived neurotoxins (EDN) and peroxidase: all these proteins are cytotoxic to the respiratory epithelium. The intracellular granules also incite histamine release by inducing the degranulation of mast cells and basophils. MBP is an endogenous antagonist of muscarinic autoreceptors M2 which activity leads to an increased bronchospasm response to the vagal nerve stimulation (30).

Eosinophils also secrete bronchoconstrictors like cysteinyl leukotriene (Cyst-LT), prostaglandins, IL-5, IL-13 and GM-CSF sustaining the ongoing airway inflammation (31-32). Other eosinophil products contributing to airway inflammation persistence and to the surface shedding of the epithelium are

lysosomal elastases (cathepsins) and matrix metalloproteases (MMPs) which intensify the responsiveness of the airways (33-34).

Along with eosinophils, mast cells are also crucial in asthma pathogenesis: they release pro-inflammatory molecules including autacoids and neutral proteases such as tryptase and chymase which have been proved to enhance bronchial responsiveness by sensitizing bronchial smooth muscle to histamine, to contribute to the airway wall remodeling by stimulating fibroblasts proliferation and to promote the increase of basement membrane thickness (35-36).

Although the presence of macrophages in asthmatic airways is very scarse, they are also involved in the induction of airway obstruction and hyperresponsiveness. Macrophages produce and secrete a group of matrix metalloproteinases (MMPs) and cathepsins that degrade various extracellular matrix macromolecules (ECM). Macrophages and neutrophils are more likely to be recruited in high number either soon after asthma attacks, to be then replaced by eosinophils after repeated sensitization, and during disease exacerbations.

Th2-cytokines (IL-4, IL-5, IL-9 and IL-13) have been demonstrated to be crucial molecules for asthma inception and persistence, driving most of the inflammatory reactions characterizing this disease. They play an important role in antigen presentation as well as in the recruitment of inflammatory cells. They are extracellular signaling proteins released by a variety of cells among which are also inflammatory cells (37). IL-5 and IL-13 have been proved to be the pivotal mediators of inflammation response (38). There are evidences that blocking either IL-5 or IL-13 activity inhibits airway hyperresponsiveness, mucus production and airway eosinophilia and that overexpression of IL-13 induces secretion of proteolytic enzymes such as matrix metalloproteinase promoting airway remodeling which may lead to emphysema (39). While IL-

13 is a potent mucus secretion stimulator that contributes to airway obstruction, IL-5 is principally responsible for eosinophil maturation, proliferation, activation and recruitment within the airway epithelium as well as of their prolonged survival; it also promotes the eosinophilic granule-mediated airway wall remodeling as well as an augmented hyperresponsiveness (40).

IL-4 is known to trigger the initiation of the inflammation response to antigen, while IL-9 is involved in mast cells infiltration in the airway and may have a role in epithelial cells hyperplasia and hyperthropy (41).

Other pro-inflammatory cytokines found to be determinants in asthma include GM-CSF (Granulocyte-Macrophage Colony Stimulating Factor) which contributes to the persistence of eosinophilic activity in the airways, and TNF-α (Tumour Necrosis Factor-α) which activates the secretion of further pro-inflammatory cytokines (42).

Chemotactic cytokines involved in the trafficking of leukocytes into airway tissues of asthmatics include eotaxins and RANTES (Regulated on Activation, Normal T cell Expressed, and Secreted) which principally regulate the infiltration of eosinophils. Matrix metalloproteinases are proteolytic enzymes which are part of the large zinc-dependent endopeptidase family. They are thought to be essential for the development, turnover and degradation of ECM components. In addition, they are also involved in epithelial repair mechanisms as well as in cytokine and chemokine activities thus controlling leukocytes trafficking in the tissue (43). These enzymes do also contribute to asthma pathogenesis since their activity on ECM might lead to the loss of lung parenchyma integrity. The MMPs found to be highly expressed in the sputum of asthmatic patients are MMP-2 *(gelatinase A)* and MMP-9 *(gelatinase B)* which are mainly released by macrophages as well as by eosinophils and they principally act on denatured collagens like gelatins hence contributing to airway remodeling . The pronounced activity of MMPs

derives from an imbalance between the activity of MMPs and the action of the tissue inhibitors of metalloproteinases (TIMPs) secreted by alveolar macrophages Together with MMPs, Cathepsins (CTS) are important contributors to lung inflammatory events. These proteolytic enzymes are intracellularly expressed and activated at the low pH found in the lysosomes of cells like eosinophils, fibroblasts, macrophages, neutophils and epithelial cells and they promote the intracellular protein turnover (44).

Cathepsins have been also seen to play a critical role in the physiological process of apoptosis by promoting protein degradation within the lysosome. However, during inflammatory conditions, their intracellular activity in the apoptosis of inflammatory cells (eosinophils and neutrophils) seems to be blocked or altered, leading to a chronic and perpetuating survival of these cells (45).

The majority of these lysosomal proteases, which activities have been found in the BAL fluid of asthmatics (cathepsins B, H, K, L and S), is cysteine proteases with papain-like activity. Their contribution to the degradation of the basement membrane and ECM components enhances the degeneration of airway remodeling (46).

Histopathological analysis shows that asthmatic epithelium presents gross denuded and/or desquamated areas thus explaining the observed hyperreactivity to non-specific agents. In asthma, epithelium undergoes different structural changes in which the increased expression of pro-inflammatory transcription factors like NFkB (Nuclear Factor kappa B) and AP-1 (Activator Protein 1) plays a crucial role.

Moreover in acute phase of the disease, airway has been inflitered by polymorphonuclear leukocytes (PMNs) in response to bacterial and viral infections represents a pivotal feature of lung inflammatory reactions and is both directly and indirectly involved in most lung pathologies (47).

Mobilization of PMNs to inflamed lungs is modulated by a complex interplay between cytokines, endothelial cells, and neutrophils. During the acute-phase response to infectious agents in human, inflammatory cytokines such as IL-1β, TNF-α and IL-8, secreted by a variety of immune and non immune cell types, induce a strong PMNs infiltration that sometimes fail to control the infection, and may even contribute to the development of lesions in the lung.

Since its discovery in 1986 (48), the role of ubiquitous NF-κB transcription factors has been extensively studied in tumorigenesis, immunity, and inflammatory responses, and its dysregulated activation has been associated to malignancies as well as to inflammatory pathological conditions. The activation of NF-κB is controlled through inhibitory IκB proteins, and the kinase that phosphorylates IκBs: the IκB kinase (IKK) complex (49). Specific NF-κB binding sites are present in promoters of a large number of genes (50), and inflammatory processes are controlled through NF-κB-dependent transcription of cytokines, chemokines, cell adhesion molecules, factors of the complement cascade, and acute phase proteins.

In the lungs, several noxious/inflammatory stimuli activate NF-κB, including intact bacteria, Gram-negative bacterial lipopolysaccharides (LPS), ozone, and silica delivered directly to the airways, as well as systemic inflammatory insults such as sepsis, haemorrhage, and direct liver injury (51). In rodent models of lung inflammation induced by LPS, pre-treatment with relatively nonspecific inhibitors of NF-κB activation was found to decrease lung inflammation, and mice deficient in both RelA (the transactivating subunit of NF-κB) and type 1 TNF receptor (TNFR1) showed impaired neutrophil recruitment to the lungs in response to LPS, when compared to wild-type controls as well as TNFR1-deficient mice (52).

Taken together, these studies suggest an important role for NF-κB in the initiation of signaling leading to an inflammatory response in the lungs.

However, it has also been suggested that NF-κB may play a role in the resolution phase of the inflammatory reaction, possibly through anti-apoptotic effects and the expression of proteins limiting inflammation (53). Therefore, cellular distribution, intensity and/or duration of NF-κB activation may result in either self-limitation of lung inflammation or its progression to tissue injury (54).

A widely used tool to evaluate the effects of inhaled pollutants, allergen or infection on the development and aggravation of asthma consists in epidemiological studies. Controlled exposure studies in humans are informative as well, but are limited by practical and ethical issues. The use of animal models leads to more insights regarding the role of inhalable pollutants during sensitization and inflammation in asthma, with a unique opportunity to unravel the effects on the different phases of the development of the asthma pathology (Figure 4). The mouse has emerged as the animal of choice for modelling this disease (55).

Because of the prevalence of asthma and the complexity of this multifactorial and multicellular disease, it has become important to establish relevant animal models to better aid in the discovery of therapeutic agents. Preclinical research using animal models of pulmonary inflammation has been critical for understanding the pathophysiology of asthma and for developing new therapies, and a variety of mouse models of asthma have been developed that capture specific inflammatory mechanisms of asthma (56). In normal healthy animals, it is necessary to immunize and challenge the mice with specific antigens (57-58) to induce allergic asthma-like pulmonary inflammation. These types of animal models have helped to establish asthma as a unique form of chronic airway inflammation involving lymphocytes, mast cells, and eosinophils. Among these, eosinophils are the predominant effector cells for tissue damage and pulmonary dysfunction, and airway eosinophil

influx correlates well with the severity of airway hyperreactivity. Once eosinophils have infiltrated the lung, numerous inflammatory changes in the airways are triggered, including the release of a wide variety of immunomodulatory molecules, which can directly damage airway epithelium, cause degranulation of basophils and mast cells (59), and prime the lung for subsequent occurrences of allergic pulmonary inflammation (60-61).

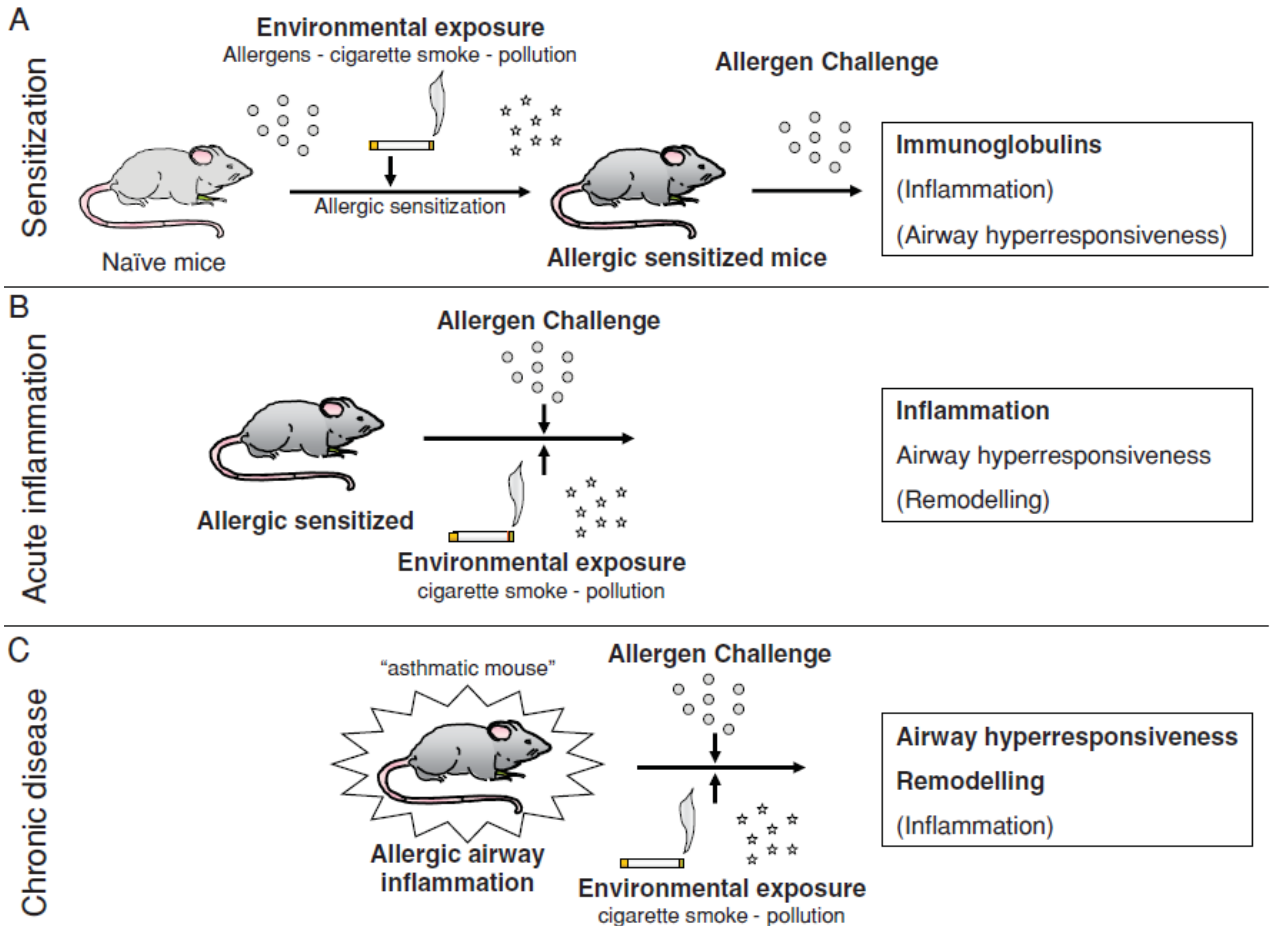

Figure 4. Schematic presentation of how the effects of environmental exposure (aero)immunization and airway challenge on the 3 different phases of the asthma pathology (sensitization, acute inflammation and chronic disease) can be dissected in mice. **(*Maes et al. Respiratory Research 2010, 11:7)***

MOLECULAR IMAGING

Morphological observations have driven the course of biology ever since the first microscope was built in the late sixteenth century. Molecular imaging is a rapidly emerging biomedical research discipline that extends such observations in living subjects to a more meaningful dimension. It may be defined as the visual representation, characterization, and quantification of biological processes at the cellular and subcellular levels within intact living organisms. It is a novel multidisciplinary field, in which the images produced reflect cellular and molecular pathways and in vivo mechanisms of disease present within the context of physiologically authentic environments. The term “molecular imaging” implies the convergence of multiple image-capture techniques, basic cell/molecular biology, chemistry, medicine, pharmacology, medical physics, biomathematics, and bioinformatics into a new imaging paradigm. Present imaging technologies rely mostly on nonspecific macroscopic physical, physiological, or metabolic changes that differentiate pathological from normal tissue rather than identifying specific molecular events (e.g., gene expression) responsible for disease. Molecular imaging usually exploits specific molecular probes as the source of image contrast. This change in emphasis from a nonspecific to a specific approach represents a significant paradigm shift, the impact of which is that imaging can now provide the potential for understanding of integrative biology, earlier detection and characterization of disease, and evaluation of treatment.

The emergence of molecular imaging strategies is largely due to recent unprecedented advances in molecular and cell biology techniques, the use of transgenic animal models, availability of newer imaging drugs and probes that are highly specific, and successful development of small-animal imaging instrumentation. These factors, along with continued expansion of scientific horizons in the current post-genomic era, have been pivotal in the drive

toward a new standard that allows linking established in vitro and cell culture experimental assays to imaging studies within living subjects. This now creates the possibility of achieving several important goals in biomedical research, namely, (62) to develop non-invasive in vivo imaging methods that reflect specific cellular and molecular processes, for example, gene expression, or more complex molecular interactions such as protein–protein interactions; to monitor multiple molecular events near-simultaneously; to follow trafficking and targeting of cells; to optimize drug and gene therapy; to image drug effects at a molecular and cellular level; to assess disease progression at a molecular pathological level; and to create the possibility of achieving all of the above goals of imaging in a rapid, reproducible, and quantitative manner, so as to be able to monitor time-dependent experimental, developmental, environmental, and therapeutic influences on gene products in the same animal or patient. Molecular imaging probes can now also be developed by taking advantage of the rapidly increasing knowledge of available cellular/molecular targets. The merger of molecular biology and medical imaging is facilitating rapid growth of this new field by providing methods to monitor cellular/molecular events adapted from conventional molecular assays, for example, reporter gene assays. The present frenetic pace of advancements in biotechnology and functional genomics (63) is resulting in parallel progress in molecular imaging innovations and applications. The development, validation, and application of these novel imaging techniques in living subjects should further en- hence our understanding of disease mechanisms and go hand in hand with the development of molecular medicine (64). Molecular imaging in living subjects offers distinct advantages when compared with conventional in vitro and cell culture research techniques in biology. Although in vitro studies in basic biological research have been, and remain, a mainstay for defining

biochemical and gene expression pathways, the in vitro approach has been less successful in deciphering physiological whole-body contributions of proteins, in which redundancies and differences in regulation can alter the outcome from that initially predicted. In contrast to cell and tissue culture, in vivo animal models allow the assessment of phenomena such as tolerances, complementation, and redundancy in biological pathways (65). Molecular imaging permits both the temporal and the spatial biodistribution of a molecular probe and related biological processes to be determined in a more meaningful manner throughout an intact living subject. Visualization of functions and interactions of a particular gene becomes easier in a more realistic manner that respects the dynamics of complex biological networks and of complete and holistic biological systems in the entire living subject.

Molecular imaging assays in intact living animals could be of further benefit in resolving biological questions raised by pharmaceutical scientists. Transgenic animals are useful in guiding early drug discovery by “validating” the target protein, evaluating test compounds, determining whether the target is involved in any toxicological effects of test compounds, and testing the efficacy of compounds to ensure that the compounds will act as expected in man (66). The implementation of molecular imaging approaches in this drug discovery process offers the strong advantage of being able to meaningfully study a potential drug labelled for imaging in an animal model, often before phenotypic changes become obvious, and then quickly move into human studies. It is likely that preclinical trials can be accelerated to rule out drugs with unfavorable biodistribution and/or pharmacokinetics prior to human studies. A further advantage over in vitro and cell culture experimentation may be achieved by repetitive study of the same animal model, using identical or alternative biological imaging assays at different time points. This reveals a dynamic and more meaningful picture of the progressive changes in

biological parameters under scrutiny, as well as possible temporal assessment of therapeutic responses, all in the same animal without recourse to its death. This yields better quality results from far fewer experimental animals. Another benefit of molecular imaging assays is their quantitative nature. The images obtained are usually not just subjective or qualitative, as is the case with standard use of several conventional medical imaging modalities, but instead, usually provide meaningful numerical measures of biological phenomena. Such quantitative data could even be considered more useful than similar data obtainable in vitro or ex vivo, on account of preserving the intactness and the physiology of the experimental subject. However, one exception to this can be made in cases in which general anesthesia of the living subject results in alteration of the biological function under investigation, as may occur; for example, in brain molecular imaging studies.

PRINCIPLES OF OPTICAL IMAGING

Optical Imaging (OI) modalities are based on the detection and quantification of bioluminescent or fluorescent light from the subject, through use of a cooled charged coupled device (CCD) camera. The relatively simple instrumentation and lack of requirement for radioactivity permits users to run experiments themselves without help or complicated chemistry and scheduling, putting the technology well within the reach of the average laboratory. The focus on optical imaging techniques for molecular imaging is driven in large part by the sensitivity for imaging optical contrast agents and reporter molecules in vivo. The lower limits of detection for optical imaging may reach picomolar or even femtomolar concentrations of an optical reporter or contrast agent. Combined with the minimal background of techniques such as bioluminescence imaging and fluorescence imaging in the near infrared

spectrum, the signal-to-background ratio for detecting specific molecular signals equals or exceeds that which can be achieved with other molecular imaging modalities.

For light in the visible spectrum, absorption by hemoglobin and other molecules may reduce optical signals by approximately 10-fold per centimeter of tissue (67). To image fluorescence in deeper tissues, investigators have developed strategies for imaging near-infrared fluorescence (NIRF) with emission wavelengths between 650 and 900 nm. At these wavelengths, absorption of light by hemoglobin, lipids, and water is lowest, and tissue autofluorescence also is greatly reduced. As a result, the sensitivity for NIRF imaging agents is greatly enhanced, potentially allowing for tomographic optical imaging signals to be detected at depths of 7–14 cm (68). Differential absorption of light by tissues also produces images that are weighted toward optical reporters and probes that are located closer to the surface of a subject. While this limitation is being overcome with 3-dimensional imaging and analysis techniques such as fluorescence molecular tomography (FMT) (69).

BIOLUMINESCENCE AND BLI SYSTEMS

Bioluminescence imaging (BLI) is based on the sensitive detection of visible light produced during enzyme (luciferase)-mediated oxidation of a molecular substrate when the enzyme is expressed *in vivo* as a molecular reporter. Bioluminescence at the emission wavelength firefly luciferase (560 nm) can be imaged as deep as several centimeters within tissue, which allows at least organ-level resolution. This technology has been applied in studies to monitor transgene expression, progression of infection and inflammation, tumor growth and metastasis, transplantation, toxicology, viral infections, and gene therapy. BLI is simple to execute and enables monitoring throughout the

course of disease, allowing localization and serial quantification of biological processes without killing the experimental animal. This powerful technique can reduce the number of animals required for experimentation because multiple measurements can be made in the same animal over time, minimizing the effects of biological variation. Bioluminescence is appealing as an approach for *in vivo* optical imaging in mammalian tissues because these tissues have low intrinsic bioluminescence; therefore, images can be generated with remarkably high signal-to-noise ratios. A variety of different bioluminescent systems have been identified in nature, each requiring a specific enzyme and substrate. Although the most commonly used bioluminescent reporter for research purposes has been luciferase from the North American firefly (*Photinus pyralis*; FLuc), useful luciferases have also been cloned from jellyfish (Aequorea), sea pansy (Renilla; RLuc), corals (Tenilla), click beetle (Pyrophorus plagiophthalamus), and several bacterial species (Vibrio fischeri, V. harveyi) (70).

Firefly luciferase was cloned in 1985 (71 Three years later, an assay to measure luciferase in mammalian cell lysates was developed (72) that enabled the luciferase gene to become a useful tool for in vivo studies of gene regulation. Luciferase is an excellent marker for gene expression because of its lack of post-translational modifications and an in vivo t1/2 of approximately 3 h (73). Firefly luciferase produces photons in a reaction that requires ATP, magnesium, and a benzothiazoyl–thiazole luciferin (figure 5).

Light emission from the firefly luciferase-catalyzed luciferin reaction is broad-band (530–640 nm) and peaks at 562 nm (74). This emission spectrum, coupled with the optical properties of biological tissue, allows light (especially with spectral content above 600 nm) to penetrate through several centimeters of tissue. Therefore, it is possible to detect light emitted from internal organs in mice that express luciferase as a reporter gene. The sensitivity of detecting

internal light sources is dependent on several factors, including the level of luciferase expression, the depth of labelled cells within the body (the distance that the photons must travel through tissue), and the sensitivity of the detection system (75).

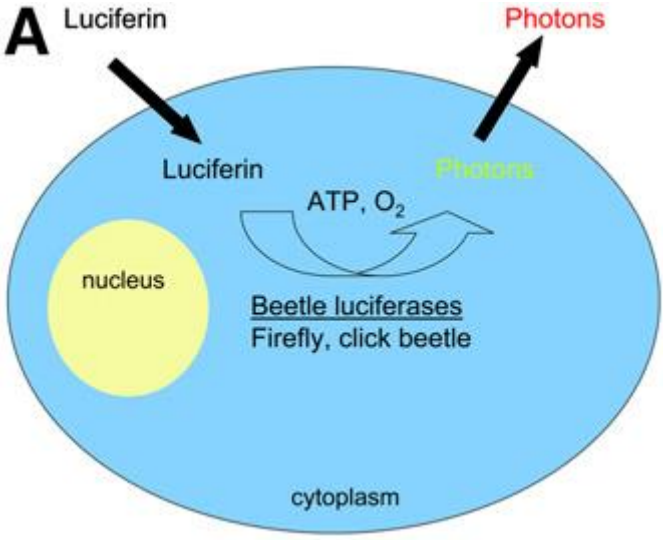

Figure 5. Schematic representation of bioluminescence imaging reporters. Beetle luciferase enzymes (firefly,click beetle) expressed in cytoplasm of engineered cells catalyze production of light photons from the substrate luciferin in the presence of oxygen and ATP. Gaussia and Renilla luciferases use a different substrate,coelenterazine, andare independent of ATP. Inits native form, Gaussia luciferaseis secreted from cellsand reacts with substrate inthe extracellular space.

Key advances in detector technology have led to substantial improvement in sensitivity and image quality. Photons are detected by specialized charge coupled device (CCD) cameras that convert photons into electrons after striking silicon wafers. CCD cameras spatially encode the intensity of incident photons into electrical charge patterns to generate an image. For BLI, the noise of the systems is reduced by super-cooling the CCD camera and mounting the camera in a light-tight box. These cameras are run by a computer for image acquisition and analysis. (Figure 6)

Although BLI has been used successfully in a variety of applications to obtain semiquantitative information regarding biological processes *in vivo*, several issues must be considered when applying this technology. Simple

quantification of light emission may not provide a true representation of the biological effect studied. The luciferase reaction is a complex interaction of a variety of molecules, including ATP, oxygen, and luciferin (substrate).

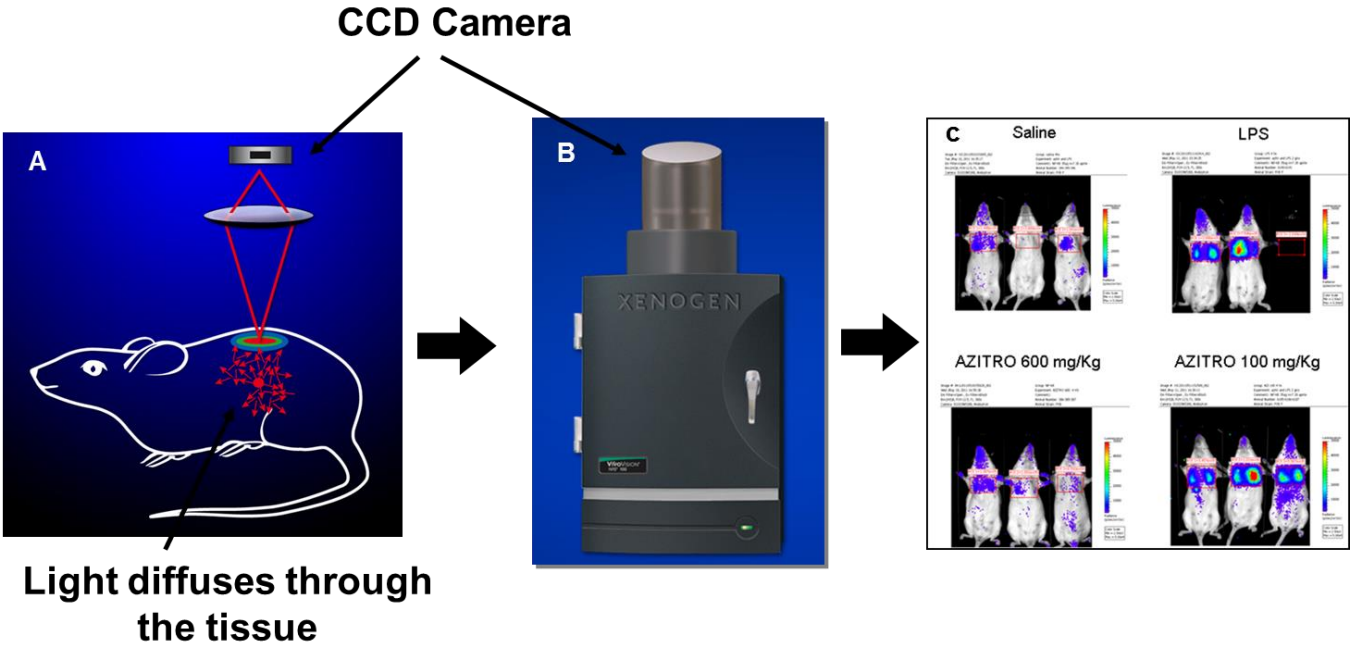

Figure 6. Schematic optical imaging instrumentation. A) mice as a light source**,** B) IVIS Lumina, which provides 2D BLI and FLI, C) example of quantification of BLI in mice.

If ATP, oxygen, or exogenously administered luciferin is not abundantly present, light emission may not be a true representation of luciferase activity. Another issue with BLI is the limited and wavelength-dependent transmission of light through animal tissues. As a general rule, there is an approximate 10-fold loss of photon intensity for each centimeter of tissue depth. Also, images are surface weighted, meaning that light sources closer to the surface of the animal appear brighter compared with deeper sources because of tissue attenuation properties. In addition, dynamic changes may occur in geometry (e.g., growing tumor, scar tissue) and/or the optical properties of tissues that affect light scatter or absorption and detected bioluminescence. Thus, although BLI provides a unique and powerful methodology, quantitative analysis must be approached with caution, and validation for each specific

application is necessary. In order to dynamically investigate in vivo the potentially different roles of NF-κB in the inflammatory response, a transgenic mouse model was developed expressing the minimal promoter of NF-κB and the luciferase gene as a reporter, allowing a direct monitoring of NF-κB activation by bioluminescence (76-77). BLI has proven to be very powerful technique for detecting luciferase reporter activity in intact animal models, facilitating real-time, molecular level analysis of disease progression. Nevertheless the generation, characterization, and colony management of transgenic mice may be difficult, and typically very expensive. An alternative, relatively inexpensive approach is represented by the use of transient transgenic mice obtained through the infusion of a polyethylenimine (PEI)/DNA complex containing plasmids with specific responsive elements (RE) and luciferase as a reporter gene. This technique yields significant transfection in vivo, as was recently shown by imaging pulmonary NF-κB activation in LPS-treated mice (78). This approach has been used in our lab to investigate in vivo the role of IL-8 in the lung. One of the most remarkable properties of interleukin 8 (CXCL8/IL-8), a chemokine with known additional functions also in angiogenesis and tissue remodeling, is the variation of its expression levels. In healthy tissues, IL-8 is barely detectable, but it is rapidly induced by several folds in response to proinflammatory cytokines, bacterial or viral products, and cellular stress. Although mouse cells do not bear a clear homologous IL-8 gene, the murine transcriptional apparatus may well be capable of activating or repressing a heterologous IL-8 gene promoter driving a reporter gene. In order to induce a transient transgenic expression, mice were systemically injected with a bovine IL-8 promoter–luciferase, construct. Subsequently mice were monitored for luciferase expression in the lung by in vivo bioluminescent image analysis over an extended period of time (up to 60 days) (79).

Generating transient transgenic mouse model where we can measure in non invasive the pathways activation of NF-kb and IL-8 it is crucial for understanding the molecular mechanic of the pathogenesis of the lung diseases and make them more druggable in order to test new anti-inflammatory drugs following a therapeutic regimen.

FLUORESCENCE AND IMAGING SYSTEM

In fluorescence imaging (FLI), an external light source excites the fluorophore (which can be protein or chemical dye) converting it to an excited state, and the transferred light energy is emitted at a different wavelength as the fluorophore returns to its ground state Figure 7.

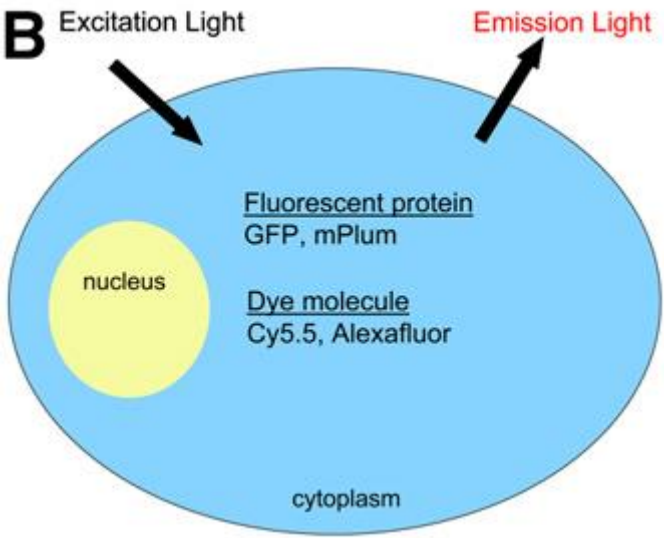

Figure 7. Fluorescence imaging requires light of appropriate wavelength to excite the reporter molecule (fluorescent protein or dye molecule), resulting in emission of light with a defined emission spectrum for each reporter protein or dye.

In contrast to bioluminescence, where light is emitted from within the subject following enzyme catalysed chemical energy release, with fluorescence, excitation light (of a specific wavelength) shined on the subject, is wave shifted by the fluorophore and emitted back out of the animal for detection using filters unique to the emitted light wavelength. Reporter strategies based

on delivery of genes coding for fluorescence proteins (FP) have been in use for many years (80). FP encoding cDNA can easily be included in vector constructs and serve as a monitoring tool for gene therapy. FP such as green fluorescent protein or GFP (from the *Aequorea victoria* jelly fish - the first isolated FP gene), have the powerful facet that they naturally fluoresce without the addition of substrates or enzymes. (Fluorophore + Excitation Light = Emission Light). These FP are suitable for cell and molecular biology as well as *in vivo* imaging since they are very stable and their chromophores form by autocatalytic cyclization without the need for cofactors. Genetic fusion of FP to proteins of interest permits 1:1 expression, facilitating quantitative imaging, particularly for in vitro imaging. There now exists a wide range of optimised and stabilised mutants of this gene emitting blue, cyan or yellow light, as well a number of fluorescent proteins isolated from other sources with orange, red and far-red spectra figure 8.

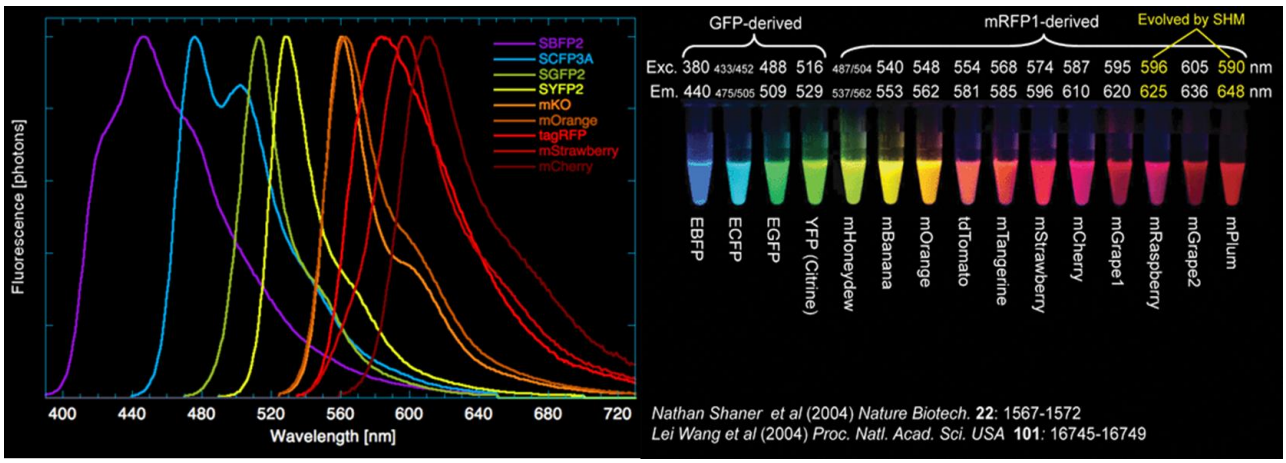

Figure 8. Monomeric or tandem dimeric fluorescent proteins derived from *Aequorea* GFP or *Discosoma* RFP, expressed in bacteria and purified. This photo is a time exposure of fluorescences excited at different wavelengths and viewed through different cut off filters.

All FP are in the region of 25 kD in size. An advantage of the availability of these various FP (which now number more than 20) is that their unique emission wavelengths permit simultaneous imaging of multiple targets in cells and tissues. However, a number of issues have been identified for in vivo

fluorescence imaging. Excitation and emission wavelengths in the green range have limited penetration in mammalian tissues (1–5 mm) (81). Tissues also absorb excitation and fluoresce when excited at these wavelengths (due to tissue chromophores, such as oxy- and deoxy-hemoglobin, water, melanin and fat) Figure 9.

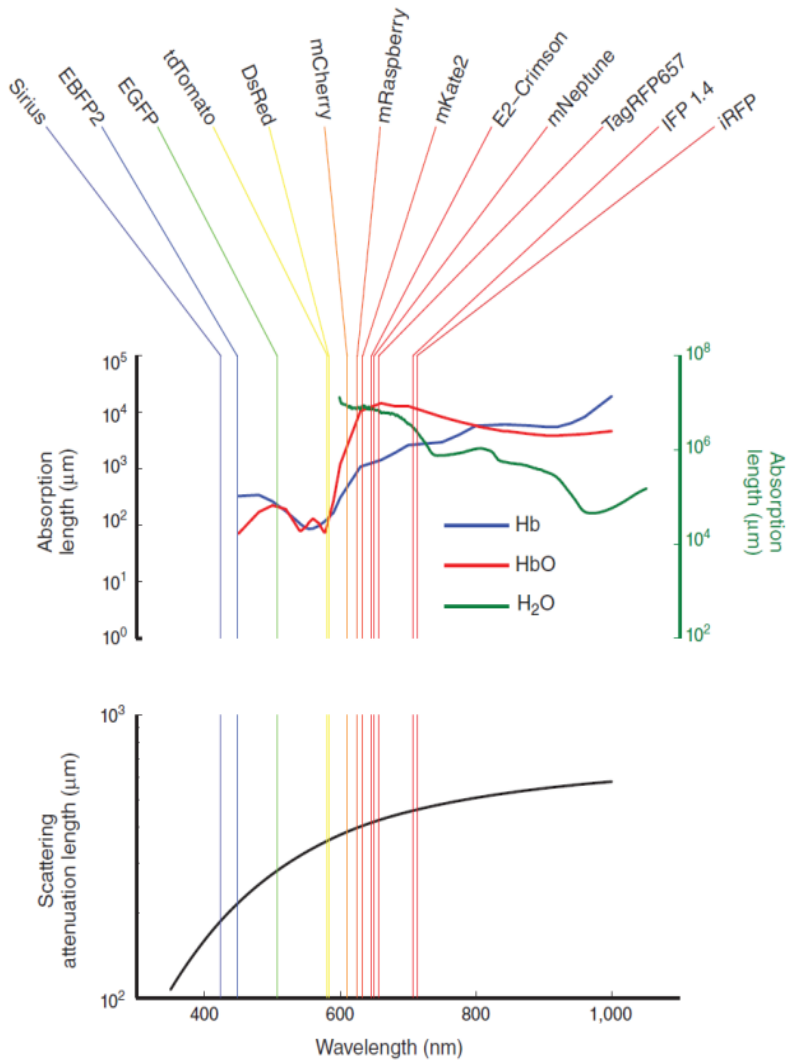

Figure 9. Absorption and scattering lengths are longer for near-infrared compared with visible light. Fluorescence emission peaks for an assortment of fluorescent proteins are shown in the top panel atop plots of the absorption lengths of deoxy-hemoglobin8 (Hb; blue curve, left axis), oxy-hemoglobin8 (HbO; red curve, left axis) and water9 (green curve, right axis). (Note that emission peaks do not necessarily convey a fluorophore's perceived color.) The absorption lengths for hemoglobin were calculated from the molar extinction coefficients assuming a concentration of 2.2 mM hemoglobin, which is representative of human and mouse blood. The bottom panel shows the wavelength dependence of the scattering attenuation length of a tissue sample of human skin (black trace)

Combined autofluorescence and emission signal absorption can result in a poor signal-to noise ratio. Imaging in the near-infrared spectrum increases tissue penetration and decreases non-specific autofluorescence. Longer wavelength such as DsRed isolated from Discosoma striata have been shown to have an advantage over GFP in that red light penetrates tissues

more efficiently than green. Hence, FP in this spectral region are currently the most useful for in vivo imaging, and include the more recent and brighter mCherry and mKate2. Nonetheless, poor signal-to-noise ratio limits usage of FLI in vivo, particularly in deep tissue. Advances in software and instrumentation are yielding improved sensitivity, quantification and spatial resolution. Modern multispectral systems are capable of capturing spectral information of each pixel of an image and with 'spectral unmixing' can separate wavelengths (including from different FP) and help remove autofluorescence. A potentially powerful approach to imaging of deep tissue involves fluorescence-mediated tomography (82). With this technique, the subject is exposed to continuous wave or pulsed light from different sources in an imaging chamber and emitted light captured by detectors arranged in a spatially defined order, followed by software processing to construct a tomographic image. Figure 10.

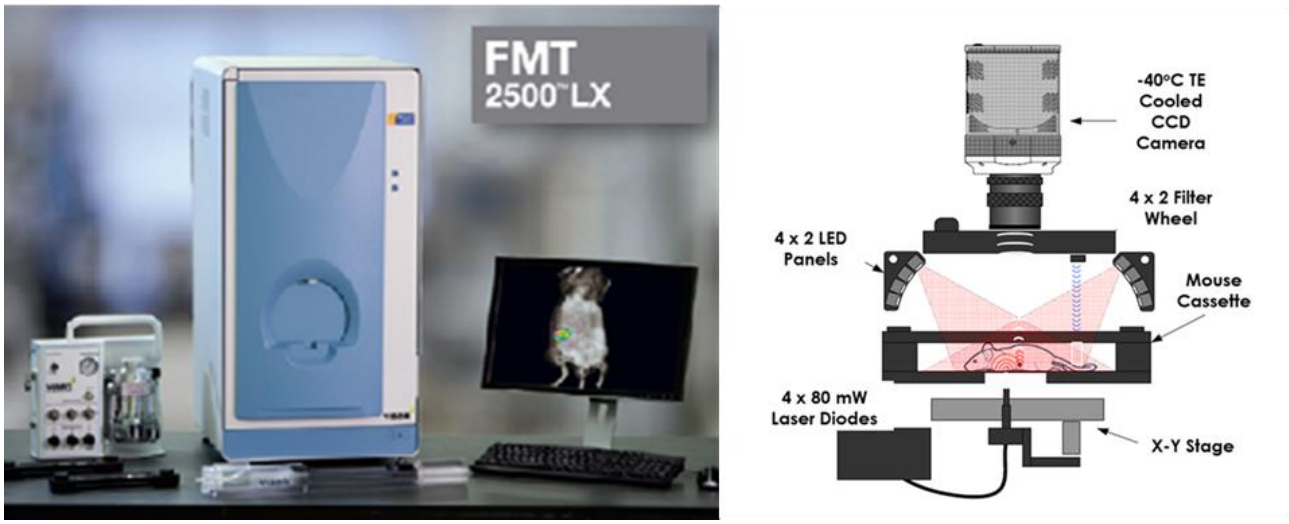

Figure 10. Fluorescent molecular tomography system (FMT) on the left. The FMT® 2000 is a workhorse 3D fluorescence tomographic system with the ability to quantitate up to two fluorophores simultaneously. The system comes with two excitation laser channels (680 and 750 nm). On the right schematic representation of imaging technology. FMT laser-driven transillumination generates paired absorption and fluorescence data maps throughout the animal. The anesthetized mouse is comfortably placed portable Animal Imaging Cassette. Imaging sessions are rapid (2-3 minutes per animal), animal handling is simple and the mouse remains stable and immobilized for consistent, repetitive imaging results. Fluorescence quantified to the picomole at each point in the subject including deep tissue targets and fluorescence measurements calculated throughout the user-selected regions of Interest (ROI).

This strategy is still undergoing development, but studies in a wide range of contexts indicate promise for this (83).

An alternative fluorescent imaging strategy to FP gene delivery involves delivery of a gene coding for a membrane bound antibody, capable of selectively binding a labelled antigen. For example, a membrane-anchored antipolyethylene glycol (anti-PEG) antibody reporter gene system has been developed and demonstrated to efficiently trap a range of pegylated imaging probes for multiple imaging systems including optical, Magnetic Resonance (MR) and PET(84). Furthermore, given the potential benefits of the more recently described quantum dot technology over traditional FP approaches, including reduced photo-bleaching and improved signal-to-noise ratio, exploitation of this approach in combination with cell/gene therapy also holds promise. FLI is also used outside of whole body imaging. For example, Intravital Microscopy refers to in vivo imaging of surface regions (in situ or invasively prepared), primarily to visualise microvasculature in real time at the cell-level (85). Fluorescently-labelled individual cells can be visualised in vivo using this approach. Fluorescence can also be utilised for ex vivo analyses of reporter gene activity, such as secreted alkaline phosphatase (SEAP), similar to the use of Gaussia luciferase.

Despite the limitations described here, in vivo FLI is nonetheless a powerful approach applicable to a wide range of situations and anatomical locations, proving its usefulness at depth penetrations, from micrometres (intravital microscopy) to centimetres (fluorescence molecular tomography) (86).

Fluorescence molecular tomography (FMT) is a technique developed to three-dimensionally visualize deeper into the animal, and it is herein considered as a noninvasive molecular lung imaging tool for small animal imaging. FMT imaging has been a useful tool for imaging *in vivo* protease activities involved in several diseases like cancer, cardiovascular and

osteoporosis and among the enzymes imaged are cathepsins and matrix metalloproteinases (87-88). The fluorescent probes used in detecting the enzymatic activities are generally called “smart probes” or “activatable probes” which emit light changing their optical properties upon protease cleavage (89). (Figure 11) The availability of these probes has made this technique exploitable for studying lung diseases: different researchers including (90-91-92), have used this approach to assess allergic airway inflammation in asthma-induced short-term OVA or LPS mice model. The technology uses multi-projection illumination of the animal thorax and combines multi-projection light measurements from the thorax with mathematical models of photon propagation in tissue in a reconstruction scheme that produces quantitative three-dimensional images of fluorochrome biodistribution. Volumetric visualization and quantification of the fluorochrome

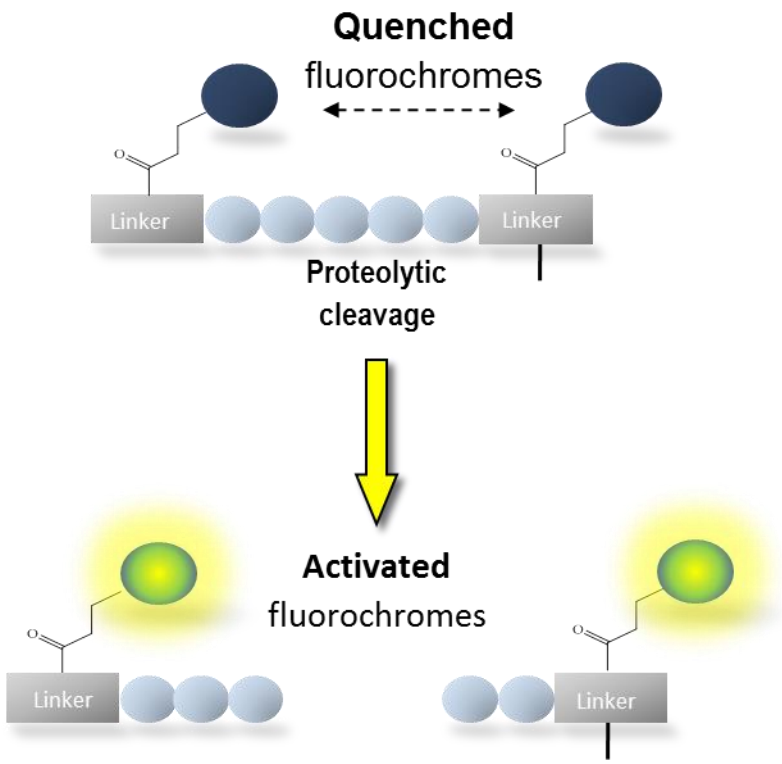

Figure 11. Schematic representation of “smart” activatable probe

in deep tissues; obtained in these studies confirmed and emphasized the role of eosinophil influx associated either with an increased protease activity in the

airway and disease severity. The FMT application to lung imaging is foreseen to play a markedly different role than microscopy, since the method achieves macroscopic resolutions similar to the ones of nuclear imaging. The benefits of FMT are associated with its ability for three-dimensional imaging and importantly the use of physical models of photon propagation that can account for the nonlinear signal variations in tissues as a function of fluorochrome depth and tissue optical properties and optical property heterogeneity (93-94). Therefore FMT can bring a new dimension in lung small animal research by allowing true quantification of optical signals and volumetric in vivo imaging of proteases using activatable probes, of receptors and other proteins by targeted probes or transgenic fluorescent protein gene-reporter technology, and of functional characteristics with more conventional agents tracking vascular changes and permeability. By imaging at different wavelengths, many of these targets may be concurrently resolved. By further using safe, nonionizing radiation, FMT may be well suited to study disease progression and longitudinally characterize drug efficacy.

GOAL OF THE STUDY

Animal Models and Luminescence *vs* Fluorescence

The use of animal models in research it is a crucial step to unravel the effects on the different phases of asthma progression and the mouse has emerged as the specie of choice for modelling this disease. Due to the complexity of asthma, it has become important to establish relevant animal models to better aid in the discovery, for understanding the pathophysiology of asthma and for developing new therapeutic approach. A variety of animal models have been developed that capture specific inflammatory mechanisms of asthma. Researchers using such established mouse models currently rely on invasive measures of pulmonary function and ex vivo characterization of pulmonary cellular infiltration. Although these assessments of disease status areused extensively and highly validated, they are terminal procedures that preclude the possibility of repeated, longitudinal assessment of test subjects.

In contrast, optical *in vivo* imaging technologies of live animals like bioluminescence (BLI) and fluorescence molecular tomography (FMT) provides a tool for non-invasive repeated assessments of *in situ* biological processes, but it is not yet validated as a widespread metric in respiratory arena. Fluorescent protein detection has shown some success at preclinical levels, high background levels and poor tissue penetration of both excitation and emission waves restrict efficacy. Luminescence-based reporting systems display fewer drawbacks and autoluminescence is almost nonexistent. This absence of autoluminescence results in low background light emission permitting much higher sensitivity and specificity than fluorescence in some *in vivo* applications. Keeping in consideration the origin of all the diseases start at molecular level, the application of this technology results to be a very useful in drug discovery, because now a days, the pharmaceuticals are

pushing their research pipeline in targeting specific molecular mechanism. Due to the BLI characteristic listed above, this technology is very suitable for investigating molecular pathways in lung disorders. On the other hand, fluorescent technology, in our specific case FMT has been applied to monitor cellular infiltration to the lung in a chronic asthma mouse model. Smart probes have been used, because they can be direct injected in to the mice and activated by a specific protease secreted from inflammatory cells recruited into the lung by a different pro-inflammatory stimuli. Upon activation the probes emit fluorescent light that can be detected by FMT and associate with the number cellular infiltration and correlated with stage of the disease.

The present study has two goals:

1. **The use of bioluminescent imaging technology to investigate the activation of IL-8 in mouse lung *in vivo* and the role the protein (quale proteina?) in acute pulmonary inflammation by a non invasive approach.**

2. **The generation of a chronic asthma mouse model with established features of asthma in order to test new anti-inflammatory drugs following a therapeutic regimen and to set-up a reliable live-animal imaging method for monitoring with a longitudinal and repeated way the pathophysiologic processes and their biomarkers. In this view, the Fluorescence Molecular Tomography (FMT) technology has been applied to quantify and visualize in a non-invasive way the progression of pulmonary inflammation in chronic asthma.**

MATERIALS AND METHODS: GOAL 1

Experimental Animals

Female inbred FVB (7–8 week-old) mice were purchased from Harlan Laboratories Italy (San Pietro al Natisone, Udine). Animals were maintained under conventional housing conditions. Prior to use, animals were acclimatized for at least 5 days to the local vivarium conditions (room temperature: 20–24°C; relative humidity: 40–70%), having free access to standard rat chow and tap water. All experiments were carried out in rodents and exclusively included painless suppression of animals. All animal experiments were carried out in agreement with the revised "Guide for the Care and Use of Laboratory Animals" (95) and were approved by the Institutional Animal Care and Use Committee at Chiesi Farmaceutici.

Reagents

LPS (E. Coli) was from Sigma (St. Louis, MO); TNF-α (10 ng/ml) (Sigma), JetPEI was from Polyplus-transfection Inc (Euroclone, Milano, Italy).

Vector Characteristic and In Vivo Gene Delivery

bIL-8-Luc was obtained by sub-cloning the 2030 bp IL8 bovine promoter, amplified by PCR from Madin-Darby bovine kidney (MDBK; ATCC #CCL-22) genomic DNA and subcloned into the digested pGL3basic vector (Promega) as previously described (96). We applied in vivo JetPEI (Polyplus Transfection) as a carrier for delivering DNA to lung tissues. The DNA and JetPEI mix was formulated according to the product manual with a final N/P ratio of 7. Briefly, 40 µg of bIL-8–luc or NF-κB-luc and 7 µL of JetPEI were each diluted into 200 µL 5% glucose. The two solutions were then mixed and incubated for 15 minutes at room temperature.The entire mixture was i.v.

injected into FVB mice and the expression of bIL-8–Luc was monitored through imaging with IVIS.

Cell Cultures

Mouse lung adenocarcinoma cell line of epithelial origin, LA-4 cells (ATTC, #CCL-196), was cultured in Dulbecco's modified essential medium (Sigma) containing 10% FBS, 2 mM of L-glutamine, 100 IU/ml of penicillin, 100 µg/ml of streptomycin, and 2.5 µg/ml of amphotericin B (Sigma). Cell culture plates or flasks were incubated at 37°C with 5% CO2 in air, in a humidified atmosphere.

LA-4 Cells Characterization by RT-PCR for TNF-αRI and II and TLRs

Total RNA from LA-4 cells was extracted with TriPure reagent (Roche) and 5 µg of total RNA were reverse transcribed using Ready-To-Go, T-Primed First-Strand Kit (Amersham Biosciences). Two microliters of the resulting cDNA were amplified in a final volume of 50 µl of 10 mM Tris–hydrochloride, pH 8.3, containing 0.2 mM deoxynucleotide triphosphates, 2.5 mM MgCl2, 50 mM KCl, 1 U of Taq polymerase (Invitrogen) and 0.25 µM of each primer listed in Table S1. The amplification program for TNF-αRI, II and GAPDH was 35 cycles, each cycle consisting of denaturation at 94°C for 1 min, primer annealing at 55°C for 1 min, and chain elongation at 72°C for 1 min [33]. The amplification program for TLRs was 35 cycles, each cycle consisting of denaturation at 94°C for 1 min, primer annealing at 55°C for 1 min, and chain elongation at 72°C for 1 min [34]. PCR products were analyzed on a 2% agarose gel.

LA-4 Cell Electroporation

LA-4 cells were cultured in a 75 cm2 flask. When growth reached 90% confluence cells were electroporated. bIL-8-Luc plasmid DNA (20 µg) diluted in 600 µl of DMEM without serum was electroporated (Equibio apparatus Wolf Laboratories Limit., York, UK) into LA-4 cells at 186 V, 960 µF, in 4-mm gap cuvettes (Wolf Laboratories Limit., York, UK)). Electroporated cells were plated in a twenty four-well plates and incubated in an atmosphere of 95% air and 5% CO2 at 37°C.

Dual Luciferase Reporter Assay

Twenty-four hours post electroporation, LA-4 cells in twenty four-well plates were treated with LPS (500 ng/ml) (Sigma) or TNF-α (10 ng/ml) (Sigma) for four hours. The luciferase reporter assay was performed with a Dual Luciferase Reporter Assay System kit (Promega Corp., Madison, WI, USA) according to the manufacturer's specification with minor modifications. Following treatment, cells were washed with PBS and lysed with 100 µl of passive lysis buffer by freeze-thawing at −80°C. Ten microliters of the cell lysate were added to 50 µl of LAR and Luciferase activity was determined with a PerkinElmer Victor3 Multilabel Counter (PerkinElmer, Waltham, MA, USA), according to the manufacturer's specifications. Experiments were performed with 4 replicates at each time point and each experiment repeated three times. Statistical differences were tested by One Way ANOVA followed by Dunnet's post hoc test for group comparisons.

Bronchoalveolar Lavage Fluid (BALF) and Cell Counting

Bronchoalveolar lavage (BAL) was performed as previously described (96). Briefly, mouse tracheas were cannulated with an 18-gauge angiocathether (Becton Dickinson). Six hundred microliters of sterile HANK'S buffer were

instilled three times in the bronchial tree and collected for subsequent analysis. After centrifugation at 400 g for 10 minutes, the cell pellet was resuspended in 0.2 ml of PBS. Total cell number was counted with a particle counter (Dasit XT 1800J). The pellets deriving from the same animal were combined and resuspended in a volume of 0.2 ml and total and differential cell counts were performed within 2 hours using an automated cell counter (Dasit xt 1800 J, Sysmex). The cell count per animal was calculated from the number of cells for 1 ml of BALF multiplied for the volume used for the resuspension of the cell pellet.

In Vivo Bioluminescence Imaging

In vivo imaging was performed using an IVIS imaging system (Caliper Life Sciences, Alameda, CA). From 10 days after DNA delivery the transient transgenic mice were imaged in order to check the baseline activation of the IL-8 pathway. The day after transgenization, the mice were intratracheally challenged with LPS (12.5 µg/mouse) or TNF-α (1 µg/mouse) and the lungs imaged using bioluminescence (BLI) after 2, 4, 7 and 24 hours following intraperitoneal injection of 150 mg/kg luciferin. The mice were anesthetized with gas anaesthesia (isoflurane 2.5%), imaged for 5 minutes, 10 minutes and 15 minutes after luciferin injection in order to minimized the pharmacokinetic variability among mice. Photons emitted from specific regions were quantified using Living Image® software (Caliper Life Sciences, Alameda, CA).

Data Analysis

Experimental values were expressed as the mean and standard error of the mean (SEM). Statistical analysis was performed using one-way analysis of variance followed by Dunnett's t test (* $p < 0.05$, ** $p < 0.01$).

RESULTS: GOAL 1

ACUTE LUNG INFLAMMATION MOUSE MODEL

The Bovine IL-8 Promoter is Responsive in Mouse Lung Cells *in vitro.*

The bovine IL-8 promoter, mapped on Bos taurus chromosome 6 (http://www.ncbi.nlm.nih.gov/mapview/maps.cgitaxid=9913&chr=6&query=uid(207248,3567299)&QSTR=280828%5Bgene%5Fid%5D&maps=gene_set&cmd=focus), was previously cloned from bovine genomic DNA template and its activation at the transcriptional level tested with a luciferase reporter construct bIL-8-Luc. The luciferase construct was generated by sub-cloning the 2030 bp IL-8 promoter in front of a pGL3 Luciferase reporter vector. The capability of mouse cells to trans-activate the bovine IL-8 promoter/luciferase reporter construct (bIL-8-Luc, Figure 12A) was first tested in an in vitro model. The expression of Toll Like receptors (TLRs,) was evaluated by RT-PCR in the LA-4 cell line, a mouse epithelial cell line from lung, TLR 1, 2, 3, 4, 5, 6, 8 and 9 were detectable, while no expression of TLR7 was identified (Figure 12B). Secondly, TNF-α and TNF-α receptor (TNF-αR) I and II were both found expressed in LA-4 cells (Figure 12C). Subsequently, LA-4 cells were transiently transfected by electroporation with the bIL-8-luc reporter construct and 24 h post transfection the cells were treated with TNF-α or LPS. In bIL-8-luc transfected LA-4 cells, a 4 hour treatment with TNF-α increased luciferase signal up to 3 folds, while, similarly, a 4 hour treatment with LPS elicited a 2-fold induction (Figure 12D). Signal intensity was expressed as folds of induction over the bIL-8-luc transfected vehicle-treated LA-4 cells. Results are reported as mean ± SD and significance attributed when $P<0.05$ (*) or $P<0.01$(**)

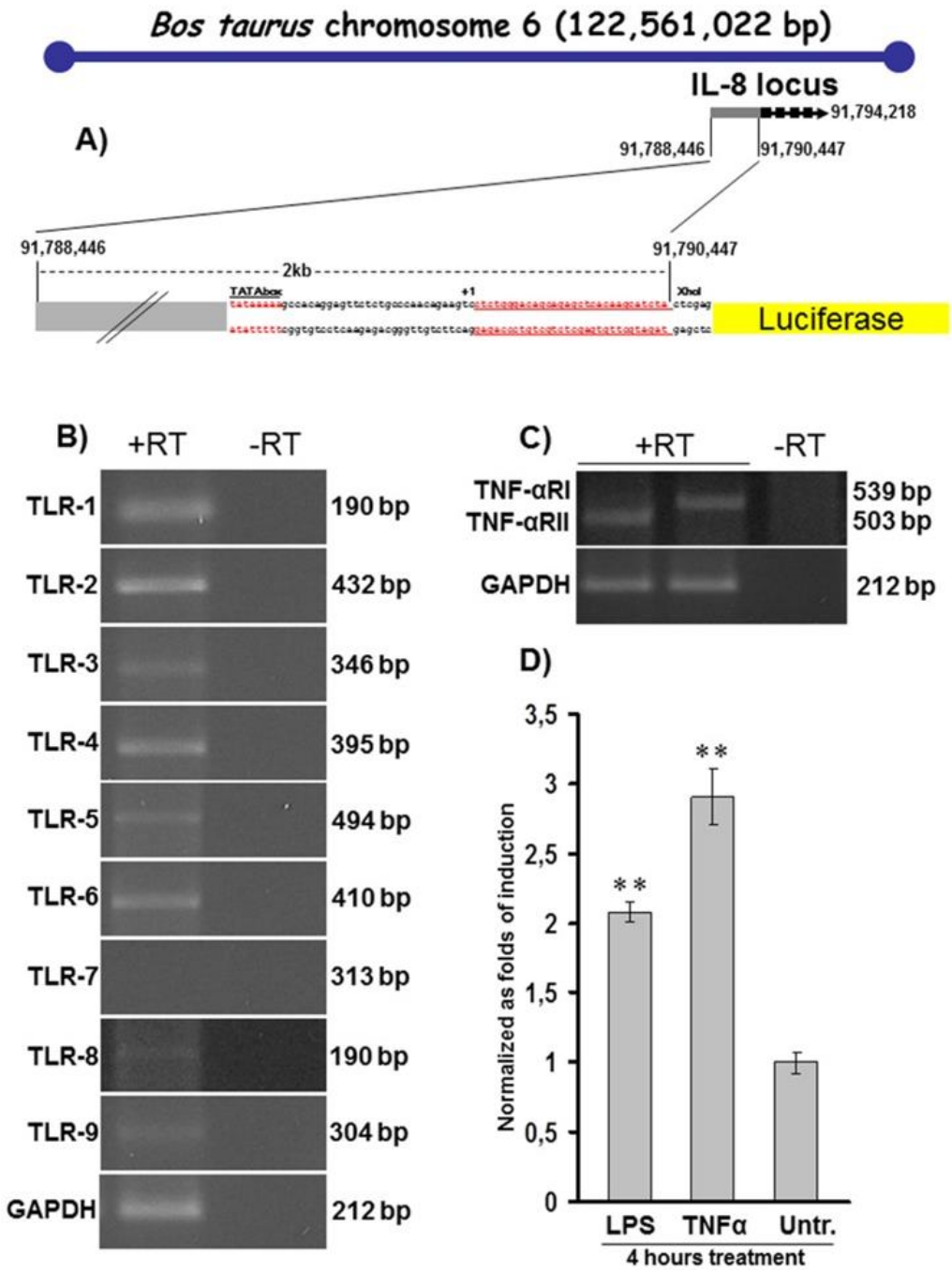

Figure 12. A) Schematic diagram (not to scale) of the Bos taurus chromosome 6 with the IL-8 gene locus comprising promoter and exons annotated by numbers. The 2 kb IL-8 promoter sequence, comprising the putative TATA box, the transcriptional start site (+1) and the UTR (red underlined) was cloned into the pGL3 basic vector in front of the open reading frame of the Luciferase reporter. B) RT-PCR products of TLRs from 1 to 9 and their corresponding amplicon size. GAPDH was used as an internal control and the amplification performed in the absence of reverse transcriptase (-RT) as a negative control. C) RT-PCR products of TNF-αRI,II and their corresponding amplicon size. GAPDH was used as an internal control and the amplification performed in the absence of reverse transcriptase (-RT) as a negative control. D) IL-8 promoter activation after treatment of bIL-8-Luc transfected LA-4 cells with LPS or TNF-α, along with the untreated control (Untr.). Each experiment was done in quadruplicate, and each point represents the mean ± standard deviation of three experiments. Data were expressed as folds of induction (2,1 and 2,8 for LPS and TNF-α respectively) over vehicle-treated cells and statistical differences were tested by One Way ANOVA followed by Dunnet's post hoc test for group comparisons. Results are reported as mean ± SD and significance attributed when $P<0.05$ (*) or $P<0.01$(**).

The Bovine IL-8 Promoter is Responsive in Mouse Lung *in vivo*

Given the positive results obtained in vitro, bIL-8-luc reporter construct was tested in vivo. Mice were first transiently transgenized with bIL-8-luc or the Empty vector control (pGL3 basic) and 10 days post transgenization were intratracheally instilled with LPS or TNF-α. At different time points (3, 5 and 24 hours) post instillation mice were monitored for luciferase expression in the lung by in vivo image analysis. Mice responded to both treatments with a robust induction already at 3 hours after instillation and the response still remained significant after 24 hours. In contrast no signal was observed for control mice treated with saline or transiently transgenized with the Empty vector (Figure 13A and B). Signal intensity was then expressed as folds of induction where the untreated control was considered as 1 (Figure 13C). This in vivo analysis demonstrated the striking specificity of the system and a better induction with a lower background compared to the data obtained in vitro. Results are reported as mean ± SD and significance attributed when $P<0.05$ (*) or $P<0.01$(**)

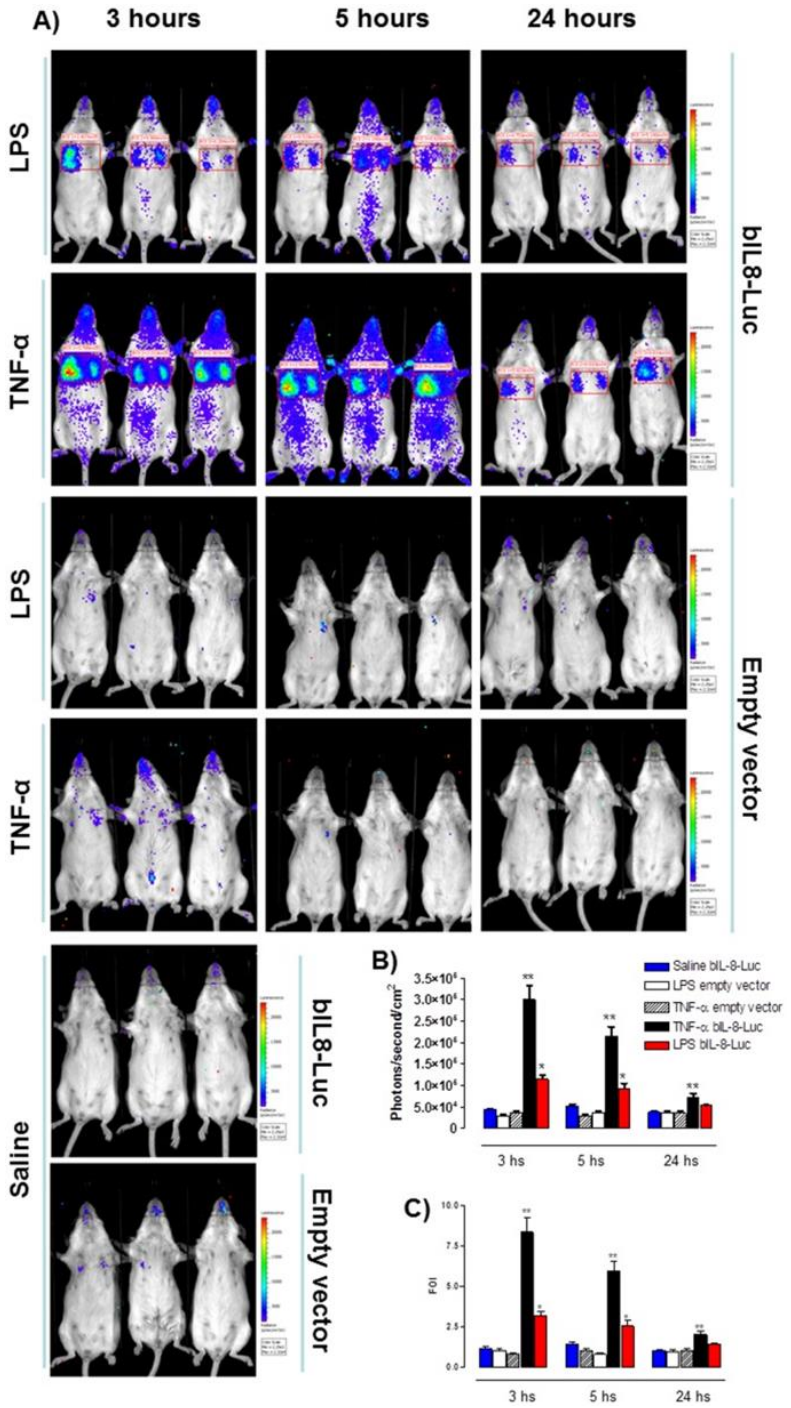

Figure 13. A) Representative images of groups of mice (n=3 per group) transiently transgenized with bIL-8-Luc or Empty vector DNA and intratracheally instilled with LPS, TNF-α or vehicle (saline solution). Mice were monitored at 3, 5 and 24 hours post stimulation by BLI drawing a region of interest (ROI) over the chest. B) Light intensity quantification of the ROI using the LivingImage software. The experiment was repeated three times and each point represents the mean ± standard deviation of 9 animals. C) Data were expressed as folds of induction over vehicle-treated mice (Saline) and statistical differences were tested by One Way ANOVA followed by Dunnet's post hoc test for group comparisons. Results are reported as mean ± SD and significance attributed when P<0.05 (*) or P<0.01(**).

Long Lasting Response of Bovine IL-8 Reporter Gene *in vivo*

Similarly to in vitro transient transfections, the gene delivery system employed in vivo is expected to result in a transient expression of the delivered bIL-8-Luc reporter construct. It was therefore important to assess the extent and the duration in vivo of the responsiveness of the bIL-8-Luc reporter construct. Mice transiently transgenized with bIL-8-Luc or the Empty vector were intratracheally instilled with LPS or TNF-α at 8, 32, 45 and 60 days post transgenization and 3, 5, or 24 h post treatment were monitored for luciferase expression in the lung by in vivo image analysis. Surprisingly, transiently transgenized mice responded to LPS or TNF-α up to 60 days after transfection (Figure 14) with the greater response at 32 days. In contrast, no signal was detectable in mice treated with saline or transiently transgenized with the Empty vector. Results are reported as mean ± SD and significance attributed when $P<0.05$ (*) or $P<0.01$(**). Thus, our data suggest that the same mice can be utilized or reutilized for at least 45 days after the administration of the reporter gene, saving animals and costs. This will offer the opportunity of monitoring every single animal over an extended time period.

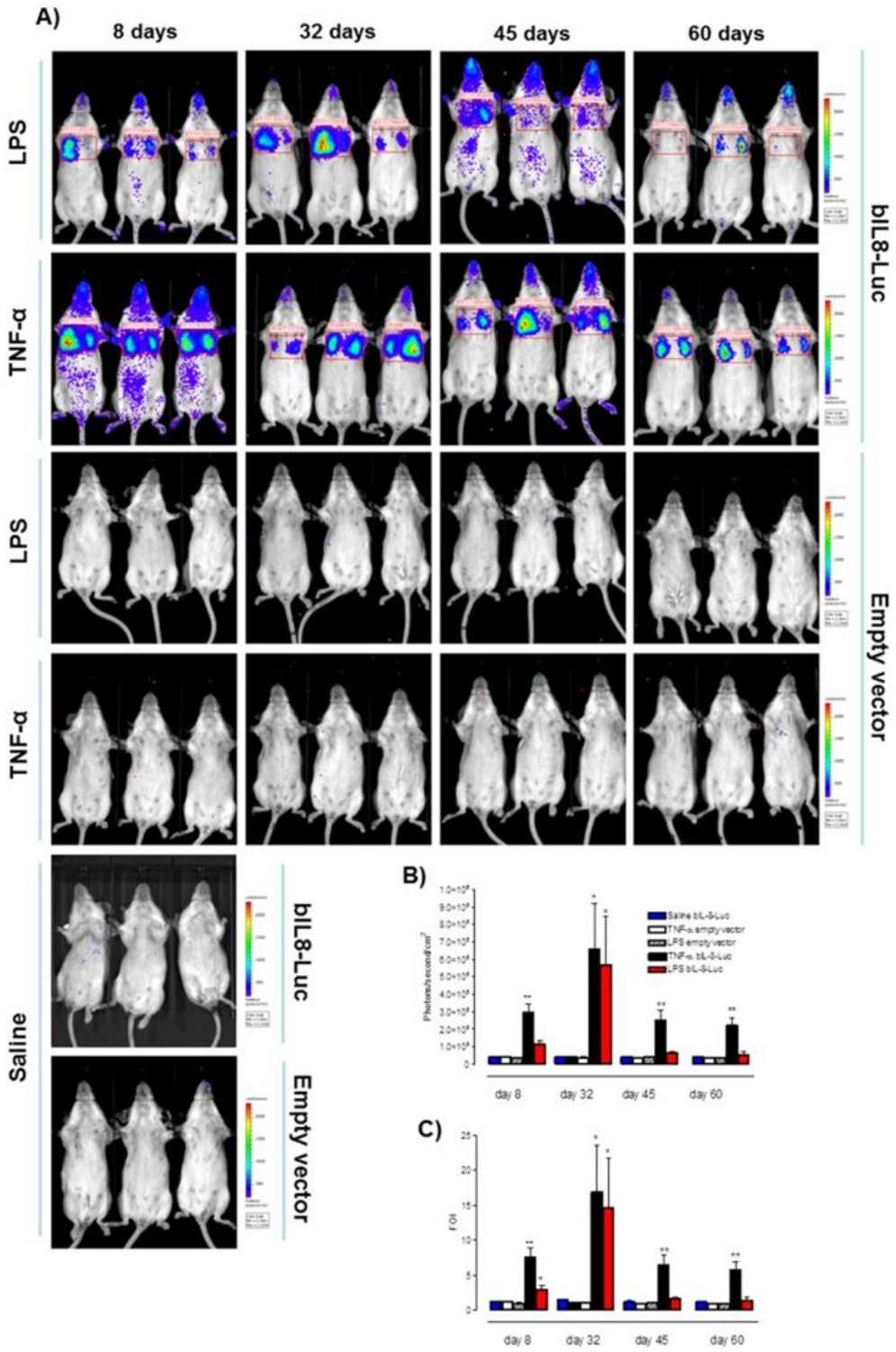

Figure 14. A) Representative images of groups of mice (n=3 per group) transiently transgenized with bIL-8-Luc or Empty vector DNA and intratracheally instilled with LPS, TNF-α or vehicle (saline solution) at 8, 32, 45 and 60 days post transgenization. Mice were monitored at 3 hours post stimulation by BLI by drawing a region of interest (ROI) over the chest. B) Light intensity quantification of the ROI using the LivingImage software. The experiment was repeated three times and each point represents the mean ± standard deviation of 9 animals. C) Data were expressed as folds of induction over vehicle-treated mice (Saline) and statistical differences were tested by One Way ANOVA followed by Dunnet's post hoc test for group comparisons. Results are reported as mean ± SD and significance attributed when P<0.05 (*) or P<0.01(**).

Bovine IL-8 Reporter Gene Response Correlates with White Blood Cells and Neutrophils Infiltration

Since IL-8 is a major chemotactic polypeptide for neutrophils, we examined the correlation between bIL-8-Luc activation and neutrophils infiltration into the lung upon LPS or TNF-α stimulation. Ten days post bIL-8-Luc transient transgenization, the mice were intratracheally instilled with LPS, TNF-α or saline solution. Three hours post treatment, which was the time corresponding to the maximal bIL-8-luc activation and at 24 h post treatment, corresponding to the decline of the signal, the lungs of the treated mice were intratracheally washed and the broncho-alveolar lavage fluid (BALF) was assayed for the presence of infiltrating total white blood cells (WBC) and neutrophils. As shown in figure 15, WBC and neutrophils significantly increased in treated mice with respect to the untreated control, whereas the number of monocytes remained constant, a finding in line with the notion that monocytic infiltration is typically a late event of inflammatory responses. However, in terms of cellular infiltration response, LPS gave a better response than TNF-α. Thus a positive correlation between bIL-8-Luc reporter construct activation and white blood cells and neutrophils infiltration was observed. Results are reported as mean ± SD and significance attributed when $P<0.05$ (*) or $P<0.01$(**).

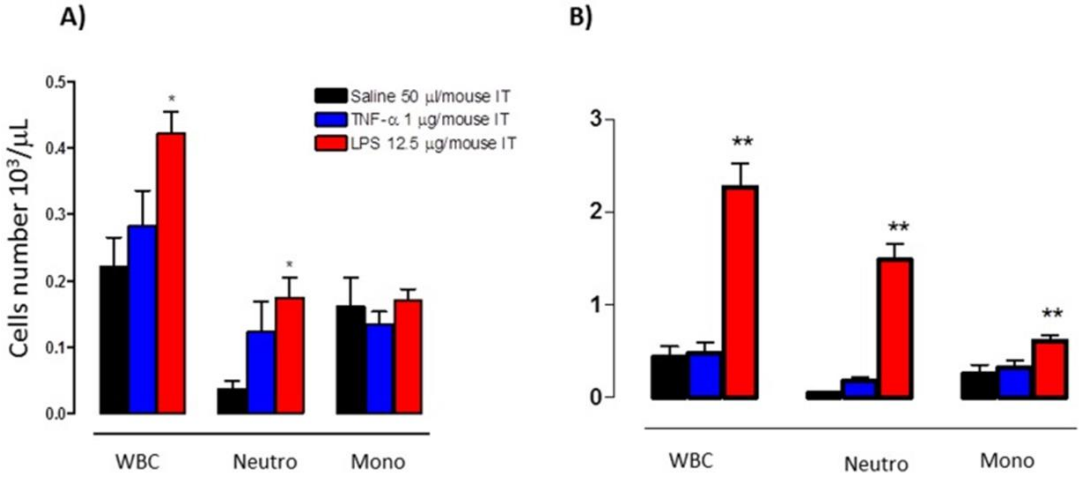

Figure 15. Cellular infiltration into the lung of mice intratracheally instilled with LPS, TNF-α or vehicle. The amount of White blood cells (WBC), Neutrophils (Neut) and Monocytes (Mono) found in BALF was expressed as number of cells per µl at 3 (A) and 24 hours (B) post treatment. The experiment was repeated three times and each point represents the mean ± standard deviation of 9 animals. Data were expressed as folds of induction over vehicle-treated mice (Saline) and statistical differences were tested by One Way ANOVA followed by Dunnet's post hoc test for group comparisons. Results are reported as mean ± SD and significance attributed when $P<0.05$ (*) or $P<0.01$(**).

MATERIALS AND METHODS: GOAL 2

Experimental Animals

Female inbred Balb-C (7–8 week-old) mice were purchased from Harlan Laboratories Italy (San Pietro al Natisone, Udine). Animals were maintained under conventional housing conditions. Prior to use, animals were acclimatized for at least 5 days to the local vivarium conditions (room temperature: 20–24°C; relative humidity: 40–70%), having free access to standard rat chow and tap water. All experiments were carried out in rodents and exclusively included painless suppression of animals. All animal experiments were carried out in agreement with the revised "Guide for the Care and Use of Laboratory Animals" (95) and were approved by the Institutional Animal Care and Use Committee at Chiesi Farmaceutici.

Allergengs

The allergens considered in this study are among those recognized to be crucial in the inception and persistence of asthma:

Dust mite (extracts of Dermatophagoides farinae),

Ragweed (extracts Ambrosia artemisiifolia),

Aspergillus (extracts of Aspergillus fumigatus).

The dose of allergen given per mouse was 0.5 µg of dust mite, 5 µg of ragweed and 0.5 µg of aspergillus.

In vivo imaging Probe

Near infrared (NIR)-activatable “smart” probe (Perkin Elmer, Inc. Boston, MA, USA) was used for imaging protease activities in chronic asthma disease.

ProSense® 680 MMPsense® 680 are protease activatable fluorescent in vivo imaging agent that is activated by key disease associated proteases such as

Cathepsin B, L, S and Plasmin and by matrix metalloproteinases (MMPs) including MMP-2, -3, -9 and -13 . Smart probes are optically silent in their unactivated state and becomes highly fluorescent following protease-mediated activation. The probes are tail vein injected at 80 nmoles/Kg.

Cytokines Analysis

The cell-free supernatant of each sample of BAL fluid stored at -80ºC was used for simultaneous quantification of cytokines and chemokines by using the Bio-Plex™ 200 (Luminex) system (Bio-Rad Laboratories, Segrate, Milano, Italy). BAL fluid supernatants were analyzed by using the 23-Plex panel Mouse Cytokine Assay kit (Bio-Rad Laboratories, Segrate, Milano, Italy).

Asthma Induction Protocol

Mice anesthetized by inhalation of isoflurane (Isoba, Shering Plough) in the vetEquip box (VetEquip - Rodent Circuit Controller Plus Anaesthesia System - RC2+ -; 0.2% of isoflurane and 2l/min oxygen). 30 µl of the three allergens combined suspension, were intra-nasally administered DRA (Dust mite 0.5µg, Ragweed 5µg, Aspergillus fumigatus 0.5µg) twice per week for 8 weeks followed by 3 weeks of rest (no challenge). The control mice were given 30 µl of saline. The experimental set up is shown in figure 16.

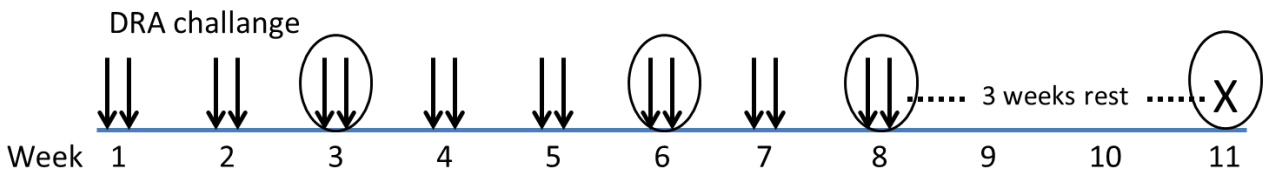

Figure 16. Asthma induction protocol. DRA challenge is represented by black arrow. Challenge lasted till 8 weeks followed by 3 weeks of rest. Circles represent time points selected for the characterization of disease progression. At 3-6-8 and 11 weeks those parameters have been evaluated: FMT, cellular count in BALF, histology and cytokines determination.

In vivo Fluorescence Imaging

Both DRA challenged and control mice were randomly divided in two groups (Saline and DRA. From week 4 on, 24 hours prior to image acquisition and just before the second challenge of the week, a group received 200 µl of 8mg/kg of ProSense 680 or MMPsense680 via tail vein injection. To minimize hair scattering in fluorescent signal, mice thorax and abdomen were completely shaved and depilated. On the day of image acquisition, animals were anesthetized with isoflurane and were properly positioned on a mouse portable imaging cassette (VisEn Medical, Inc. Bedford, MA, USA) which was then placed in the imaging chamber of the FMT 1500 (Fluorescence Molecular Tomography) imaging system (VisEn Medical, Inc. Bedford, MA, USA). The imaging chamber was heated and gas anesthesia maintained (0.2% of isoflurane and 2l/min oxygen).

Through FMT "truequant" software version 2.2 (VisEn Medical, Inc. Bedford, MA, USA), the specific optical filters, for the detection of both exciting and emitting light of the NIR probes used, were set up in the FMT 1500 system. As imaging process began, a NIR diode laser, turned on the excitation wavelength of the fluorochhrome in use, transilluminated the animal's thorax region. The light that propagated through the mouse was then collected by thermoelectrically cooled charge-device (CCD) placed on the opposite side of the imaged animal. Image acquisition lasted from 4 to 5 minutes per animal. The fluorescence data obtained were then reconstituted through specific algorithms by the FMT 1500 system "truequant" software to generate a three-dimensional picture of fluorescence signal which was quantified in picomoles (pM). The quantification of the fluorochromes was relative to internal standards generated with known concentration of the specific NIR dye used.

Histological Analysis

The lungs excided were delicately inflated with 0.6 μl of formalin through a tracheal blunt needle, fixed in 10% neutral formalin and embedded longitudinally. The histological sections (3 μm) were stained with hematoxylin (a basic dye that stains the nuclei of cells in blue) and erythrosine (a food dye with properties similar to eosin that stains cell cytoplasm in pink).

To evaluate Airway Inflammatory Infiltrates (AII) and Airway Epithelial Hyperplasia (AEH) in the lung specimens, seven airways per mouse were taken into consideration. In order to be regarded as suitable for this evaluation, airways needed to be completely intact and entirely contained in a 200X microscopic field. Oblong airways were excluded from the analysis.

AII and AEH, quantified in digitally acquired images analyzed with SIS software (Soft Imaging System GmbH), were measured as the area of inflammatory infiltrates and area of epithelium (in square micrometers) divided by the airway's basement membrane perimeter (in micrometers).

In detail, airway measurements included the perimeter of the basal membrane of the epithelium (AP), the area of the region circumscribed by the basal membrane (AA), the area of the lumen (AL) and the area covered by inflammatory infiltrates (AII). AEH score, corresponding to (AA – AL) / AP and AII score corresponding to AII/AP was calculated for each airway. A mouse mean score and a mean total score for each group of mice were then calculated.

Data Analysis

Experimental values were expressed as the mean and standard error of the mean (SEM). Statistical analysis was performed using one-way analysis of variance followed by Dunnett's t test (* $p < 0.05$, ** $p < 0.01$).

RESULTS: GOAL 2

CHRONIC ASTHMA MOUSE MODEL

In Vivo DRA -Induced Eosinophilia

An increase in white blood cells (WBC) was observed in BALFs of DRA-exposed animals starting from the first time-point at week 3 and picking up to week 8 figure 16 a. Three weeks after the last allergen sensitization (week 11), the WBC infiltration decreased in the DRA mice remain 2.5 fold higher compare to the saline group. The same disease progression has been confirmed by histological analysis, figure 17. Among the inflammatory cells infiltrating the airways of DRA mice, eosinophils were the predominant population figure 16 b. In fact, the eosinophil infiltration was robust during the time points 3,6,8 weeks ($p<0.01$ vs saline control). At week 11, the eosinophil count in BALF decreased to a very low level, but still higher than the saline ($p<0.05$ vs saline control). The infiltration of lymphocytes was moderate but significant in DRA mice at the considered weeks 3,6,8 weeks ($p<0.01$ vs saline control), whereas the neutrophil counts were lower showing ($p<0.05$ vs saline control) only at week 3. On the other hand, control mice (saline-sensitized) showed a very low influx of white blood cells in their lungs, with a predominance of macrophages, including pulmonary resident monocytes, data not shown. The lung tissue from DRA-challenged mice went through marked structural changes at both week 6 and 8 which persisted at a lower degree at week 11, as it can been seen in figure 17. After 6 and 8 weeks of DRA sensitization, mice showed a severe airway inflammation characterized by cellular infiltrates figure 18 a, airway epithelial hyperplasia accompanied by a thickening of bronchial airways which appeared moderate at week 6 increasing markedly at week 8. Epithelial changes persisted at week 11 decreasing to the level observed at week 6, figure 18 b.

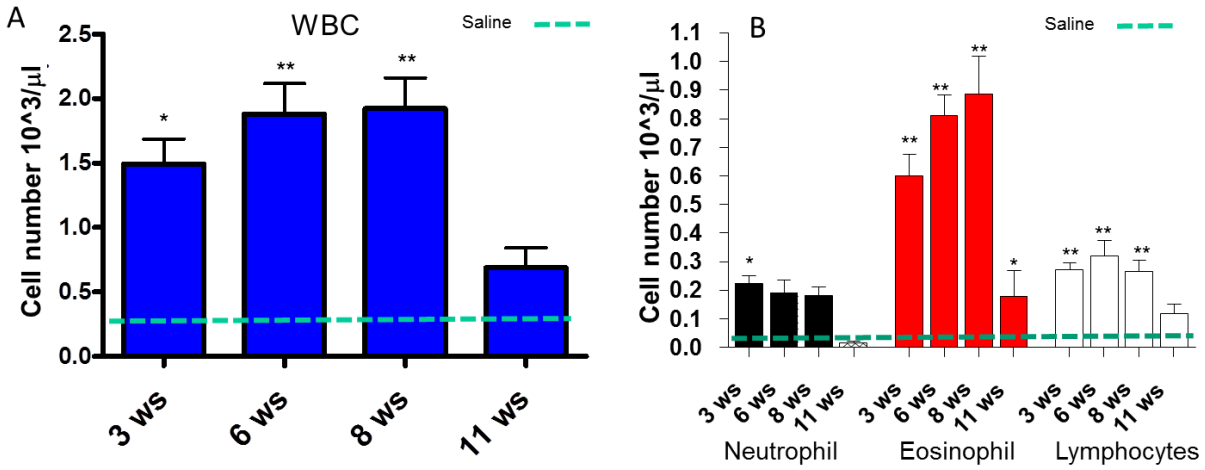

Figure 16. Analysis of DRA-induced inflammatory cells in BAL fluids. The BAL cells analysis was conducted at 3, 6, and 8 weeks of DRA challenge, and at 11 weeks (3 weeks after the last DRA exposure). At every time points animals were sacrificed 24h after the second sensitization per week and just a few minutes after imaging acquisition. One Way ANOVA followed by Dunnet's post hoc test for group comparisons. Results are reported as mean ± SEM and significance attributed when P<0.05 (*) or P<0.01(**).

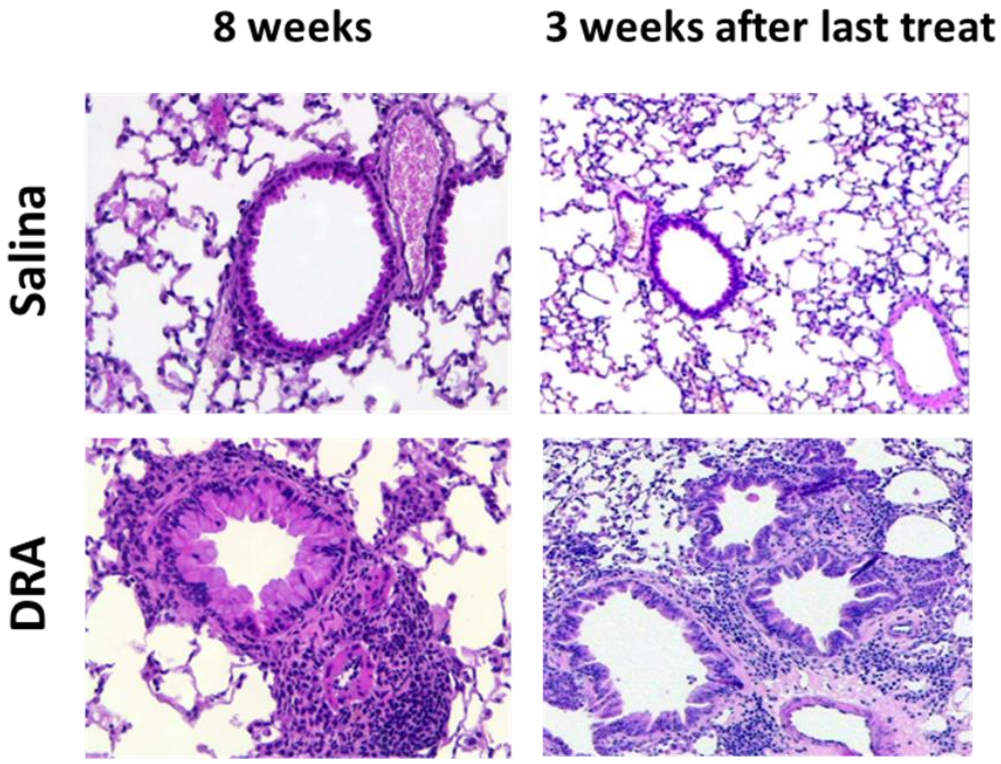

Figure 17. Histology time course: Representation of lung sections, at 8 and 11 weeks, of saline and DRA challenged group. Hematoxilin/erythrosin-stained examined by light microscopy.

DRA sensitization was proved to increase the levels of pro-inflammatory mediators such as IL-5, IL-4, KC, IL-17, RANTES and IL-12(p40) in the lungs of mice. The increase of these cytokines are in agreement with the cellular phenotype found in BAL fluid.

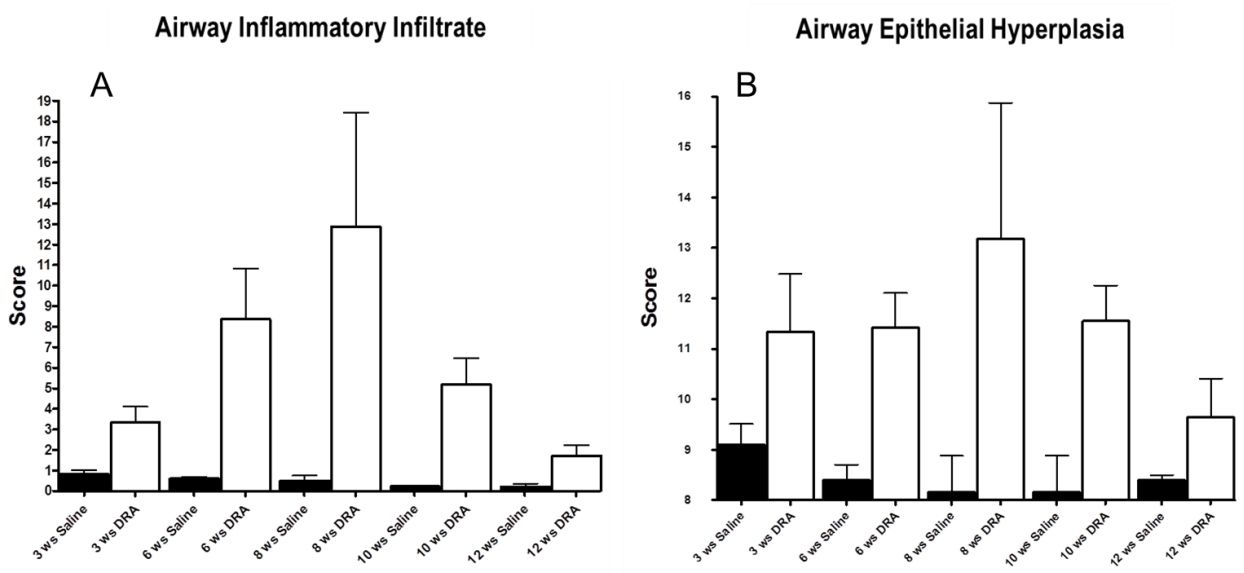

Figure 18. Histological findings of Airway Inflammatory Infiltrate and Airway Epithelial Hyperplasia were scored at 3 6-8-10 and 12 weeks. The time course of histological evaluation was in agreement with cellular infiltration in BALF. (n=6 animals/time point)

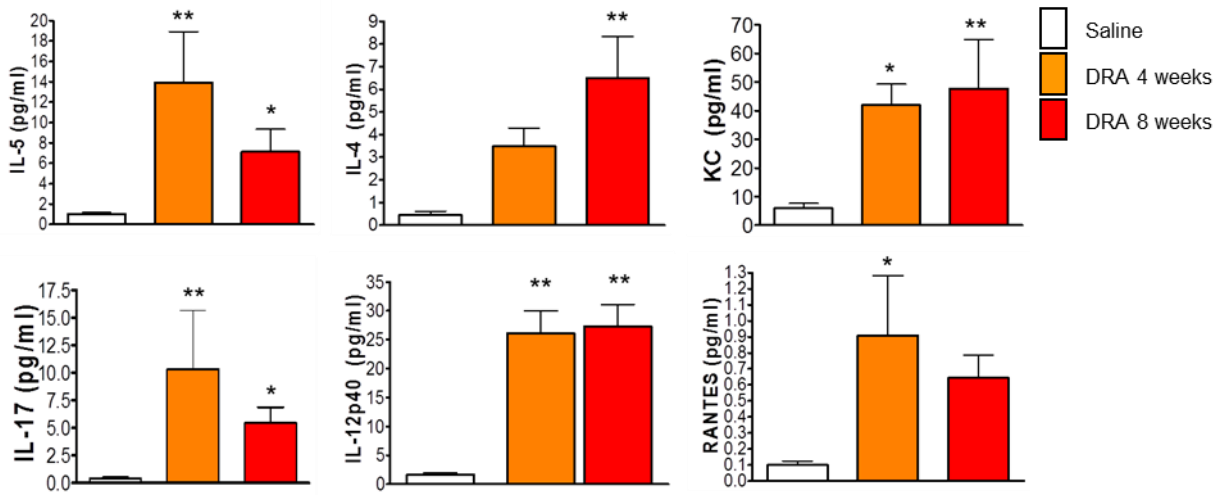

Figure 19. Analysis of DRA-induced pro-inflammatory mediators in BAL fluids. Pro-inflammatory mediators were measured with Bio-Plex assay system. Animals were sacrificed 24h after the second sensitization at week 8 and just after image acquisition. One Way ANOVA followed by Dunnet's post hoc test for group comparisons. Results are reported as mean ± SEM and significance attributed when P<0.05 (*) or P<0.01(**).

CHRONIC ASTHMA MOUSE MODEL

In Vivo Fluorescent Molecular Tomography Imaging

DRA-challenged mice and control mice were administered cathepsins (CTS) and metalloproteinases (MMPs) specific detector probes: ProSense 680 and MMPSense 680. The florescent light observed derives from the activation of the probes (optically silenced) as they contact their molecular targets, CTS and MMPs secreted by inflammatory cells (eosinophils, macrophages and epithelial cells). Here we imaged the activity of these proteases within the lung region of the mice, by selecting the region of interest (ROI) delimitated by the purple boxes as it can be seen in figure 20 c and figure 21 c.

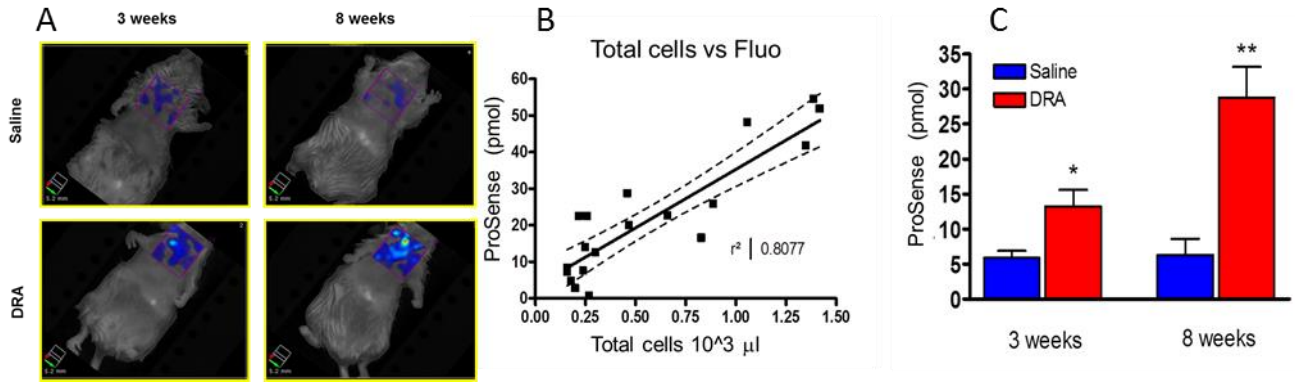

Figure 20. A) Representative images of same saline and DRA mice at 3 and 8 week treated with ProSense680. B) Correlation between WBC and fluorescence signal .C) Quantification of the fluorescent signal in pmoles in the ROI designed.

The ROIs are presented in a three-dimensional form that allows the localization of the enzymatic activities and their spread through lung tissue: from the surface into the deep inner part of lung tissue.

FMT *in vivo* imaging of mice thorax revealed high levels of fluorescent signal in the DRA-challenged animals compared to the control animal figure 20 c treated with ProSense. Cellular infiltrates in BAL fluid was plotted against ProSense fluorescent signal that showed a positive correlation with the total number of WBC present in BAL fluids, figure 20 b.

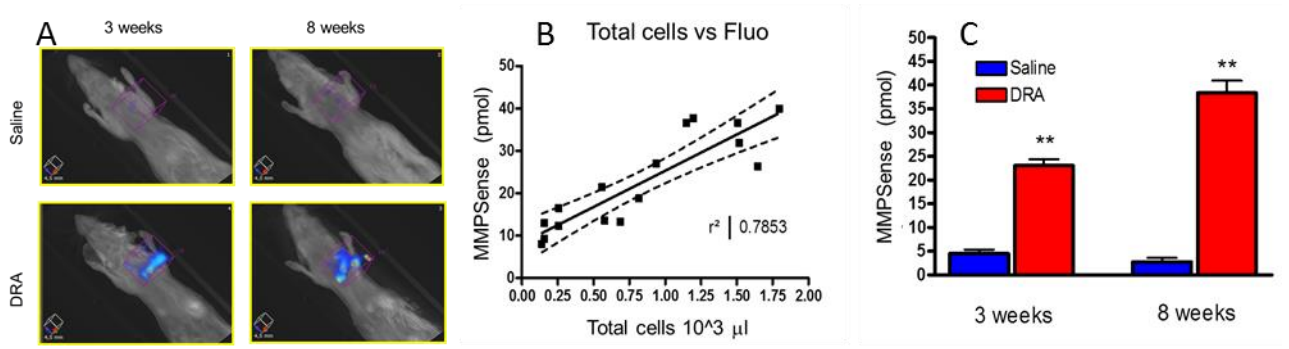

Figure 21. A) Representative images of same saline and DRA mice at 3 and 8 week treated with MMPSense680. B) Correlation between WBC and fluorescence signal .C) Quantification of the fluorescent signal in pmoles in the ROI designed.

In vivo imaging of the activity of MMPs in DRA-sensitized mice showed a good signal at 3 and 8 week figure 20 c and again a good correlation, figure 20 c has been found. This experiment suggested that, both probes can be used for evaluating chronic asthma progression in mouse, even if all the classical analysis such as histology, cellular phonotype need to be done.

DISCUSSION

A hallmark of tissue inflammation following chemical, physical or microbiological insults is the recruitment of white blood cells to the injured tissue, which is orchestrated by chemotactic polypeptides named chemokines, among which IL-8 is one of the most remarkable. A significant correlation between IL-8 levels and neutrophil infiltration in diseases has been reported. IL-8 is an essential factor for acute inflammation and induces the infiltration of T lymphocytes into inflamed tissue. Recent studies have also demonstrated that IL-8 is involved in non-inflammatory reactions like angiogenesis (97). In addition, systemic administration of IL-8 rapidly induces migration of hematopoietic stem cells from bone marrow to peripheral blood (98). These results suggest that IL-8 also regulates non-inflammatory physiological reactions in vivo.

IL-8 transcriptional activation is closely correlated with the initiation of acute inflammatory responses and thus is an ideal indirect read-out for monitoring the activation of inflammatory pathways targeting IL-8 expression. IL-8 homologs in many species have been cloned, including human (99), macaque (100), Sooty mangabey (101), bovine (102), sheep (103), pig (104), dog (105), rabbit (106), Guinea pig (107) and chicken (108); however, a homolog of IL-8 has not been described in small rodents, including mice. In this study we developed a useful murine model for monitoring IL-8 expression in vivo. To this aim the bovine IL-8 promoter was chosen for two main reasons. First, lung inflammation-associated diseases in ruminants are very important in terms of economic loss for the beef meat industry; according to a report of the Committee for Animal Health Research Programs, major disease-related losses attributed to respiratory infections were calculated to be ~400 million Euros per year; therefore the creation of an innovative in vivo platform for testing new respiratory anti-inflammatory drugs targeting specific

pathways, such as IL-8, would be highly desirable. Second, all the information obtained on IL-8 bovinized mice can be easily employed for the human lung inflammation associated diseases, due to the high similarity existing between respiratory diseases in ruminants and human.

Although the minimal responsive sequence for the bovine IL-8 promoter is represented by the first 200 bp starting from the putative transcriptional initiation site, a 2 kb large version of the promoter was utilized (96) in order to include most of the potentially relevant binding sites for transcription factors. Moreover, recently two IL-8 promoter haplotypes have been characterized: the type 1, less sensitive to LPS and TNF-α and the type 2 with higher sensitivity to LPS and TNF-α (109).

Because IL-8 was previously shown to be expressed by a human epithelial cell line derived from lung after specific stimuli (110), the bIL-8 reporter construct was initially tested in vitro in a mouse lung epithelial cell line, LA-4, which expresses TLRs and TNF-αRs. Although mice and rats do not have IL-8 gene, bovine IL-8 promoter/luciferase reporter construct was expressed at detectable levels in transfected LA-4 cells and was significantly induced upon treatment with LPS or TNF-α. This simple but extremely informative experiment demonstrates that mouse cells have the transcriptional machinery for transactivating a heterologous IL-8 promoter/luciferase reporter construct.

To functionally test the IL-8 promoter/luciferase reporter construct in mice, an in vivo bioluminescent imaging (BLI) approach was exploited. BLI is a sensitive tool that is based on the detection of light emission from cells or tissues (111). The utility of reporter gene technology makes it possible to analyze specific cellular and biological processes in a living animal through in vivo imaging methods. Bioluminescence from luciferase gene expression, as is the case of the reporter construct employed during this study, is the most widely used. Because mammalian tissues do not naturally emit

bioluminescence, in vivo BLI has considerable appeal because images can be generated with absence of background signal. BLI requires an expression cassette consisting of the bioluminescence reporter gene (in this case was luciferase) under the control of a selected promoter (in this experimental setting a bovine IL-8 gene promoter) driving the reporter. In order to induce light production, the substrate luciferin must be provided by intravascular or intraperitoneal injection.

Furthermore, a more robust fold-induction in response to LPS or TNF-α was obtained in the lung of bIL-8-luc DNA injected. Noteworthy, bIL-8-luc transiently transgenized mice could be stimulated with LPS or TNF-α up to 60 days. Thus, the capability to monitor a biological process longitudinally in the same mouse represents an obvious advance for functional as well as pharmacological studies. The correlation between WBC and neutrophils infiltration and luciferase expression following LPS or TNF-α stimulation is in accordance with the recognized IL-8 role as a key factor in orchestrating inflammation, thus further validating the association between IL-8 transcriptional activation and pulmonary inflammation in the experimental setting that we here adopted. Although a bovine promoter was used in this study as a proof of concept, the results of the study suggest that IL-8 promoter regions derived from other species, including primates, could also be utilized in this experimental setting.

IL-8 exerts a wide variety of actions on pulmonary disease pathophysiology in ruminants and human during bacterial or viral infection, acute respiratory distress syndrome (ARDS), reperfusion injury and transplantation, lung injuries due to physical and chemical conditions, allergic inflammation and asthma, idiopathic pulmonary fibrosis and other diffuse lung diseases, including lung cancer (112-113). The absence of IL-8 and its receptor orthologs in small rodents hindered the possibility of testing novel strategies

targeting IL-8 using mice as a convenient small size experimental animal model. We filled the gap by generating a mouse model transiently expressing a reporter gene under the control of an IL-8 promoter which is suitable to functionally study IL-8 promoter in a convenient small size experimental animal model.

The other part of thesis, we therefore focus on:

1) set-up of a model of chronic asthma, where animals were exposed intranasally to a combination of 3 natural allergens (dust mite, ragweed and aspergillus: DRA) for 8 weeks, twice a week, followed by a 3-4 week rest period.

2) access to disease progression in non-invasive way using fluorescent molecular tomography

Asthma is an example of a “complex disease,” a term that has become popular for characterizing those pathologies that appear to have multifaceted etiologies and an entanglement of underlying mechanisms. Asthma is a chronic inflammatory disease of the airways characterized by a T cell-driven eosinophil and mast cell inflammation that leads to intermittent, reversible airway obstruction. Not surprisingly, allergy heads the list of causative suspects, but it is by no means alone. As with most human diseases, studies in laboratory animals have produced much of what we currently think we know about the mechanisms responsible for asthma. Obviously, the relevance and validity of these studies are tied to how well we can produce accurate animal equivalents of human asthma. The development of such “animal models” is still very much a work in progress; although many of the various features of asthma have been convincingly recapitulated in animals, invariably every animal model misses some important aspect of the human syndrome. Accordingly, much of the challenge in studying animal models of

asthma lies in phenotyping them properly, particularly as asthma is defined in humans in terms of phenotype rather than underlying pathology.

In a recent paper by Goplen (114) it was reported that chronic exposure to multiple allergens(extracts of dust mite, ragweed, and aspergillus species), leads to the development of chronic asthma. DRA model could represent a step forward in asthma modelling because it can be used to test therapeutic agents without performing a de novo allergen challenge once the chronic inflammation is established. We decided to set-up a DRA mouse model because the experimental models have been developed so far, did not reproduce specific mechanisms of human asthma. These models are useful for the investigation of immunological mechanisms and of cellular recruitment but fail to reproduce most of the morphological and functional features of the human disease. An additional drawback of these models has been the transient nature of the airway pathology that peaks 24 to 72 hours after challenge with the antigen and resolves in 1 to 2 weeks. It is thus a common practice in preclinical drug development to pre-treat animals with a therapeutic agent before an allergen challenge and then study the outcome: this represents a simplistic approach, since in human chronic asthma a preventive treatment is unrealistic. Modelling chronic asthma in mice is problematic since repeated exposure to a single antigen can down-regulate the inflammation, greatly limiting usefulness of these experimental systems. Therefore, more realistic model of asthma are needed for the investigation of the pathophysiology of the disease and for the identification of novel therapeutic agents. Another limitation is due to the conventional assessments of asthma that currently relies on invasive measures of pulmonary function and ex vivo characterization of pulmonary cellular infiltration. Although these assessments of disease status are used extensively and highly validated, they are terminal procedures that preclude the possibility of repeated,

longitudinal assessment of test subjects. The ability to noninvasively visualize and quantify the underlying biological processes in mouse pulmonary models in vivo would provide a significant advance in characterizing disease processes and the effects of therapeutics.

Our results confirm that multiple allergen exposure breaks tolerance and induces an airway pathology that persists long after the allergen exposure.

DRA administration led to reactive changes consisting of inflammation and epithelial hyperplasia reaching a maximum score at week 8 that persisted till week 11 in treated animals after a rest period of three weeks, even if with a lower degree of severity.

In particular, we observed an increase in airway inflammation and epithelial hyperplasia at morphometric analysis, increased number of inflammatory cells as lymphocytes and eosinophils.

Access to asthma progression with fluorescent molecular tomography in non–invasive way showed a good correlation between ProSense and MMPsense fluorescent signal and cellular infiltration, this data suggesting that cathepsin and metalloproteases activation could be a good read-out for measuring the disease progression.

Our study demonstrated the utility of quantitative fluorescence tomography, paired with a proteases-activatable imaging agent to quickly, noninvasively, and accurately measure the severity of pulmonary cellular infiltration in mice.

In conclusion we developed a chronic asthma model characterized by an eight-week, twice a week, intranasal challenge of triple allergens (DRA) in female Balb/C mice. This model reproduces some features of human chronic asthma consisting of inflammation and epithelial hyperplasia that persists after allergen withdrawal. Moreover, we have demonstrated the ability of the FMT imaging to noninvasively visualize and quantify inflammation in the lung in a robust and consistent manner. The consistency of the quantitative

tomography and its excellent correlation with BAL assessment and histology provides a powerful tool for monitoring the disease and probably quantifying the effect of therapeutic interventions. The DRA mouse model and FMT technology are good example where many expertise has to work together in order to understand the complexity of asthma. DRA reproduces many of the feature of the human disease, and it could represent a valuable tool for drug discovery approach, mimic what is real happen in the clinic. In the next future we intend to go deeper in understanding the DRA model using FMT technology to screen the mice before entering in the experiments in order to redefine the treated group in more precise manner, less mice used, less variability, each mouse will be the control of itself and the evaluation will be based on individual analysis. Moreover we intend to apply DRA model and FMT for evaluating pharmacological responses in longitudinal studies, where test subjects could be monitored before during and after the pharmacological intervention. Non-invasive technology are unique tool for monitoring molecular events and the disease progression in chronic asthma models and acute lung injury.

The fusion between BLI and FMT is one of next step of our research commitment as well, by using the same mice previously transgenized with a specific plasmid DNA and after challenged with DRA. BLI will be used to look at the pathology at molecular level and FMT to stage the disease progression in the same mice.

This new insight open up a new door in preclinical research where a specific molecular events and the consequence of it will be monitor in the latter stage of the disease in the same mouse longitudinally and science will make a step further.

We keep working hard in the field and we strongly believe that the way will be very long, but we know that is the right path to follow.

REFERENCES

1) World Health Organisation, 2008a

2) World Health Organisation, 2008b

3) Brusasco V, Pellegrino R. Complexity of factors modulating airway narrowing in vivo: relevance to assessment of airway hyperresponsiveness. *J Appl Physiol*. 2003. 95(3):1305-13.

4) Expert Panel Report 3 (EPR-3): Guidelines for the Diagnosis and Management of Asthma-Summary Report 2007. National Asthma Education and Prevention Program. *J Allergy Clin Immunol*. 2008. 121(6):1330.

5) Haldar P, Pavord ID, Shaw DE, Berry MA, Thomas M, Brightling CE, Wardlaw AJ, Green RH. Cluster analysis and clinical asthma phenotypes. *Am J Respir Crit Care Med*. 2008. 1;178(3):218-24.

6) Wenzel SE. Asthma: defining of the persistent adult phenotypes. *Lancet*. 2006. 26;368(9537):804-13.

7) Zosky GR, Larcombe AN, White OJ, Burchell JT, Janosi TZ, Hantos Z, Holt PG, Sly PD, Turner DJ. Ovalbumin-sensitized mice are good models for airway hyperresponsiveness but not acute physiological responses to allergen inhalation. *Clin Exp Allergy*. 2008. 38(5):829-38.

8) Padrid P, Snook S, Finucane T, Shiue P, Cozzi P, Solway J, Leff AR. Persistent airway hyperresponsiveness and histologic alterations after chronic antigen challenge in cats. *Am J Respir Crit Care Med,* 1995.151: 184–193.

9) Couetil LL, Hoffman AM, Hodgson J, Buechner-Maxwell V, Viel L, Wood JL, Lavoie JP. Inflammatory airway disease of horses. *J Vet Int Med/Am Coll Vet Int Med* 2007. 21: 356–361.

10) From the Global Strategy for Asthma Management and Prevention, Global Initiative for Asthma (GINA) 2011. Available from: http://www.ginasthma.org/.

11) Kim H, Mazza J. Asthma. *Allergy Asthma Clin Immunol*. 2011. 10;7 Suppl 1:S2.
12) From the Global Strategy for the Diagnosis and Management of Asthma in Children 5 Years and Younger, Global Initiative for Asthma (GINA) 2009. Available from: http://www.ginasthma.org/.

13) Baxi SN, Phipatanakul W. The role of allergen exposure and avoidance in asthma. *Adolesc Med State Art Rev*. 2010. 21(1):57-71
14) O'byrne PM, Postma DS. The many faces of airway inflammation. Asthma and chronic obstructive pulmonary disease. Asthma Research Group. *Am J Respir Crit Care Med*. 1999. 159(5 Pt 2):S41-63.
15) Lemanske RF Jr, Busse WW. Asthma: clinical expression and molecular mechanisms. *J Allergy Clin Immunol*. 2010. 125(2 Suppl 2):S95-102.
16) Vercelli D. Discovering susceptibility genes for asthma and allergy. *Nat Rev Immunol.* 2008. 8(3):169-82
17) Kumar A. and Ghosh B. Genetics of asthma: a molecular biologist perspective. *Clinical and Molecular Allergy*. 2009. 7: 7.
18) Shin Y.S., Takeda K. and Gelfand E.W. Understanding asthma using animal models. *Allergy Asthma Immunol Res*. 2009.1: 10-18.
19) Pillai P, Corrigan CJ, Ying S. Airway epithelium in atopic and nonatopic asthma: similarities and differences. *ISRN Allergy*. 2011. 195846
20) Madore AM, Laprise C. Immunological and genetic aspects of asthma and allergy. *J Asthma Allergy*. 2010, 3:107-21.
21) Durrani SR, Viswanathan RK, Busse WW. What effect does asthma treatment have on airway remodeling? Current perspectives. *J Allergy Clin Immunol*. 2011. 128(3):439-48.

22) Nakawah MO, Hawkins C, Barbandi F. Asthma, Chronic Obstructive Pulmonary Disease (COPD), and the Overlap Syndrome. *J Am Board Fam Med*. 2013. 26(4):470-7.

23) Shum BO, Rolph MS, Sewell WA. Mechanisms in allergic airway inflammation - lessons from studies in the mouse. *Expert Rev Mol Med.* 2008. 10:e15.

24) Sohal SS, Ward C, Danial W, Wood-Baker R, Walters EH. Recent advances in understanding inflammation and remodeling in the airways in chronic obstructive pulmonary disease. *Expert Rev Respir Med*. 2013. 7(3):275-88.

25) Girodet PO, Ozier A, Bara I, Tunon de Lara JM, Marthan R, Berger P Airway remodeling in asthma: new mechanisms and potential for pharmacological intervention. *Pharmacol Ther*. 2011. 130(3):325-37

26) J. Kelley Bentley and Marc B. Hershenson "Airway Smooth Muscle Growth in Asthma", *Proceedings of the American Thoracic Society*. 2008. 5,(1): 89-96.

27) Ankathatti Munegowda M, Xu S, Freywald A, Xiang J. CD4+ Th2 cells function alike effector Tr1 and Th1 cells through the deletion of a single cytokine IL-6 and IL-10 gene. *Molecular immunology*. 2012. 143-9.

28) Balzar S, Chu HW, Silkoff P, Cundall M, Trudeau JB, Strand M, Wenzel S. Increased TGF-beta2 in severe asthma with eosinophilia. *J Allergy Clin Immunol*. 2005. 115(1):110-7.

29) Rutgers SR, Timens W, Kaufmann HF, van der Mark TW, Koëter GH, Postma DS. Comparison of induced sputum with bronchial wash, bronchoalveolar lavage and bronchial biopsies in COPD. *Eur Respir J*. 2000. 15(1):109-15.

30) Costello RW, Jacoby DB, Fryer AD. Pulmonary neuronal M2 muscarinic receptor function in asthma and animal models of hyperreactivity. *Thorax*. 1998. 53(7):613-6.

31) Neves JS, Radke AL, Weller PF. Cysteinyl leukotrienes acting via granule membrane-expressed receptors elicit secretion from within cell-free human eosinophil granules. *J Allergy Clin Immunol.* 2010.125(2):477-82.

32) Uhm TG, Kim BS, Chung IY. Eosinophil development, regulation of eosinophil-specific genes, and role of eosinophils in the pathogenesis of asthma. *Allergy Asthma Immunol Res*. 2012. 4(2):68-79.

33) Yasukawa A, Hosoki K, Toda M, Miyake Y, Matsushima Y, Matsumoto T, Boveda-Ruiz D, Gil-Bernabe P, Nagao M, Sugimoto M, Hiraguchi Y, Tokuda R, Naito M, Takagi T, D'Alessandro-Gabazza CN, Suga S, Kobayashi T, Fujisawa T, Taguchi O, Gabazza EC. Eosinophils promote epithelial to mesenchymal transition of bronchial epithelial cells. *PLoS One*. 2013. 21;8(5):e64281.

34) Possa SS, Charafeddine HT, Righetti RF, da Silva PA, Almeida-Reis R, Saraiva-Romanholo BM, Perini A, Prado CM, Leick-Maldonado EA, Martins MA, Tibério Ide F. Rho-kinase inhibition attenuates airway responsiveness, inflammation, matrix remodeling, and oxidative stress activation induced by chronic inflammation. *Am J Physiol Lung Cell Mol Physiol*. 2012. 1;303(11):L939-52.

35) Venkatasamy R, Spina D. Protease inhibitors in respiratory disease: focus on asthma and chronic obstructive pulmonary disease. *Expert Rev Clin Immunol*. 2007. 3(3):365-81.

36) Al Heialy S, McGovern TK, Martin JG. Insights into asthmatic airway remodelling through murine models. *Respirology.* 2011. 16(4):589-97

37) Bhakta NR, Woodruff PG. Human asthma phenotypes: from the clinic, to cytokines, and back again. *Immunol Rev*. 2011. 242(1):220-32.

38) Desai D, Brightling C. Cytokines and cytokine-specific therapy in asthma. *Adv Clin Chem*. 2012. 57:57-97.

39) Elias JA, Kang MJ, Crothers K, Homer R, Lee CG. State of the art. Mechanistic heterogeneity in chronic obstructive pulmonary disease: insights from transgenic mice. *Proc Am Thorac Soc*. 2007. 15;4(5):473.

40) Lanone S, Zheng T, Zhu Z, Liu W, Lee CG, Ma B, Chen Q, Homer RJ, Wang J, Rabach LA, Rabach ME, Shipley JM, Shapiro SD, Senior RM, Elias JA. Overlapping and enzyme-specific contributions of matrix metalloproteinases-9 and -12 in IL-13-induced inflammation and remodeling. *J Clin Invest*. 2002.110(4):463-74.

41) Kearley J, Erjefalt JS, Andersson C, Benjamin E, Jones CP, Robichaud A, Pegorier S, Brewah Y, Burwell TJ, Bjermer L. IL-9 governs allergen-induced mast cell numbers in the lung and chronic remodeling of the airways. *Am J Respir Crit Care Med.* 2011. 183(7):865-75.

42) Choi J, Callaway Z, Kim HB, Fujisawa T, Kim CK. The role of TNF-alpha in eosinophilic inflammation associated with RSV bronchiolitis. *Pediatr Allergy Immunol*. 2010. 21(3):474-9.

43) Parks WC, Wilson CL, López-Boado YS. Matrix metalloproteinases as modulators of inflammation and innate immunity. *Nat Rev Immunol*. 2004. 4(8):617-29.

44) Oikonomidi S, Kostikas K, Tsilioni I, Tanou K, Gourgoulianis KI, Kiropoulos TS. Matrix metalloproteinases in respiratory diseases: from pathogenesis to potential clinical implications. *Curr Med Chem*. 2009. 16(10):1214-28.

45) Conus S, Simon HU. Cathepsins: key modulators of cell death and inflammatory responses. *Biochem Pharmacol*. 2008. 1;76(11):1374-82.

46) Serveau-Avesque C., Ferrer-Di Matino M., Hervé-Grépinet V., Hazouard E., Gauthier F., Diot E. and Lalmanach G. . Active cathepsins B, H, K, L

and S in human inflammatory broncho-alveolar lavage fluids. *Bio. Cell* 2005. 98: 15-22.

47) Murugan V, Peck MJ. Signal transduction pathways linking the activation of alveolar macrophages with the recruitment of neutrophils to lungs in chronic obstructive pulmonary disease. *Exp Lung Res* 2009;35:439-485.

48) Sen R, Baltimore D. Inducibility of kappa immunoglobulin enhancer-binding protein nf-kappa b by a posttranslational mechanism. *Cell* 1986;47:921-928.

49) Mercurio F, Zhu H, Murray BW, Shevchenko A, Bennett BL, Li J, Young DB, Barbosa M, Mann M, Manning A, et al. Ikk-1 and ikk-2: Cytokine-activated ikappab kinases essential for nf-kappab activation. *Science* 1997;278:860-866.

50) Pahl HL. Activators and target genes of rel/nf-kappab transcription factors. *Oncogene* 1999;18:6853-6866.

51) Blackwell TS, Yull FE, Chen CL, Venkatakrishnan A, Blackwell TR, Hicks DJ, Lancaster LH, Christman JW, Kerr LD. Multiorgan nuclear factor kappa b activation in a transgenic mouse model of systemic inflammation. *Am J Respir Crit Care Med* 2000;162:1095-1101.

52) Alcamo E, Mizgerd JP, Horwitz BH, Bronson R, Beg AA, Scott M, Doerschuk CM, Hynes RO, Baltimore D. Targeted mutation of tnf receptor i rescues the rela-deficient mouse and reveals a critical role for nf-kappa b in leukocyte recruitment. *J Immunol* 2001;167:1592-1600.

53) Lawrence T, Gilroy DW, Colville-Nash PR, Willoughby DA. Possible new role for nf-kappab in the resolution of inflammation. *Nat Med* 2001;7:1291-1297.

54) Everhart MB, Han W, Sherrill TP, Arutiunov M, Polosukhin VV, Burke JR, Sadikot RT, Christman JW, Yull FE, Blackwell TS. Duration and intensity of

nf-kappab activity determine the severity of endotoxin-induced acute lung injury. *J Immunol* 2006;176:4995-5005.

55) Zosky GR, Sly PD. Animal models of asthma.*Clin Exp Allergy*. 2007;37(7):973-88.

54) Bice DE, Seagrave J, Green FH. Animal models of asthma: potential usefulness for studying health effects of inhaled particles. *Inhal Toxicol*. 2000;12(9):829-62.

57) Zhou D, Chen G, Kim JT, Lee LY, and Kang BC. A dose-response relationship between exposure to cockroach allergens and induction of sensitization in an experimental asthma in Hartley guinea pigs. *J Allergy Clin Immunol.* 1998; 101:653–659.

58) Clarke AH, Thomas WR, Rolland JM, Dow C, and O'Brien RM. Murine allergic respiratory responses to the major house dust mite allergen Der p 1. *Int Arch Allergy Immunol* .1999.120:126–134.

59) Fireman P. Understanding asthma pathophysiology. *Allergy Asthma Proc*. 2003. 24(2):79-83.

60) Jones CP, Pitchford SC, Lloyd CM, Rankin SM. CXCR2 mediates the recruitment of endothelial progenitor cells during allergic airways remodeling. *Stem Cells*. 2009; 27(12):3074-81

61) Busse W.W. and Lemanske R.F. Asthma. *N. Engl. J. Med*. 2001, Vol 344(5) pp 350-362.

62) Adams, J.Y., Johnson, M., Sato, M., Berger, F., Gambhir, S.S., Carey, M., Iruela-Arispe, M.L., and Wu, L. Visualization of advanced human prostate cancer lesions in living mice by a targeted gene transfer vector and optical imaging. *Nat. Med.* 2002, 8: 891–897.

63) Subramanian, G., Adams, M.D., Venter, J.C., and Broder, S. Implications of the human genome for understanding human biology and medicine. *JAMA,* 2001, 286: 2296–2307.

64) Phelps ME., Nuclear medicine, molecular imaging, and molecular medicine. *J Nucl Med*. 2002 ;43(2):13N-14N.

65) Gassmann M, Hennet T. From Genetically Altered Mice to Integrative Physiology. *News Physiol Sci*. 1998;13:53-57.

66) Livingston JN. Genetically engineered mice in drug development. *J Intern Med.* 1999 Jun;245(6):627-35.

67) Contag CH, Contag PR, Mullins JI, Spilman SD, Stevenson DK, Benaron DA. *Mol Microbiol*. 1995;18(4):593-603.

Photonic detection of bacterial pathogens in living hosts.

68) Weissleder R, Ntziachristos V., Shedding light onto live molecular targets. *Nat Med*. 2003;9(1):123-8.

69) Montet X, Ntziachristos V, Grimm J, Weissleder R. Tomographic fluorescence mapping of tumor targets. *Cancer Res*. 2005; 65(14):6330-6

70) Hastings JW. Chemistries and colors of bioluminescent reactions: a review. *Gene* 1996;173:5–11.

71) Wet JR, Wood KV, Helinski DR, DeLuca M. Cloning of firefly luciferase cDNA and the expression of active luciferase in Escherichia coli. *Proc Natl Acad Sci USA* 1985;82:7870–7873.

72 Nguyen VT, Morange M, Bensaude O. Firefly luciferase luminescence assays using scintillation counters for quantitation in transfected mammalian cells. *Anal Biochem* 1988;171:404–408.

73) Lipshutz GS, Gruber CA, Cao Y, Hardy J, Contag CH, Gaensler KM. In utero delivery of adeno-associated viral vectors: intraperitoneal gene transfer produces long-term expression. *Mol Ther* 2001;3:284– 292.

74) Rice BW, Cable MD, Nelson MB. In vivo imaging of light-emitting probes. *J Biomed Opt* 2001;6:432–440.

75) Wilson T, Hastings JW. Bioluminescence. *Annu Rev Cell Dev Biol* 1998; 14:197–230.

76) Everhart MB, Han W, Sherrill TP, Arutiunov M, Polosukhin VV, Burke JR, Sadikot RT, Christman JW, Yull FE, Blackwell TS. Duration and intensity of nf-kappab activity determine the severity of endotoxin-induced acute lung injury. *J Immunol.* 2006;176:4995-5005.

77) Kielland A, Carlsen H. Molecular imaging of transcriptional regulation during inflammation. *J Inflamm (Lond)* 2010;7:20.

78) Ansaldi D, Hod EA, Stellari F, Kim JB, Lim E, Roskey M, Francis KP, Singh R, Zhang N. Imaging pulmonary nf-kappab activation and therapeutic effects of mln120b and tdzd-8. *PLoS One* 2011;6:e25093.

79) Stellari FF, Franceschi V, Capocefalo A, Ronchei M, Facchinetti F, Villetti G, Donofrio G. In vivo imaging of transiently transgenized mice with a bovine interleukin 8 (CXCL8) promoter/luciferase reporter construct. *PLoS One*. 2012;7; 6:e39716.

80) Chuang K, Cheng T. Noninvasive Imaging of Reporter Gene Expression and Distribution *In Vivo*. *Fooyin J Health Sci* 2010;2(1):1-11.

81) Ntziachristos V, Tung CH, Bremer C, Weissleder R. Fluorescence molecular tomography resolves protease activity in vivo. *Nat Med*. 2002 Jul;8(7):757-60.

82) Min J-J, Nguyen V, Gambhir S. Molecular Imaging of Biological Gene Delivery Vehicles for Targeted Cancer Therapy: Beyond Viral Vectors. *Nuclear Medicine and Molecular Imaging 2010*;44(1):15-24.

83) Korideck H, Peterson JD. Noninvasive quantitative tomography of the therapeutic response to dexamethasone in ovalbumin-induced murine asthma. *J Pharmacol Exp Ther*. 2009 Jun;329(3):882-9

84) Chuang KH, Wang HE, Cheng TC*, et al.* Development of a universal anti-polyethylene glycol reporter gene for noninvasive imaging of PEGylated probes. *J Nucl Med* 2010;51(6):933-41.

85) Fukumura D, Duda DG, Munn LL, Jain RK. Tumor microvasculature and microenvironment: novel insights through intravital imaging in pre-clinical models. *Microcirculation* 2010;17(3):206-25.

86) Waerzeggers Y, Monfared P, Viel T*, et al.* Methods to monitor gene therapy with molecular imaging. *Methods.* 2009;48(2):146-60.

87) Blum G., Weimer R.B., Edgington L.E., Adams W. and Bogyo M. Comparative Assessment of Substrates and Activity Based Probes as Tools for Non-Invasive Optical Imaging of Cysteine Protease Activity*. PLoS ONE* 2009, 4(7): e6374.

88) Yang Y., Hong H., Zhang Y., and Cai W. Molecular Imaging of Proteases in *Cancer. Cancer Growth Metastasis*. 2009, 2: 13-27.

89) Ntziachritos V., Bremer C., Grave E.E., Ripoll J. and Weissleder R. In Vivo Tomograhic Imaging of Near-Infrared Fluorescent Probes. *Molecular imaging*, 2002. Vol 1(2) pp. 82-88.

90) Ntziachristos V. Optical imaging of molecular signatures in pulmonary inflammation. *Proc Am Thorac Soc*. 2009. 15;6(5):416-8

91) Cortez-Retamozo V., Swirski F.K., Waterman P., Yuan H., Figueiredo J.L., Newton A.P., Upadhyay R., Vinegoni C., Kohler R., Blois J., Smith A., Nahrendorf M., Josephson L., Weissleder R. and Pittet M.J.Real-time assessment of inflammation and treatment response in a mouse model of allergic airway inflammation. *J. Clin. Invest*. 2008. 118: 4058-4066.

92) Haller J, Hyde D, Deliolanis N, de Kleine R, Niedre M, Ntziachristos V. Visualization of pulmonary inflammation using noninvasive fluorescence molecular imaging. *J Appl Physiol*. 2008. 104(3):795-802

93) Jones H, Marino P, Shakur B, Morrell N. In vivo assessment of lung inflammatory cell activity in patients with COPD and asthma. *Eur Respir J* 2003;21:567–573.

94) Cataldo D, Gueders M, Rocks N, Sounni N, Evrard B, Bartsch P, LouisR, Noel A, Foidart J. Pathogenic role of matrix metalloproteases andtheir inhibitors in asthma and chronic obstructive pulmonary diseaseand therapeutic relevance of matrix metalloproteases inhibitors. *Cell Mol Biol* 2003;49:875–884.

95) Guide for the care and use of laboratory animals. Washington, D.C.: *National Academy Press*; 1996.

94) Donofrio G, Capocefalo A, Franceschi V, Price S, Cavirani S, Sheldon IM The chemokine IL8 is up-regulated in bovine endometrial stromal cells by the BoHV-4 IE2 gene product, ORF50/Rta: a step ahead toward a mechanism for BoHV-4 induced endometritis. *Biol Reprod*. 2010; 83(6):919-28

97) Rosenkilde MM, Schwartz TW. The chemokine system – a major regulator of angiogenesis in health and disease. APMIS : *acta pathologica, microbiologica, et immunologica Scandinavica.* 2004.112: 481–495.

98) Laterveer L, Lindley IJ, Hamilton MS, Willemze R, Fibbe WE Interleukin-8 induces rapid mobilization of hematopoietic stem cells with radioprotective capacity and long-term myelolymphoid repopulating ability. *Blood* .1995. 85: 2269–2275.

99) Matsushima K, Morishita K, Yoshimura T, Lavu S, Kobayashi Y. Molecular cloning of a human monocyte-derived neutrophil chemotactic factor (MDNCF) and the induction of MDNCF mRNA by interleukin 1 and tumor necrosis factor. 1988. *J Exp Med* 167: 1883–1893.

100) Minnerly JC, Baganoff MP, Deppeler CL, Keller BT, Rapp SR. Identification and characterization of rhesus macaque interleukin-8. *Inflammation*.1995.19: 313–331.

101) Villinger F, Brar SS, Mayne A, Chikkala N, Ansari AA. Comparative sequence analysis of cytokine genes from human and nonhuman primates. *J Immunol*.1995.155: 3946–3954.

102) Morsey MA, Popowych Y, Kowalski J, Gerlach G, Godson D. Molecular cloning and expression of bovine interleukin-8. *Microb Pathog.*1996*.* 20:203-212.

103) Legastelois I, Greenland T, Arnaud P, Mornex JF, Cordier G. Sequencing of the ovine interleukin-8-encoding cDNA using the polymerase chain reaction. *Gene*.1994.150: 367–369.

104) Lin G, Pearson AE, Scamurra RW, Zhou Y, Baarsch MJ. Regulation of interleukin-8 expression in porcine alveolar macrophages by bacterial lipopolysaccharide. *J Biol Chem.* 1994. 269: 77–85.

105) Kukielka GL, Smith CW, LaRosa GJ, Manning AM, Mendoza LH. Interleukin-8 gene induction in the myocardium after ischemia and reperfusion in vivo. J Clin Invest.*1995*. 95: 89–103.

106) Yoshimura T, Yuhki N. Neutrophil attractant/activation protein-1 and monocyte chemoattractant protein-1 in rabbit. cDNA cloning and their expression in spleen cells. *J Immunol*. 1991. 146: 3483–3488.

107) Yoshimura T. cDNA cloning of guinea pig monocyte chemoattractant protein-1 and expression of the recombinant protein. *J Immunol* .1993.150: 5025–5032.

108) Dehbi M, Mbiguino A, Beauchemin M, Chatelain G, Bedard PA. Transcriptional activation of the CEF-4/9E3 cytokine gene by pp60v-src. *Mol Cell Biol*. 1992. 12: 1490–1499.

109) Meade KG, O'Gorman GM, Narciandi F, Machugh DE, O'Farrelly C. Functional characterisation of bovine interleukin 8 promoter haplotypes in vitro. *Mol Immunol*. 2012.50: 108–116.

110) Standiford TJ, Kunkel SL, Basha MA, Chensue SW, Lynch JP. Interleukin-8 gene expression by a pulmonary epithelial cell line. A model for cytokine networks in the lung. *J Clin Invest*.1990. 86: 1945–1953.

111) Doyle TC, Burns SM, Contag CH. In vivo bioluminescence imaging for integrated studies of infection. *Cell Microbiol*. 2004. 6: 303–317.

112) Malazdrewich C, Ames TR, Abrahamsen MS, Maheswaran SK. Pulmonary expression of tumor necrosis factor alpha, interleukin-1 beta, and interleukin-8 in the acute phase of bovine pneumonic pasteurellosis. *Vet Pathol.* 2001. 38: 297–310.

113) Mukaida N. Pathophysiological roles of interleukin-8/CXCL8 inpulmonary diseases. *Am J Physiol Lung Cell Mol Physiol*. 2003. 284: L566 - 577.

114) Goplen N, Karim MZ, Liang Q, Gorska MM, Rozario S, Guo L, Alam R. Combined sensitization of mice to extracts of dust mite, ragweed, and Aspergillus species breaks through tolerance and establishes chronic features of asthma. *J Allergy Clin Immunol*. 2009;123(4):925-32.e11

.

In Vivo Imaging of Transiently Transgenized Mice with a Bovine Interleukin 8 (CXCL8) Promoter/Luciferase Reporter Construct

Fabio Franco Stellari[1,2], Valentina Franceschi[1], Antonio Capocefalo[1], Marcello Ronchei[1], Fabrizio Facchinetti[2], Gino Villetti[2], Gaetano Donofrio[1]*

1 Dipartimento di Salute Animale, Sezione di Malattie Infettive degli Animali, Università di Parma, Parma, Italy, **2** Chiesi Farmaceutici S.p.A, Parma, Italy

Abstract

One of the most remarkable properties of interleukin 8 (CXCL8/IL-8), a chemokine with known additional functions also in angiogenesis and tissue remodeling, is the variation of its expression levels. In healthy tissues, IL-8 is barely detectable, but it is rapidly induced by several folds in response to proinflammatory cytokines, bacterial or viral products, and cellular stress. Although mouse cells do not bear a clear homologous IL-8 gene, the murine transcriptional apparatus may well be capable of activating or repressing a heterologous IL-8 gene promoter driving a reporter gene. In order to induce a transient transgenic expression, mice were systemically injected with a bovine IL-8 promoter–luciferase construct. Subsequently mice were monitored for luciferase expression in the lung by *in vivo* bioluminescent image analysis over an extended period of time (up to 60 days). We demonstrate that the bovine IL-8 promoter–luciferase construct is transiently and robustly activated 3–5 hours after LPS and TNF-α instillation into the lung, peaking at 35 days after construct delivery. Bovine IL-8 promoter–luciferase activation correlates with white blood cell and neutrophil infiltration into the lung. This study demonstrates that a small experimental rodent model can be utilized for non-invasively monitoring, through a reporter gene system, the activation of an IL-8 promoter region derived from a larger size animal (bovine). This proof of principle study has the potential to be utilized also for studying primate IL-8 promoter regions.

Citation: Stellari FF, Franceschi V, Capocefalo A, Ronchei M, Facchinetti F, et al. (2012) *In Vivo* Imaging of Transiently Transgenized Mice with a Bovine Interleukin 8 (CXCL8) Promoter/Luciferase Reporter Construct. PLoS ONE 7(6): e39716. doi:10.1371/journal.pone.0039716

Editor: Bernhard Kaltenboeck, Auburn University, United States of America

Received February 22, 2012; **Accepted** May 25, 2012; **Published** June 28, 2012

Copyright: © 2012 Stellari et al. This is an open-access article distributed under the terms of the Creative Commons Attribution License, which permits unrestricted use, distribution, and reproduction in any medium, provided the original author and source are credited.

Funding: This study received financial support from Chiesi Farmaceutici and the Italian Ministry of University and Scientific Research. The funders had no role in study design, data collection and analysis, decision to publish, or preparation of the manuscript.

Competing Interests: Fabio Stellari, Fabrizio Facchinetti. and Gino Villetti are affiliated to Chiesi Farmaceutici group. Chiesi Farmaceutici provided financial support for this study, however this does not alter the authors' adherence to all the Plos One policies on sharing data and materials.

* E-mail: gaetano.donofrio@unipr.it

Introduction

Severe respiratory diseases in ruminants and human are characterized by pneumonia with extensive infiltration of polymorphonuclear inflammatory cells (PMNs) in small airways and alveoli, by the accumulation of fibrinous oedema in the alveoli, pleura surface and interlobular septa, by hemorrhage, vascular thrombosis and coagulative parenchymal necrosis of the lung [1,2].

Several bacteria and viruses overcoming host defense mechanisms and proliferating in the lung are the main triggering factors of lung inflammation and polymorphonuclear leukocytes (PMNs) are directly and indirectly responsible for most of the lung pathologies and lesions [2,3]. Mobilization of PMNs in the inflamed lung is modulated by the interactions of leucocytes and cytokines. During the acute-phase response of the pneumonic process caused by infectious agents in ruminants and human, the inflammatory cytokines such as IL-1β, TNF-α and IL-8, secreted by a variety of immune and non immune cell types, induce a strong PMNs mobilization and an increased inflammatory response [2,3]. PMNs mobilization does not always effectively combat the infection and may also contribute to the development of lesions in the lung. During the development of lung inflammation IL-1β and TNF-α are initially produced, thereby inducing a strong IL-8 secretion, the most potent PMNs chemotactic and activating factor. IL-1β, TNF-α and especially IL-8, promote PMNs-mediated tissue injury by stimulating degranulation of PMNs and extracellular release of arachidonic acid metabolites, toxic oxygen radicals and proteolytic enzymes [4]. Hence, IL-8 could be considered a downstream event that is dependent, at least in part, on the prior secretion of early response cytokines such as IL-1β and TNF-α [1,2,4] and this assumption has very important implications for therapeutic strategies directed toward the modulation of inflammatory cytokines. First of all pharmacologic molecules inhibiting or antagonizing the biological effect of inflammatory cytokines should be mainly directed toward IL-8. Next, anti-cytokine drugs should be administrated very early to prevent irreversible lung lesions [5,6].

Interleukin-8 (CXCL8/IL-8) is secreted by a variety of immune and non immune cell types. The human chemokine IL-8 is an 8.5-kDa C-X-C chemokine member of the CXC chemokine family, which acts through the G protein-coupled receptors CXCR1 and CXCR2. IL-8/CXCL8 complex is capable of activating the expression of adhesion molecules in endothelial cells [7] and is an important chemoattractant for neutrophils [8] as well as T-cells [9] and monocytes [10]. In neutrophils, in particular, IL-8 induces shape changes, exocytosis of stored proteins, and the respiratory

burst, resulting in the release of superoxide anions and hydrogen peroxide. IL-8 is also involved in a wide variety of pathological processes, including host defenses against bacterial infections, angiogenesis and immune disorders [11]. One of the most remarkable property of IL-8 is the rapid variation of its expression levels in response to numerous stimuli. In healthy tissues, IL-8 is barely detectable, but it is rapidly induced in response to pro-inflammatory cytokines such as tumor necrosis factor alpha (TNF-α) or IL-1, bacterial or viral products, and cellular stress.

Different signaling pathways coordinately regulate IL-8 transcription as well as mRNA stabilization in response to external stimuli. Maximal IL-8 amounts are generated by a combination of three different mechanisms: first, derepression of the gene promoter; second, transcriptional activation of the gene by nuclear factor-kappaB (NF-*k*B) and JUN-N-terminal protein kinase (JNK) pathways; and third, stabilization of the mRNA by the p38 mitogen-activated protein kinase pathway. This complex regulation renders cells capable of rapidly increasing and, at the same time, to fine-tuning the amount of IL-8 secreted, thereby tightly controlling the extent of leukocytes attracted to the site of tissue injury.

Although post-transcriptional regulation of IL-8 expression has been shown to be important, transcriptional regulation linked to the activation of pro-inflammatory molecule receptors, such as TLRs, IL-1 and TNF-α receptors, remains crucial in modulating IL-8 expression [12]. Available data suggested that the NF-*k*B and JNK pathways are indispensable for the transcriptional regulation of IL-8 expression. Using the chromatin immune-precipitation technique, Nissen and Yamamoto demonstrated the binding of p65 NF-*k*B to the IL-8 promoter and the subsequent formation of a TNF-α-stimulated pre-initiation complex containing inducible phosphorilated RNA polymerase II [13,14]. Therefore, establishing an *in vivo* molecular read-out to monitor IL-8 induction following a specific inflammatory stimulus would be of great value for testing new strategies directed toward the transcriptional modulation of IL-8 production. Although the manifestation of lung diseases in ruminants overlaps in most respect the manifestation of lung diseases in human [2,3], the use of ruminants (bovine, sheep or goat) as animal models is very costly and demanding in terms of maintenance and the availability of advanced genetic or immunologic resources is significantly limited when compared with those available for rodent studies. On the other hand, no clear-cut IL-8 homolog in rat or mouse has been identified so far, although MIP-2 and KC may be functional homologs of IL-8 in mice [15]. Furthermore, IL-8 binds to two types of IL-8 receptors in humans, while mouse has only one potential IL-8 receptor (homolog of human CXCR2). Although mice lack an exact homolog of IL-8, the murine CXCR2 homolog is activated by other neutrophils chemoattractants, namely MIP-2 and KC. Indeed, gene targeting of CXCR2 in mice exhibited inhibition of neutrophil infiltration into inflamed tissue [16] and mice transiently overexpressing IL-8 exhibit excessive accumulation of neutrophils in the microcirculation of the lung, liver, and spleen [15]. Based on the above information it was hypothesized that, although mouse cells do not bear a clear homologous of IL-8 gene, murine transcriptional apparatus may nonetheless be capable of activating or repressing a heterologous IL-8 gene promoter driving a reporter gene. The possibility of monitoring in small rodents *in vivo* luciferase reporter genes under the control of cytokine promoters derived from other species would be of great value for studying the pathophysiology of inflammatory responses as well as to test interventions aimed at modulating such responses. In the present study this hypothesis was successfully tested by utilizing a molecular imaging approach based on a previously well characterized bovine IL-8 promoter/luciferase reporter construct [17] in mice. This study paves the way to non-invasive imaging approaches for studying mechanisms and signaling pathways underlying regulation of IL-8 expression.

Results

The Bovine IL-8 Promoter is Responsive in Mouse Lung Cells *in vitro*

The bovine IL-8 promoter, mapped on *Bos taurus* chromosome 6 (http://www.ncbi.nlm.nih.gov/mapview/maps.cgitaxid=9913&chr=6&query=uid(207248,3567299)&QSTR=280828%5Bgene%5Fid%5D&maps=gene_set&cmd=focus), was previously cloned from bovine genomic DNA template and its activation at the transcriptional level tested with a luciferase reporter construct bIL-8-Luc. The luciferase construct was generated by sub-cloning the 2030 bp IL-8 promoter in front of a pGL3 Luciferase reporter vector [17]. The capability of mouse cells to trans-activate the bovine IL-8 promoter/luciferase reporter construct (bIL-8-Luc, **Fig. 1A**) was first tested in an *in vitro* model. The expression of Toll Like receptors (TLRs,) was evaluated by RT-PCR in the LA-4 cell line, a mouse epithelial cell line from lung, TLR 1, 2, 3, 4, 5, 6, 8 and 9 were detectable, while no expression of TLR7 was identified (**Fig. 1B**). Secondly, TNF-α and TNF-α receptor (TNF-αR) I and II were both found expressed in LA-4 cells (**Fig. 1C**). Subsequently, LA-4 cells were transiently transfected by electroporation with the bIL-8-luc reporter construct and 24 h post transfection the cells were treated with TNF-α or LPS. In bIL-8-luc transfected LA-4 cells, a 4 hour treatment with TNF-α increased luciferase signal up to 3 folds, while, similarly, a 4 hour treatment with LPS elicited a 2-fold induction (**Fig. 1D**). Signal intensity was expressed as folds of induction over the bIL-8-luc transfected vehicle-treated LA-4 cells. Results are reported as mean ± SD and significance attributed when $P<0.05$ (*) or $P<0.01$(**).

The Bovine IL-8 Promoter is Responsive in Mouse Lung *in vivo*

Given the positive results obtained *in vitro*, bIL-8-luc reporter construct was tested *in vivo*. Mice were first transiently transgenized with bIL-8-luc or the Empty vector control (pGL3 basic) and 10 days post transgenization were intratracheally instilled with LPS or TNF-α. At different time points (3, 5 and 24 hours) post instillation mice were monitored for luciferase expression in the lung by *in vivo* image analysis. Mice responded to both treatments with a robust induction already at 3 hours after instillation and the response still remained significant after 24 hours. In contrast no signal was observed for control mice treated with saline or transiently transgenized with the Empty vector (**Fig. 2A and B**). Signal intensity was then expressed as folds of induction where the untreated control was considered as 1 (**Fig. 2C**). A further control was established with mice transiently transgenized with different promoter reporter constructs such as STAT-1-Luc and ELK-1-Luc and no signal was detected after LPS or TNF-α treatment (**Figure S1**).

This *in vivo* analysis demonstrated the striking specificity of the system and a better induction with a lower background compared to the data obtained *in vitro*. Results are reported as mean ± SD and significance attributed when $P<0.05$ (*) or $P<0.01$(**).

Long Lasting Response of Bovine IL-8 Reporter Gene *in vivo*

Similarly to *in vitro* transient transfections, the gene delivery system employed *in vivo* is expected to result in a transient expression of the delivered bIL-8-Luc reporter construct. It was therefore important to assess the extent and the duration *in vivo* of the responsiveness of the bIL-8-Luc reporter construct. Mice

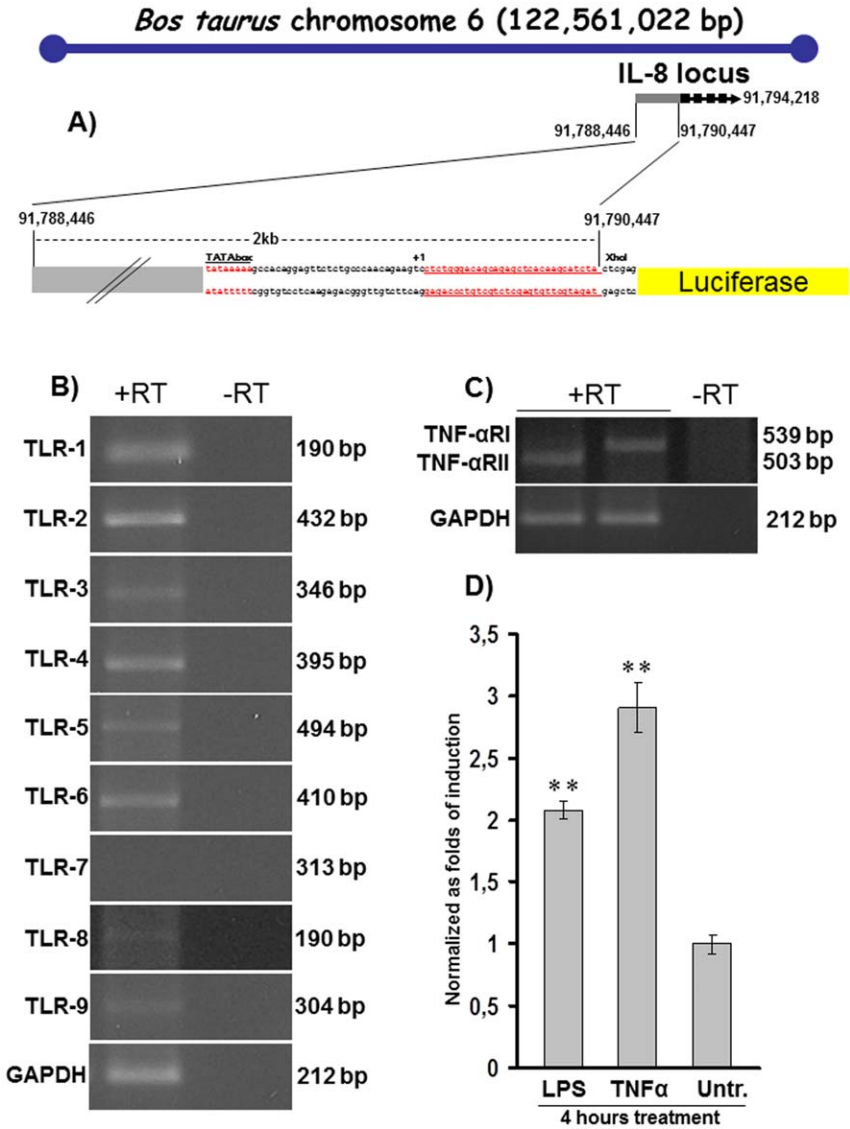

Figure 1. *In vitro* characterization of bIL-8-Luc reporter construct. A) Schematic diagram (not to scale) of the *Bos taurus* chromosome 6 with the IL-8 gene locus comprising promoter and exons annotated by numbers. The 2 kb IL-8 promoter sequence, comprising the putative TATA box, the transcriptional start site (+1) and the UTR (red underlined) was cloned into the pGL3 basic vector in front of the open reading frame of the Luciferase reporter. **B**) RT-PCR products of TLRs from 1 to 9 and their corresponding amplicon size. GAPDH was used as an internal control and the amplification performed in the absence of reverse transcriptase (-RT) as a negative control. **C**) RT-PCR products of TNF-αRI,II and their corresponding amplicon size. GAPDH was used as an internal control and the amplification performed in the absence of reverse transcriptase (-RT) as a negative control. D) IL-8 promoter activation after treatment of bIL-8-Luc transfected LA-4 cells with LPS or TNF-α, along with the untreated control (Untr.). Each experiment was done in quadruplicate, and each point represents the mean ± standard deviation of three experiments. Data were expressed as folds of induction (2,1 and 2,8 for LPS and TNF-α respectively) over vehicle-treated cells and statistical differences were tested by One Way ANOVA followed by Dunnet's post hoc test for group comparisons. Results are reported as mean ± SD and significance attributed when $P<0.05$ (*) or $P<0.01$(**).
doi:10.1371/journal.pone.0039716.g001

transiently transgenized with bIL-8-Luc or the Empty vector were intratracheally instilled with LPS or TNF-α at 8, 32, 45 and 60 days post transgenization and 3, 5, or 24 h post treatment were monitored for luciferase expression in the lung by *in vivo* image analysis. Surprisingly, transiently transgenized mice responded to LPS or TNF-α up to 60 days after transfection (**Fig. 3**) with the greater response at 32 days. In contrast, no signal was detectable in mice treated with saline or transiently transgenized with the Empty vector. Results are reported as mean ± SD and significance attributed when $P<0.05$ (*) or $P<0.01$(**).

Thus, our data suggest that the same mice can be utilized or reutilized for at least 45 days after the administration of the reporter gene, saving animals and costs. This will offer the opportunity of monitoring every single animal over an extended time period.

Bovine IL-8 Reporter Gene Response Correlates with White Blood Cells and Neutrophils Infiltration

Since IL-8 is a major chemotactic polypeptide for neutrophils, we examined the correlation between bIL-8-Luc activation and neutrophils infiltration into the lung upon LPS or TNF-α stimulation. Ten days post bIL-8-Luc transient transgenization, the mice were intratracheally instilled with LPS, TNF-α or saline solution. Three hours post treatment, which was the time

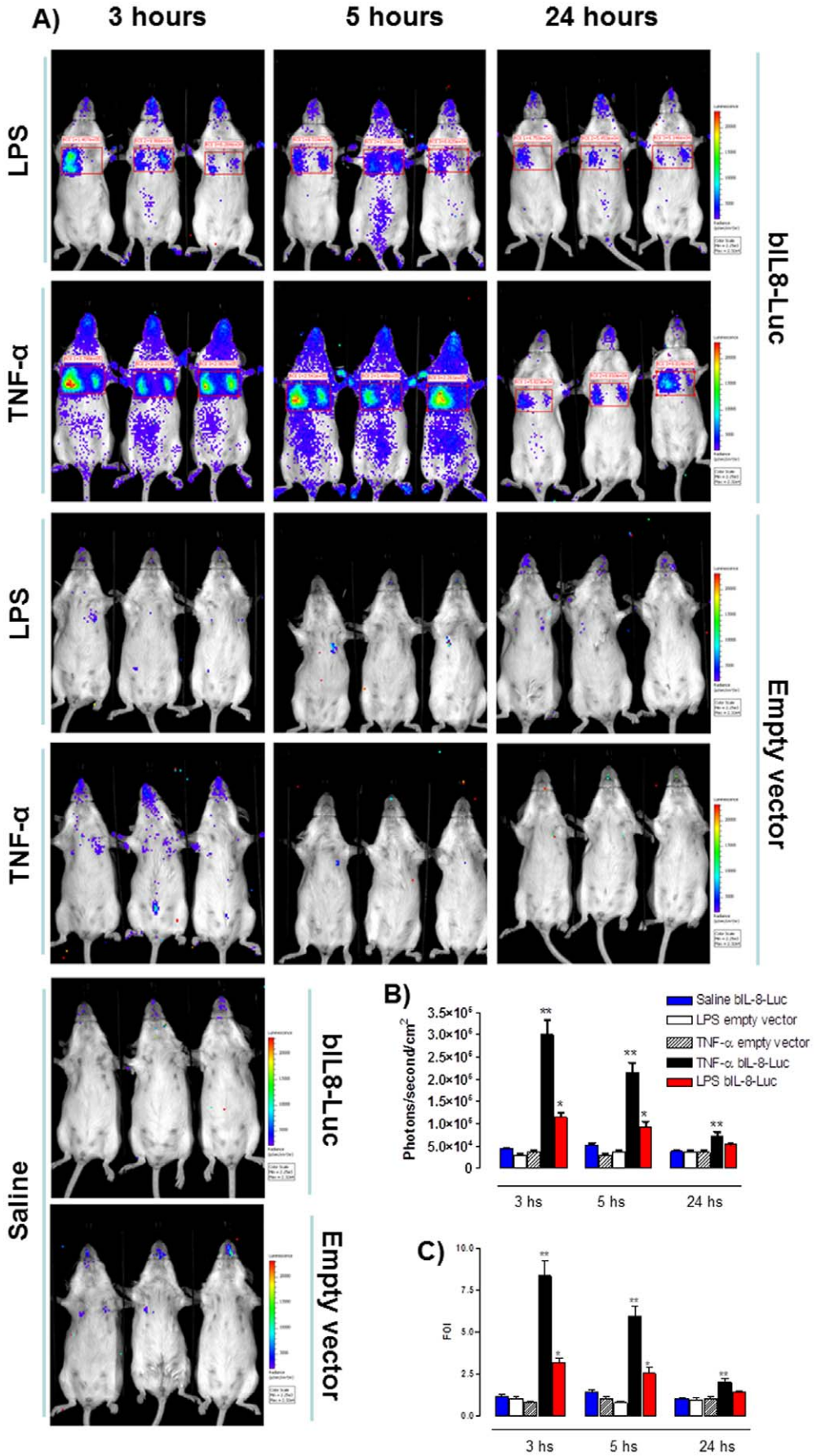
A)
3 hours
5 hours
24 hours
LPS
TNF-α
bIL8-Luc
LPS
TNF-α
Empty vector
Saline
bIL8-Luc
Empty vector
B)
Photons/second/cm²
3.5×10⁶
3.0×10⁶
2.5×10⁶
2.0×10⁶
1.5×10⁶
1.0×10⁶
5.0×10⁴
0
Saline bIL-8-Luc
LPS empty vector
TNF-α empty vector
TNF-α bIL-8-Luc
LPS bIL-8-Luc
3 hs
5 hs
24 hs
C)
FOI
10.0
7.5
5.0
2.5
0.0
3 hs
5 hs
24 hs

Figure 2. bIL-8-Luc reporter construct response *in vivo*. A) Representative images of groups of mice (n = 3 per group) transiently transgenized with bIL-8-Luc or Empty vector DNA and intratracheally instilled with LPS, TNF-α or vehicle (saline solution). Mice were monitored at 3, 5 and 24 hours post stimulation by BLI drawing a region of interest (ROI) over the chest. **B**) Light intensity quantification of the ROI using the LivingImage software. The experiment was repeated three times and each point represents the mean ± standard deviation of 9 animals. **C**) Data were expressed as folds of induction over vehicle-treated mice (Saline) and statistical differences were tested by One Way ANOVA followed by Dunnet's post hoc test for group comparisons. Results are reported as mean ± SD and significance attributed when $P<0.05$ (*) or $P<0.01$(**).
doi:10.1371/journal.pone.0039716.g002

corresponding to the maximal bIL-8-luc activation and at 24 h post treatment, corresponding to the decline of the signal, the lungs of the treated mice were intratracheally washed and the broncho-alveolar lavage fluid (BALF) was assayed for the presence of infiltrating total white blood cells (WBC) and neutrophils. As shown in **Fig. 4**, WBC and neutrophils significantly increased in treated mice with respect to the untreated control, whereas the number of monocytes remained constant, a finding in line with the notion that monocytic infiltration is typically a late event of inflammatory responses. However, in terms of cellular infiltration response, LPS gave a better response than TNF-α. Thus a positive correlation between bIL-8-Luc reporter construct activation and white blood cells and neutrophils infiltration was observed. Results are reported as mean ± SD and significance attributed when $P<0.05$ (*) or $P<0.01$(**).

Discussion

A hallmark of tissue inflammation following chemical, physical or microbiological insults is the recruitment of white blood cells to the injured tissue, which is orchestrated by chemotactic polypeptides named chemokines, among which IL-8 is one of the most remarkable. A significant correlation between IL-8 levels and neutrophil infiltration in diseases has been reported. IL-8 is an essential factor for acute inflammation and induces the infiltration of T lymphocytes into inflamed tissue. Recent studies have also demonstrated that IL-8 is involved in non-inflammatory reactions like angiogenesis [18]. In addition, systemic administration of IL-8 rapidly induces migration of hematopoietic stem cells from bone marrow to peripheral blood [19]. These results suggest that IL-8 also regulates non-inflammatory physiological reactions *in vivo*.

L-8 transcriptional activation is closely correlated with the initiation of acute inflammatory responses and thus is an ideal indirect read-out for monitoring the activation of inflammatory pathways targeting IL-8 expression. IL-8 homologs in many species have been cloned, including human [12], macaque [20], Sooty mangabey [21], bovine [22], sheep [23], pig [24], dog [25], rabbit [26], Guinea pig [27] and chicken [28]; however, a homolog of IL-8 has not been described in small rodents, including mice. In this study we developed a useful murine model for monitoring IL-8 expression in vivo. To this aim the bovine IL-8 promoter was chosen for two main reasons. First, lung inflammation-associated diseases in ruminants are very important in terms of economic loss for the beef meat industry; according to a report of the Committee for Animal Health Research Programs, major disease-related losses attributed to respiratory infections were calculated to be ~400 million Euros per year; therefore the creation of an innovative in vivo platform for testing new respiratory anti-inflammatory drugs targeting specific pathways, such as IL-8, would be highly desirable. Second, all the information obtained on IL-8 bovinized mice can be easily employed for the human lung inflammation associated diseases, due to the high similarity existing between respiratory diseases in ruminants and human.

Although the minimal responsive sequence for the bovine IL-8 promoter is represented by the first 200 bp starting from the putative transcriptional initiation site, a 2 kb large version of the promoter was utilized [17] in order to include most of the potentially relevant binding sites for transcription factors. Moreover, recently two IL-8 promoter haplotypes have been characterized: the type 1, less sensitive to LPS and TNF-α and the type 2 with higher sensitivity to LPS and TNF-α [29].

Because IL-8 was previously shown to be expressed by a human epithelial cell line derived from lung after specific stimuli [30,31], the bIL-8 reporter construct was initially tested *in vitro* in a mouse lung epithelial cell line, LA-4, which expresses TLRs and TNF-αRs. Although mice and rats do not have IL-8 gene, bovine IL-8 promoter/luciferase reporter construct was expressed at detectable levels in transfected LA-4 cells and was significantly induced upon treatment with LPS or TNF-α. This simple but extremely informative experiment demonstrates that mouse cells have the transcriptional machinery for transactivating a heterologous IL-8 promoter/luciferase reporter construct.

To functionally test the IL-8 promoter/luciferase reporter construct in mice, an *in vivo* bioluminescent imaging (BLI) approach was exploited. BLI is a sensitive tool that is based on the detection of light emission from cells or tissues [32]. The utility of reporter gene technology makes it possible to analyze specific cellular and biological processes in a living animal through *in vivo* imaging methods. Bioluminescence from luciferase gene expression, as is the case of the reporter construct employed during this study, is the most widely used. Because mammalian tissues do not naturally emit bioluminescence, *in vivo* BLI has considerable appeal because images can be generated with absence of background signal. BLI requires an expression cassette consisting of the bioluminescence reporter gene (in this case was luciferase) under the control of a selected promoter (in this experimental setting a bovine IL-8 gene promoter) driving the reporter. In order to induce light production, the substrate luciferin must be provided by intravascular or intraperitoneal injection. To date, there have been no reports of toxicity related to repeated dosing of substrates [32].

Although delivery of cationic polyethylenimine (PEI)/DNA complex could cause mortality when injected in mice in a strain dependent manner, we observed 100% survival rate when bIL-8-luc DNA was intravenously injected in FVB mice. Furthermore, a more robust fold-induction in response to LPS or TNF-α was obtained in the lung of bIL-8-luc DNA injected mice than in bIL-8-luc DNA transfected LA-4 cells. Indeed, bIL-8-luc DNA may have transfected several lung cell types, leading to the signal amplification orchestrated by the complex cellular network of the lung parenchyma. Although this is an important issue to be explored, it is out of the scope of the present study.

Noteworthy, bIL-8-luc transiently transgenized mice could be stimulated with LPS or TNF-α up to 60 days. Thus, the capability to monitor a biological process longitudinally in the same mouse represents an obvious advance for functional as well as pharmacological studies. The correlation between WBC and neutrophils infiltration and luciferase expression following LPS or TNF-α stimulation is in accordance with the recognized IL-8 role

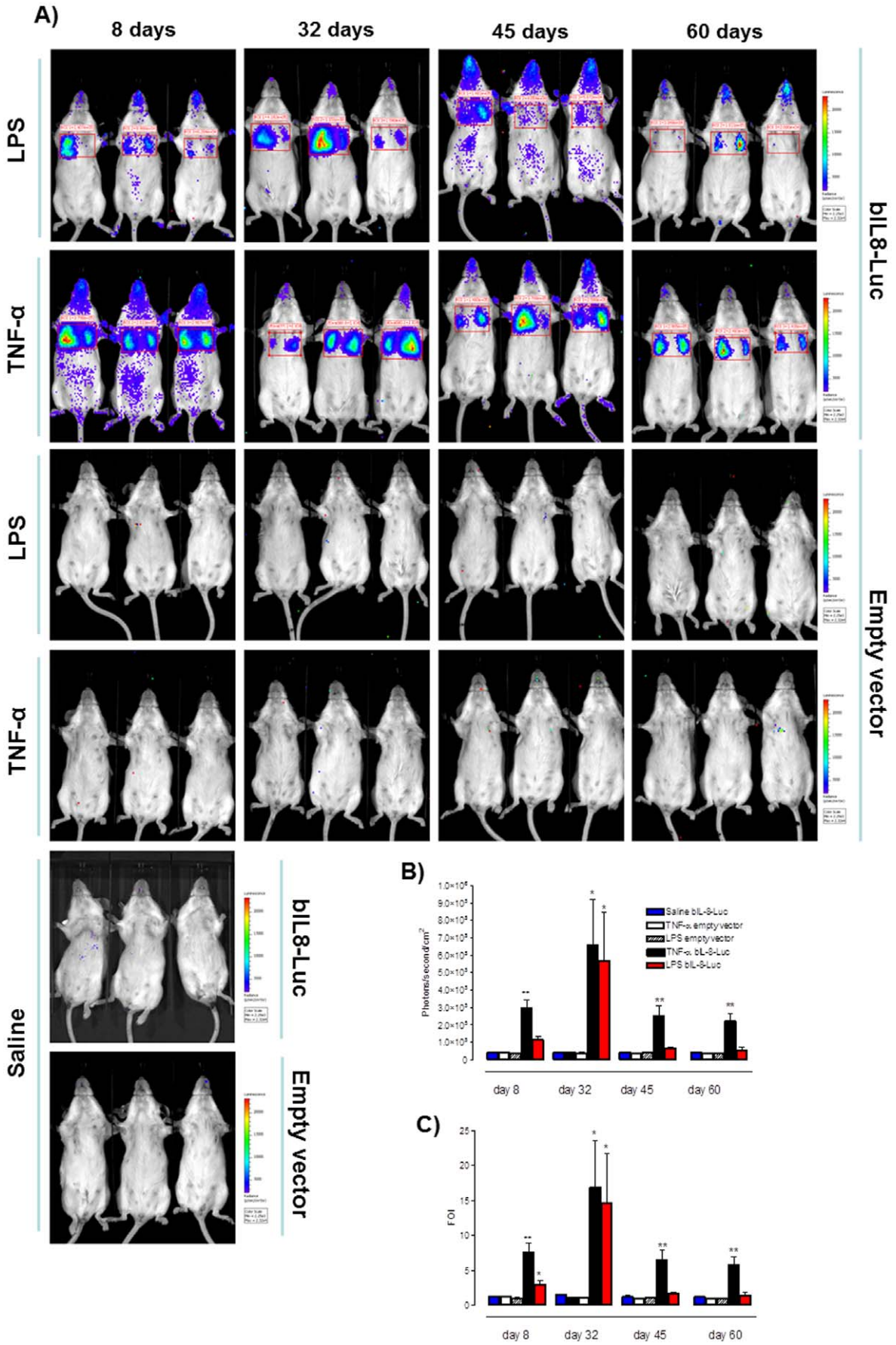
A)
8 days
32 days
45 days
60 days
LPS
TNF-α
bIL8-Luc
LPS
TNF-α
Empty vector
Saline
bIL8-Luc
Empty vector
B)
Photons/second/cm²
Saline bIL-8-Luc
TNF-α empty vector
LPS empty vector
TNF-α bIL-8-Luc
LPS bIL-8-Luc
day 8
day 32
day 45
day 60
C)
FOI
day 8
day 32
day 45
day 60

Figure 3. Long lasting response of bIL-8-Luc reporter construct. A) Representative images of groups of mice (n = 3 per group) transiently transgenized with bIL-8-Luc or Empty vector DNA and intratracheally instilled with LPS, TNF-α or vehicle (saline solution) at 8, 32, 45 and 60 days post transgenization. Mice were monitored at 3 hours post stimulation by BLI by drawing a region of interest (ROI) over the chest. **B**) Light intensity quantification of the ROI using the LivingImage software. The experiment was repeated three times and each point represents the mean ± standard deviation of 9 animals. **C**) Data were expressed as folds of induction over vehicle-treated mice (Saline) and statistical differences were tested by One Way ANOVA followed by Dunnet's post hoc test for group comparisons. Results are reported as mean ± SD and significance attributed when $P<0.05$ (*) or $P<0.01$(**).
doi:10.1371/journal.pone.0039716.g003

as a key factor in orchestrating inflammation, thus further validating the association between IL-8 transcriptional activation and pulmonary inflammation in the experimental setting that we here adopted. Although a bovine promoter was used in this study as a proof of concept, the results of the study suggest that IL-8 promoter regions derived from other species, including primates, could also be utilized in this experimental setting.

IL-8 exerts a wide variety of actions on pulmonary disease pathophysiology in ruminants and human during bacterial or viral infection, acute respiratory distress syndrome (ARDS), reperfusion injury and transplantation, lung injuries due to physical and chemical conditions, allergic inflammation and asthma, idiopathic pulmonary fibrosis and other diffuse lung diseases, including lung cancer [2,4]. The absence of IL-8 and its receptor orthologs in small rodents hindered the possibility of testing novel strategies targeting IL-8 using mice as a convenient small size experimental animal model. We filled the gap by generating a mouse model transiently expressing a reporter gene under the control of an IL-8 promoter which is suitable to functionally study IL-8 promoter in a convenient small size experimental animal model.

Materials and Methods

Construct

bIL-8-Luc was obtained by sub-cloning the 2030 bp IL8 bovine promoter, amplified by PCR from Madin-Darby bovine kidney (MDBK; ATCC #CCL-22) genomic DNA and subcloned into the digested pGL3basic vector (Promega) as previously described [17]. Whereas STAT-1-Luc and ELK-1-Luc containing the minimal promoter of STAT-1 and ELK-1 human gene were obtained from Switchgear Genomics.

Cell Cultures

Mouse lung adenocarcinoma cell line of epithelial origin, LA-4 cells (ATTC, #CCL-196), was cultured in Dulbecco's modified essential medium (Sigma) containing 10% FBS, 2 mM of L-glutamine, 100 IU/ml of penicillin, 100 μg/ml of streptomycin, and 2.5 μg/ml of amphotericin B (Sigma). Cell culture plates or flasks were incubated at 37°C with 5% CO_2 in air, in a humidified atmosphere.

LA-4 Cells Characterization by RT-PCR for TNF-αRI and II and TLRs

Total RNA from LA-4 cells was extracted with TriPure reagent (Roche) and 5 μg of total RNA were reverse transcribed using

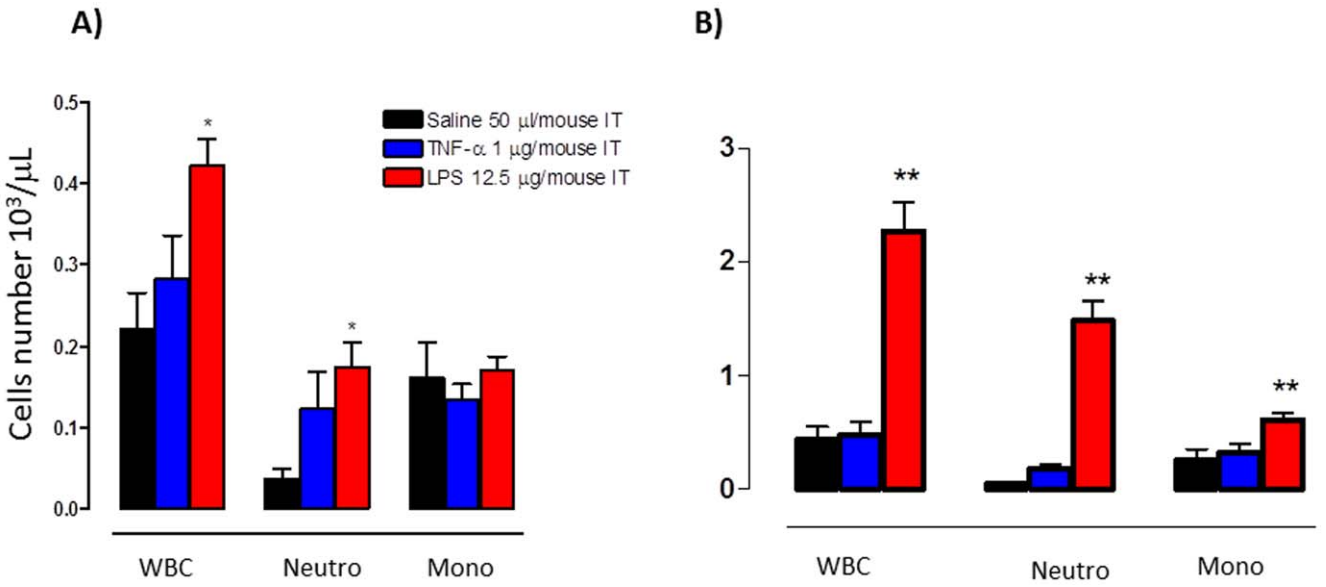

Figure 4. White blood cells and neutrophils infiltration. Cellular infiltration into the lung of mice intratracheally instilled with LPS, TNF-α or vehicle. The amount of White blood cells (WBC), Neutrophils (Neut) and Monocytes (Mono) found in BALF was expressed as number of cells per μl at 3 (A) and 24 hours (B) post treatment. The experiment was repeated three times and each point represents the mean ± standard deviation of 9 animals. Data were expressed as folds of induction over vehicle-treated mice (Saline) and statistical differences were tested by One Way ANOVA followed by Dunnet's post hoc test for group comparisons. Results are reported as mean ± SD and significance attributed when $P<0.05$ (*) or $P<0.01$(**).
doi:10.1371/journal.pone.0039716.g004

Ready-To-Go, T-Primed First-Strand Kit (Amersham Biosciences). Two microliters of the resulting cDNA were amplified in a final volume of 50 µl of 10 mM Tris–hydrochloride, pH 8.3, containing 0.2 mM deoxynucleotide triphosphates, 2.5 mM $MgCl_2$, 50 mM KCl, 1 U of Taq polymerase (Invitrogen) and 0.25 µM of each primer listed in **Table S1**. The amplification program for TNF-αRI, II and GAPDH was 35 cycles, each cycle consisting of denaturation at 94°C for 1 min, primer annealing at 55°C for 1 min, and chain elongation at 72°C for 1 min [33]. The amplification program for TLRs was 35 cycles, each cycle consisting of denaturation at 94°C for 1 min, primer annealing at 55°C for 1 min, and chain elongation at 72°C for 1 min [34]. PCR products were analyzed on a 2% agarose gel.

LA-4 Cell Electroporation

LA-4 cells were cultured in a 75 cm^2 flask. When growth reached 90% confluence cells were electroporated. bIL-8-Luc plasmid DNA (20 µg) diluted in 600 µl of DMEM without serum was electroporated (Equibio apparatus Wolf Laboratories Limit., York, UK) into LA-4 cells at 186 V, 960 µF, in 4-mm gap cuvettes (Wolf Laboratories Limit., York, UK)). Electroporated cells were plated in a twenty four-well plates and incubated in an atmosphere of 95% air and 5% CO_2 at 37°C.

Dual Luciferase Reporter Assay

Twenty-four hours post electroporation, LA-4 cells in twenty four-well plates were treated with LPS (500 ng/ml) (Sigma) or TNF-α (10 ng/ml) (Sigma) for four hours.

The luciferase reporter assay was performed with a Dual Luciferase Reporter Assay System kit (Promega Corp., Madison, WI, USA) according to the manufacturer's specification with minor modifications. Following treatment, cells were washed with PBS and lysed with 100 µl of passive lysis buffer by freeze-thawing at −80°C. Ten microliters of the cell lysate were added to 50 µl of LAR and Luciferase activity was determined with a PerkinElmer Victor^3 Multilabel Counter (PerkinElmer, Waltham, MA, USA), according to the manufacturer's specifications. Experiments were performed with 4 replicates at each time point and each experiment repeated three times. Statistical differences were tested by One Way ANOVA followed by Dunnet's post hoc test for group comparisons.

Experimental Animals

Female inbred FVB (7–8 week-old) mice were purchased from Harlan Laboratories Italy (San Pietro al Natisone, Udine). Animals were maintained under conventional housing conditions. Prior to use, animals were acclimatized for at least 5 days to the local vivarium conditions (room temperature: 20–24°C; relative humidity: 40–70%), having free access to standard rat chow and tap water. All experiments were carried out in rodents and exclusively included painless suppression of animals. The experiments comply with the Principles of Animal Care (publication no. 85–23, revised 1985) of the National Institutes of Health and with the current law of the European Union and Italy (D. L.vo 116/92). The present project was approved by the Ethical Committee of the University of Parma (Italy).

In vivo Gene Delivery

We applied *in vivo* JetPEI (Polyplus Transfection) as a carrier for delivering DNA to lung tissues. The DNA and JetPEI mix was formulated according to the product manual with a final N/P ratio of 7. Briefly, 40 µg of bIL-8–luc, STAT-1-Luc, ELK-1-Luc or pGL3 basic reporters and 7 µL of JetPEI were each diluted into 200 µL 5% glucose. The two solutions were then mixed and incubated for 15 minutes at room temperature. The entire mixture was i.v. injected into FVB mice and the expression of bIL-8–Luc, STAT-1-Luc, ELK-1-Luc or pGL3 basic reporters was monitored through imaging with IVIS.

In vivo Bioluminescence Imaging (BLI)

In vivo imaging was performed using an IVIS imaging system (Caliper Life Sciences, Alameda, CA). From 10 days after DNA delivery the transient transgenic mice were imaged in order to check the baseline activation of the IL-8 pathway. The day after transgenization, the mice were intratracheally challenged with LPS (12.5 µg/mouse) or TNF-α (1 µg/mouse) and the lungs imaged using bioluminescence (BLI) after 2, 4, 7 and 24 hours following intraperitoneal injection of 150 mg/kg luciferin. The mice were anesthetized with gas anaesthesia (isoflurane 2.5%), imaged for 5 minutes, 10 minutes and 15 minutes after luciferin injection in order to minimized the pharmacokinetic variability among mice. Photons emitted from specific regions were quantified using Living Image® software (Caliper Life Sciences, Alameda, CA).

Bronchoalveolar Lavage Fluid (BALF) and Cell Counting

Bronchoalveolar lavage (BAL) was performed as previously described [35]. Briefly, mouse tracheas were cannulated with an 18-gauge angiocathether (Becton Dickinson). Six hundred microliters of sterile HANK'S buffer were instilled three times in the bronchial tree and collected for subsequent analysis. After centrifugation at 400 g for 10 minutes, the cell pellet was resuspended in 0.2 ml of PBS. Total cell number was counted with a particle counter (Dasit XT 1800J). The pellets deriving from the same animal were combined and resuspended in a volume of 0.2 ml and total and differential cell counts were performed within 2 hours using an automated cell counter (Dasit xt 1800 J, Sysmex). The cell count per animal was calculated from the number of cells for 1 µl of BALF multiplied for the volume used for the resuspension of the cell pellet.

Statistics

Experiments were performed with 4 replicates at each time point and each experiment repeated three times. Data were analysed using One Way ANOVA followed by Dunnet's post hoc test for group comparisons. Results are reported as mean ± SD and significance attributed when $P<0.05$ (*) or $P<0.01$(**).

Supporting Information

Figure S1 Representative images of groups of mice (n = 3 per group) transiently transgenized with ELK-1-Luc or STAT-1-Luc DNA and intratracheally instilled with LPS or TNF-α. Mice were monitored at 3, 5 and 24 hours post stimulation by BLI and no signal was detectable.
(TIF)

Table S1 List of primers used in this work.
(DOC)

Acknowledgments

We would like to thank Chiara Sartori for English editing.

Author Contributions

Conceived and designed the experiments: GD FFS. Performed the experiments: GD FFS VF CA MR. Analyzed the data: GD FFS. Wrote the paper: GD. Intellectual contributions: GV FF.

References

1. Donnelly SC, Strieter RM, Kunkel SL, Walz A, Robertson CR, et al. (1993) Interleukin-8 and development of adult respiratory distress syndrome in at-risk patient groups. Lancet 341: 643–647.
2. Malazdrewich C, Ames TR, Abrahamsen MS, Maheswaran SK (2001) Pulmonary expression of tumor necrosis factor alpha, interleukin-1 beta, and interleukin-8 in the acute phase of bovine pneumonic pasteurellosis. Vet Pathol 38: 297–310.
3. Murugan V, Peck MJ (2009) Signal transduction pathways linking the activation of alveolar macrophages with the recruitment of neutrophils to lungs in chronic obstructive pulmonary disease. Exp Lung Res 35: 439–485.
4. Mukaida N (2003) Pathophysiological roles of interleukin-8/CXCL8 in pulmonary diseases. Am J Physiol Lung Cell Mol Physiol 284: L566–577.
5. Zhao X, Town JR, Li F, Zhang X, Cockcroft DW, et al. (2009) ELR-CXC chemokine receptor antagonism targets inflammatory responses at multiple levels. J Immunol 182: 3213–3222.
6. Zhao X, Town JR, Li F, Li W, Zhang X, et al. (2010) Blockade of neutrophil responses in aspiration pneumonia via ELR-CXC chemokine antagonism does not predispose to airway bacterial outgrowth. Pulm Pharmacol Ther 23: 22–28.
7. Luscinskas FW, Gerszten RE, Garcia-Zepeda EA, Lim YC, Yoshida M, et al. (2000) C-C and C-X-C chemokines trigger firm adhesion of monocytes to vascular endothelium under flow conditions. Ann N Y Acad Sci 902: 288–293.
8. Jorens PG, Richman-Eisenstat JB, Housset BP, Graf PD, Ueki IF, et al. (1992) Interleukin-8 induces neutrophil accumulation but not protease secretion in the canine trachea. Am J Physiol 263: L708–713.
9. Gesser B, Lund M, Lohse N, Vestergaad C, Matsushima K, et al. (1996) IL-8 induces T cell chemotaxis, suppresses IL-4, and up-regulates IL-8 production by CD4+ T cells. J Leukoc Biol 59: 407–411.
10. Srinivasan S, Yeh M, Danziger EC, Hatley ME, Riggan AE, et al. (2003) Glucose regulates monocyte adhesion through endothelial production of interleukin-8. Circ Res 92: 371–377.
11. Harada A, Mukaida N, Matsushima K (1996) Interleukin 8 as a novel target for intervention therapy in acute inflammatory diseases. Mol Med Today 2: 482–489.
12. Matsushima K, Morishita K, Yoshimura T, Lavu S, Kobayashi Y, et al. (1988) Molecular cloning of a human monocyte-derived neutrophil chemotactic factor (MDNCF) and the induction of MDNCF mRNA by interleukin 1 and tumor necrosis factor. J Exp Med 167: 1883–1893.
13. Schmitz ML, Bacher S, Kracht M (2001) I kappa B-independent control of NF-kappa B activity by modulatory phosphorylations. Trends Biochem Sci 26: 186–190.
14. Nissen RM, Yamamoto KR (2000) The glucocorticoid receptor inhibits NFkappaB by interfering with serine-2 phosphorylation of the RNA polymerase II carboxy-terminal domain. Genes Dev 14: 2314–2329.
15. Simonet WS, Hughes TM, Nguyen HQ, Trebasky LD, Danilenko DM, et al. (1994) Long-term impaired neutrophil migration in mice overexpressing human interleukin-8. J Clin Invest 94: 1310–1319.
16. Cacalano G, Lee J, Kikly K, Ryan AM, Pitts-Meek S, et al. (1994) Neutrophil and B cell expansion in mice that lack the murine IL-8 receptor homolog. Science 265: 682–684.
17. Donofrio G, Capocefalo A, Franceschi V, Price S, Cavirani S, et al. (2010) The chemokine IL8 is up-regulated in bovine endometrial stromal cells by the BoHV-4 IE2 gene product, ORF50/Rta: a step ahead toward a mechanism for BoHV-4 induced endometritis. Biol Reprod 83: 919–928.
18. Rosenkilde MM, Schwartz TW (2004) The chemokine system – a major regulator of angiogenesis in health and disease. APMIS : acta pathologica, microbiologica, et immunologica Scandinavica 112: 481–495.
19. Laterveer L, Lindley IJ, Hamilton MS, Willemze R, Fibbe WE (1995) Interleukin-8 induces rapid mobilization of hematopoietic stem cells with radioprotective capacity and long-term myelolymphoid repopulating ability. Blood 85: 2269–2275.
20. Minnerly JC, Baganoff MP, Deppeler CL, Keller BT, Rapp SR, et al. (1995) Identification and characterization of rhesus macaque interleukin-8. Inflammation 19: 313–331.
21. Villinger F, Brar SS, Mayne A, Chikkala N, Ansari AA (1995) Comparative sequence analysis of cytokine genes from human and nonhuman primates. J Immunol 155: 3946–3954.
22. Morsey MA, Popowych Y, Kowalski J, Gerlach G, Godson D, et al. (1996) Molecular cloning and expression of bovine interleukin-8. Microb Pathog 20: 203–212.
23. Legastelois I, Greenland T, Arnaud P, Mornex JF, Cordier G (1994) Sequencing of the ovine interleukin-8-encoding cDNA using the polymerase chain reaction. Gene 150: 367–369.
24. Lin G, Pearson AE, Scamurra RW, Zhou Y, Baarsch MJ, et al. (1994) Regulation of interleukin-8 expression in porcine alveolar macrophages by bacterial lipopolysaccharide. J Biol Chem 269: 77–85.
25. Kukielka GL, Smith CW, LaRosa GJ, Manning AM, Mendoza LH, et al. (1995) Interleukin-8 gene induction in the myocardium after ischemia and reperfusion in vivo. J Clin Invest 95: 89–103.
26. Yoshimura T, Yuhki N (1991) Neutrophil attractant/activation protein-1 and monocyte chemoattractant protein-1 in rabbit. cDNA cloning and their expression in spleen cells. J Immunol 146: 3483–3488.
27. Yoshimura T (1993) cDNA cloning of guinea pig monocyte chemoattractant protein-1 and expression of the recombinant protein. J Immunol 150: 5025–5032.
28. Dehbi M, Mbiguino A, Beauchemin M, Chatelain G, Bedard PA (1992) Transcriptional activation of the CEF-4/9E3 cytokine gene by pp60v-src. Mol Cell Biol 12: 1490–1499.
29. Meade KG, O'Gorman GM, Narciandi F, Machugh DE, O'Farrelly C (2012) Functional characterisation of bovine interleukin 8 promoter haplotypes in vitro. Mol Immunol 50: 108–116.
30. Standiford TJ, Kunkel SL, Basha MA, Chensue SW, Lynch JP 3rd, et al. (1990) Interleukin-8 gene expression by a pulmonary epithelial cell line. A model for cytokine networks in the lung. J Clin Invest 86: 1945–1953.
31. Moretto N, Facchinetti F, Southworth T, Civelli M, Singh D, et al. (2009) alpha,beta-Unsaturated aldehydes contained in cigarette smoke elicit IL-8 release in pulmonary cells through mitogen-activated protein kinases. Am J Physiol Lung Cell Mol Physiol 296: L839–848.
32. Doyle TC, Burns SM, Contag CH (2004) In vivo bioluminescence imaging for integrated studies of infection. Cell Microbiol 6: 303–317.
33. Bette M, Kaut O, Schafer MK, Weihe E (2003) Constitutive expression of p55TNFR mRNA and mitogen-specific up-regulation of TNF alpha and p75TNFR mRNA in mouse brain. J Comp Neurol 465: 417–430.
34. Golden JM, LaCasse CJ, Simova DV, Murphy TR, Kurt RA (2008) Differential mediator production by dendritic cells upon toll-like receptor stimulation does not impact T cell cytokine expression. Immunol Lett 118: 30–35.
35. Koay MA, Gao X, Washington MK, Parman KS, Sadikot RT, et al. (2002) Macrophages are necessary for maximal nuclear factor-kappa B activation in response to endotoxin. Am J Respir Cell Mol Biol 26: 572–578.